Geochemistry of apatite from the carbonatite and associated alkaline rocks of the Magnet Cove Igneous Complex, Hot Spring County, Arkansas

Rebecca Ohly
Thesis advisor: Dr. Philip Piccoli
April 29, 2011
GEOL 394

Table of contents

1. Abstract

Apatite from carbonatite and alkaline rocks from the Magnet Cove Igneous Complex in Arkansas was analyzed for major and trace element composition. Particular elements of interest were REE and halogens, which were used for geochemical modeling of the evolution of the igneous system. Major and minor elemental concentrations in apatite were compared to determine the presence and nature of potential substitutions in crystallographic sites. Halogen concentrations were used, along with both calculated and assumed temperatures and pressures, to determine changes in HF and HCl fugacities over the time of crystallization of the magma. Additionally, apatite was analyzed for REE concentrations. These data were used to estimate the degree of fractionation between rock types that occurred over the crystallization history of the complex. Concentrations of major and minor elements (including halogens) in apatite were determined by electron probe microanalysis, and trace element concentrations were measured using laser ablation-inductively coupled plasma mass spectrometry. Results were interpreted in the context of information on bulk rock chemistry and relative ages provided by Erickson and Blade (1963). Modeled fugacity ratios determined from halogen concentrations in apatite indicated a systematic decrease in both HF and HCl fugacity as the rocks decreased in age, while REE concentrations indicated that trace element partitioning was strongly controlled by phases in the individual rock types in the Magnet Cove Igneous Complex. These results suggest that geochemical evolution in the complex was influenced by both continuous (fractional crystallization) and episodic (multiple episodes of magmatism from the same parental magma) processes.

2. Introduction

Carbonatites are igneous rocks that are composed of >50% carbonate minerals. They are, therefore, unlike all other igneous rocks, which consist almost entirely of silicate minerals. They are relatively uncommon, with ~330 known occurrences. Carbonatites are typically associated with silica-undersaturated rocks, and mainly occur as small intrusions surrounded by ring dikes of silica-deficient rocks (Wooley, 1989).

It has been established that, due to these associations and other geochemical, spatial, and tectonic signatures, carbonatites are likely the result of high levels of magmatic differentiation. The mechanisms of differentiation that have been proposed include fractional crystallization, liquid immiscibility, or partial mantle melting (e.g. Dalou et al., 2009, Gaillard et al., 2008). All of these processes are supported by various lines of geological evidence, but the mechanism of formation of carbonatites has not been fully defined.

Analysis of minerals common to carbonatites and associated rocks is one method that may shed some light onto how igneous systems evolve into a carbonatitic composition. If the composition of one mineral present in all rock types in a carbonatite-silicate igneous complex changes throughout the rock types, it may be possible to infer the nature of magmatic evolution from these compositional variations.

Two such ways of doing so are the use of mineral volatile concentrations to model changes in fugacities of volatiles in a magma, and examination of trace elemental composition of

a mineral to determine mechanisms of fractionation that may be occurring. Volatiles (halogens and water, in particular) can exert significant control on the solidus of a magma, and, in systems with extremely low solidus temperatures like those seen in carbonatites, they may play a major role in magmatic evolution. By allowing a system to remain liquid over a longer than normal period (or greater temperature range), high concentrations of volatiles in a magma can affect processes of differentiation, and allow them to proceed for a longer time than would usually occur, leading to the extremely differentiated compositions seen in carbonatites. Alternately, REE can be used to determine sequence of crystallization: changes in relative and absolute concentrations, along with "kinked" shapes in chondrite-normalized REE plots, can indicate timing of crystallization, and which crystallizing phases in the rock took in the REE (Walker et al., 1986).

Apatite is common in the silicate and carbonatite rocks of the Magnet Cove Igneous Complex (MCIC). It occurs as either a trace or primary phase, ranging in modal abundance from ~1% to 24% through the various rock types. Because of its ubiquity and composition (the compositional properties of apatite that allow its use in this study are detailed in Section 4), and its resistance to subsolidus change, it is an ideal mineral to use as a proxy for multiple elemental systems that can elucidate the manner of geochemical evolution that occurred as the magma that formed the MCIC differentiated and cooled.

Carbonatites are likely products of extreme magmatic differentiation. Past studies have shown that these rocks tend to be highly enriched in trace and incompatible elements (for instance, REE) and volatiles (particularly, halogens). Assuming that the MCIC is representative of a magma that evolved into a carbonatite, with various rock types representing periods in its cooling history (Erickson and Blade, 1963), there will be systematic changes in both halogens and REE throughout the rock types.

2.1 Hypothesis

The magmatic differentiation typical of carbonatite systems will be manifested by an increase in REE concentration and REE fractionation as the MCIC rocks decrease in age (and tend more towards a carbonatitic composition), as well as changes in HF and HCl fugacities between rock types. Based on the high levels of F enrichment seen in carbonatites (up to 15 weight percent (Jago and Gittins, 1991)), and its generally incompatible behavior in magmatic systems, modeled fugacities will show an increase in HF fugacity as the rocks decrease in age, with a corresponding decrease in HCl fugacity, also indicating increasing differentiation with decreasing age in the MCIC rock types.

3. Carbonatites

3.1 Geologic settings and structural features

Carbonatites tend to occur in continental rift settings. They occur almost exclusively as intrusive complexes, though there are rare carbonatite volcanoes. Carbonatite complexes are generally a series of ring-shaped silicate intrusions surrounding a carbonatite core (Wooley, 1989). Complexes are small, generally no more than a few km in diameter. There is only one active carbonatite volcano, Oldoinyo Lengai, which is located in Tanzania. It erupts alkalic

carbonate lavas at very low temperatures, at times approaching a mere 200^{o} C (Keller et al., 2010).

Though there are carbonatite occurrences worldwide, there are several regions were complexes occur in clusters, which generally represent extinct (or, in the case of African carbonatites, active) rift systems. Notable occurrences are in Brazil, Scandinavia, Africa, and parts of the United States (including the Arkansas alkaline belt, the location of the MCIC). (Wooley, 1989)

Carbonatite magmatism is episodic, and has increased in frequency over time, though the reasons for these patterns are not well understood (Wooley, 1989).

3.2 Mineralogy of carbonatites

Carbonatites are defined as having at least 50% carbonate minerals, but they generally have much higher percentages (sometimes close to 100%). Characteristic accessory minerals include oxides (magnetite, rutile), micas (phlogopite), olivine (monticellite), halides (halite, sylvite, fluorite (which is especially important as a F-bearing phase)), and phosphates (monazite, apatite). In addition to monazite, pyrochlore is another common REE-rich phase sometimes present in carbonatites. Apatite is a characteristic accessory mineral in carbonatites, and can be present as a major phase (several tens of percent).

Carbonatites are generally composed of calcium, magnesium and/or iron carbonates, with a progression from calcium-rich to iron-rich carbonates, generally following the sequence $CaCO_3$→ $(Ca,Mg)(CO_3)_2$→ $(Ca,Fe)(CO_3)_2$→ $FeCO_3$ (i.e. more evolved magmas will tend to have more iron carbonates) (Wooley and Kempe, 1989). When specific carbonate minerals (Ca, Mg or Fe rich) are dominant, rocks are called calciocarbonatites, magnesiocarbonatites, and

Figure 1. Calciocarbonatite from the Oka complex in Canada. Major minerals visible are calcite and biotite.

ferrocarbonatites, respectively. Carbonatite lavas, as in the case at Oldoinyo Lengai, contain sodium and potassium carbonates, chiefly nyerereite ($Na_2Ca(CO_3)_2$) and gregoryite ($(Na_2,K_2,Ca)CO_3$). These alkalic lavas are classified as natrocarbonatites, and may represent the most primitive form of carbonatite magma (Wooley and Kempe, 1989). It is possible that more natrocarbonatites have erupted in the past, but the highly reactive nature of the minerals in these lavas causes them to weather extremely rapidly once exposed to atmospheric water, which alters the erupted carbonate material into hydrated alkaline carbonate minerals such as trona and nahcolite, as well as calcium-alkali carbonates such as pirssonite and shortite, and even pure calcite (Zaitsev and Keller, 2006). The presence of these alteration products may disguise the former existence of these alkali carbonate lavas by obliterating the anhydrous sodium and potassium carbonates seen in natrocarbonatites, obscuring the original composition and origin of the rock.

3.3 Incompatible elements

As carbonatites are thought to be products of highly differentiated magmas, they tend to be enriched in incompatible elements. By the time a carbonatite crystallizes, nearly all of the common (i.e. those in silicate systems) rock-forming minerals and elements have partitioned into crystalline phases. The remaining melt is then highly enriched in incompatible elements that normally exist at trace levels (for instance, REE may be at several weight percent in carbonatite vs. ppm to ppb levels in a typical silicate rock). Fluorine is perhaps the most important incompatible element in this study, and it is abundant (up to 15 weight %) in many carbonatites (Wooley and Kempe, 1989; Jago and Gittins, 1991). Other incompatible elements that are characteristically enriched in carbonatites are elements from the LILE (Rb, Cs, Ba) and HFSE (Nb, lanthanides, actinides) groups.

3.4 Rare earth elements

Carbonatites are highly enriched in REE, and generally have the highest LREE:HREE ratios as well as overall REE content of any igneous rock (Wooley and Kempe, 1989). REE can exist in carbonatites in high enough concentrations to be of economic importance, and they have been mined for REE ores in some locations (e.g. Mountain Pass, California).

Minerals rich in REE in carbonatites include apatite, monazite, and pyrochlore. Both monazite and pyrochlore are REE minerals (REE are an essential structural constituent of the mineral): monazite is a REE phosphate, and pyrochlore is a REE hydroxide-fluoride.

3.5 Volatiles in carbonatites

Volatiles in igneous systems consist of fluid phases and light elements (halogens, water, CO_2, B, etc.) that are either dissolved in a melt, or exist as a separate, immiscible vapor or liquid phase in a system. One of the most significant properties of volatiles in magmatic systems is their ability to significantly alter the solidus of a melt system. Since carbonatites can be highly enriched in volatiles, this has significant implications for the genesis of rocks of carbonatitic composition.

Carbonatite melts tend to have very high levels of halogens (fluorine and chlorine) and very low levels of water (in some cases under 1%). Lavas at Oldoinyo Lengai have been found to contain up to 15 weight percent fluorine and chlorine (Jago and Gittins, 1991). In intrusive

carbonatites, volatiles tend to partition into several minerals. Fluorite is a common fluorine-bearing phase, as are apatite and phlogopite. Phlogopite and, in particular, apatite, are both important in determining the halogen budget of a magma because they exist as a solution of three of the most abundant volatiles in igneous systems: F, Cl and OH (H_2O). Because of its common occurrence in many types of igneous rocks and its frequently high abundance in carbonatites, apatite can be an important tool in determining the changing volatile concentrations in a melt over its cooling history.

The halogens primarily exist in magmatic systems as HF and HCl, and thus fugacities calculated for this project were modeled by using elemental halogen content of apatite to determine HCl and HF fugacities. H_2O in carbonatites is primarily partitioned into hydrous minerals such as micas (usually phlogopite) and apatite, with a lesser amount going into less abundant minerals such as pyrochlore. The solid solution behavior of apatite may be somewhat mirrored by that of certain micas, but, due to the effect of Fe/Mg avoidance ratios, halogen partitioning into micas tends to be more complex, and less reflective of absolute halogen concentrations in carbonatite magmas without more complete corrections for composition of micas (Piccoli, personal communication, 2011).

3.6 Petrogenesis of carbonatites

Most proposed mechanisms of carbonatite formation invoke some form of unusually high levels of differentiation. Parental melts may be derived from very deep partial melting of the mantle (Dalou et al., 2009, Gaillard et al., 2008). Carbonatites are commonly associated with silica-undersaturated rocks (Wooley, 1989). Intrusive complexes tend to be concentric rings of rocks that become progressively poorer in silica inwards, with the cores of the complexes being the carbonatites themselves, which is the opposite sequence seen in most zoned complexes, which become more enriched in silica inwards. This spatial relationship and chemical gradation points to a magmatic evolution of some sort that alters the crystallization products of the magma over time. What is unknown is exactly what causes this evolution, and what allows it to go to such an extent that it results in rocks nearly free of silica and almost entirely carbonate. There are three favored mechanisms by which carbonatites are thought to form: fractional crystallization, liquid immiscibility, and direct mantle melting. Additionally, assimilation has been proposed in the past, but has since been ruled out by isotopic differences between carbonatites and potentially assimilated rocks. However, this highlights the fact that carbonatite melt systems tend to alter surrounding rocks (producing a type of metasomatism called fenitization) rather than be altered by connate or meteoric water, which is further evidence that carbonatite melts are rich in fluid phases/volatiles, as is manifested by the abundance of fenitization that is seen with carbonatite intrusive bodies (e.g. Andersen and Austrheim, 1991).

Fractional crystallization is an igneous differentiation process in which elements are systematically removed from a melt at varying rates by crystallizing minerals as a magma body cools. As common rock-forming elements and minerals crystallize from a melt, the remaining melt composition will become enriched in incompatible and trace elements. The high concentrations of such elements in carbonatites may suggest that fractional crystallization is responsible for the formation of these rocks.

Liquid immiscibility may be a mechanism which facilitates the formation of carbonatites as well. In this scenario, a magma will separate into multiple fluid phases that cannot mix

together (in the case of carbonatites, this would likely be due to the formation of an immiscible carbonate fluid phase rich in halogens and incompatible elements). Bühn et al. (2002) proposed in that fluid inclusions in quartz in the Okorusu fluorite deposit (and nearby carbonatite) in Namibia might provide evidence of an immiscible liquid phase present at the time of formation of the carbonatite.

The mechanism of magmatic assimilation of country rock and/or inclusions is generally no longer in favor, as it has been shown that little assimilation of carbonate rocks occurs in parental melts of carbonatites. However, though carbonatites may cause metasomatism around intrusions (fenitization), they are generally not altered by any inclusion of surrounding rocks. This may be due to the low temperature of carbonatite melts: xenoliths and wall rocks may not melt at temperatures where carbonatite magmas exist.

Comparison of Sr isotopic ratios ($^{87}Sr/^{86}Sr$) in carbonatites and other materials (sedimentary carbonates, strontianites) has been particularly helpful in eliminating assimilation as a mechanism contributing to the formation of carbonatites. $^{87}Sr/^{86}Sr$ ratios in carbonatites (ranging from 0.7060-0.7065) are consistently lower than those of limestones, limestone xenoliths within carbonatites, and strontianites (~0.7090-0.7140) (Powell et al., 1962, Hamilton and Deans, 1963).

4. Apatite

Apatite is a hydrous calcium phosphate that can contain halogens in its crystal structure, with the formula $Ca_5(PO_4)_3(F,Cl,OH)$. The crystal structure of apatite allows extensive substitutions, so a more general formula for apatite group minerals may also be used: $A_5(XO_4)_3Z_n$. It has three endmember compositions based on the solid solution of halogens and water in its structure (hereafter referred to as volatiles): apatite-(CaF), apatite-(CaCl), and apatite-(CaOH). Apatite is typically found as an accessory mineral in igneous rocks, and in biological settings. Igneous apatite generally tends toward the apatite-(CaF) end member (Piccoli and Candela, 2002), whereas apatite found in biologic settings (e.g. teeth and bones) is typically apatite-(CaOH). Apatite-(CaCl) is uncommon in most rock types. A fourth type of apatite, carbonate apatite, occurs when some of the phosphate groups and volatiles are replaced with carbonate anions. This type of apatite has been seen in carbonatites. Carbonate apatite is significant in terms of volatile contents because it may lead to measurements of volatiles in excess of the maximum molar concentration possible as determined by the mineral formula, as halogens may enter the crystal site for the phosphate group to maintain a charge balance with the carbonate anion.

4.1 Coupled substitutions

Apatite can take in a variety of elements into its crystal sites, through both regular (i.e. similar ionic radius, same charge) and coupled (multiple ions substitute to maintain an overall charge balance) substitutions. For the purposes of this study, coupled substitutions involving REE were of particular significance (the two most frequent mechanisms are $REE^{3+} + Si^{4+} \rightarrow Ca^{2+} + P^{5+}$, and $REE^{3+} + Na^{1+} \rightarrow 2Ca^{2+}$), but the vast range of compositions of apatite that exist attest to the ability of the mineral's structure to accommodate a diverse mix of elements. Many

mineral structures allow for regular substitutions; this is demonstrated by the existence of solid solution behaviors seen in so many common minerals. Coupled substitutions are less common among minerals, but are frequently seen in apatite.

4.2 Compositional implications

The solid solution behavior of apatite makes it a valuable proxy for volatile concentrations in an igneous system at the time of crystallization. Determining the relative volatile concentrations in apatite may be used to model fugacities of volatile elements in melts. Determining volatile concentrations in igneous systems is useful because of the significant control volatiles can exert on the solidus of an igneous system.

REE concentrations are another proxy for geochemical evolution: magmatic systems can experience systematic enrichment or depletion in REE (all REE, or between the heavy and light rare earths) as phases crystallize out. Compositional changes that are consistent through apatite in various rock types may indicate compositional changes in the igneous intrusion that formed the MCIC at different points in its cooling history. Fractionation of REE, as well as depletion or enrichment of specific elements, is useful in determining the order in which minerals crystallized, the abundance of each mineral type, and, ultimately, how the igneous body changed as it cooled to form the various rock types seen in the MCIC.

5. The Magnet Cove Igneous Complex

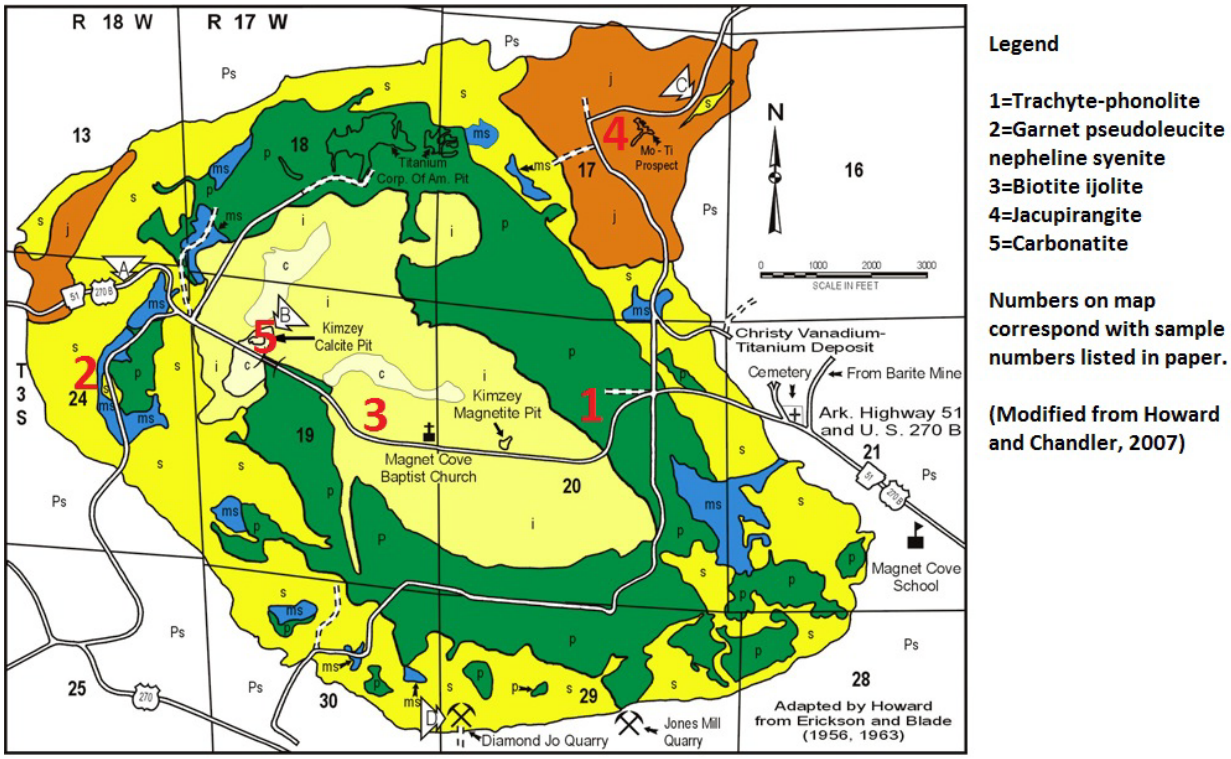

Figure 2. Geologic map of the MCIC showing major rock types in the complex.

The Magnet Cove Igneous Complex is a series of ring-shaped intrusions located in Hot Spring County, Arkansas, in the Arkansas Alkaline Belt. It is ~2 km in diameter, and is Cretaceous in age (~94 Ma) (Erickson and Blade, 1963). The intrusions are emplaced in country rock consisting of metamorphosed chert (novaculite), and consist of trachyte-phonolite, garnet pseudoleucite nepheline syenite, biotite ijolite (hereafter referred to as phonolite, syenite, and ijolite, respectively), jacupirangite, and carbonatite (Erickson and Blade, 1963). Listed below is a the generalized mineralogy of the rock types sampled for this study (a detailed description of rock types and their mineralogy is located in Appendix 2).

a) Trachyte-phonolite (MCIC-1): a rock composed primarily of alkali feldspar and nepheline.

b) Garnet pseudoleucite nepheline syenite (MCIC-2): a silica-undersaturated rock composed primarily of nepheline and alkali feldspars. It may have other feldspathoids as well. This sample contains pseudomorphs of euhedral leucite phenocrysts, which have been replaced with nepheline and feldspar.

c) Biotite ijolite (MCIC-3): a rock composed mainly of nepheline and an alkali-bearing pyroxene (generally in the aegirine-augite series). This sample also has abundant biotite.

d) Jacupirangite (MCIC-4): an ultramafic rock composed almost entirely of Ti-bearing augite and magnetite, with small amounts of nepheline.

e) Carbonatite (MCIC-5): an igneous rock composed of euhedral calcite with apatite, magnetite and diopside as the primary accessory minerals.

The outer rocks of the complex roughly correspond with being the oldest (earliest portions of the intrusion), and the inner rocks as the youngest (Erickson and Blade, 1963). Thus, the concentric zones of the complex can be assumed to be decreasing in age as one moves towards the core of the complex. The core is composed of a calciocarbonatite that makes up ~1.2% of the exposed rock in the complex (Erickson and Blade, 1963).

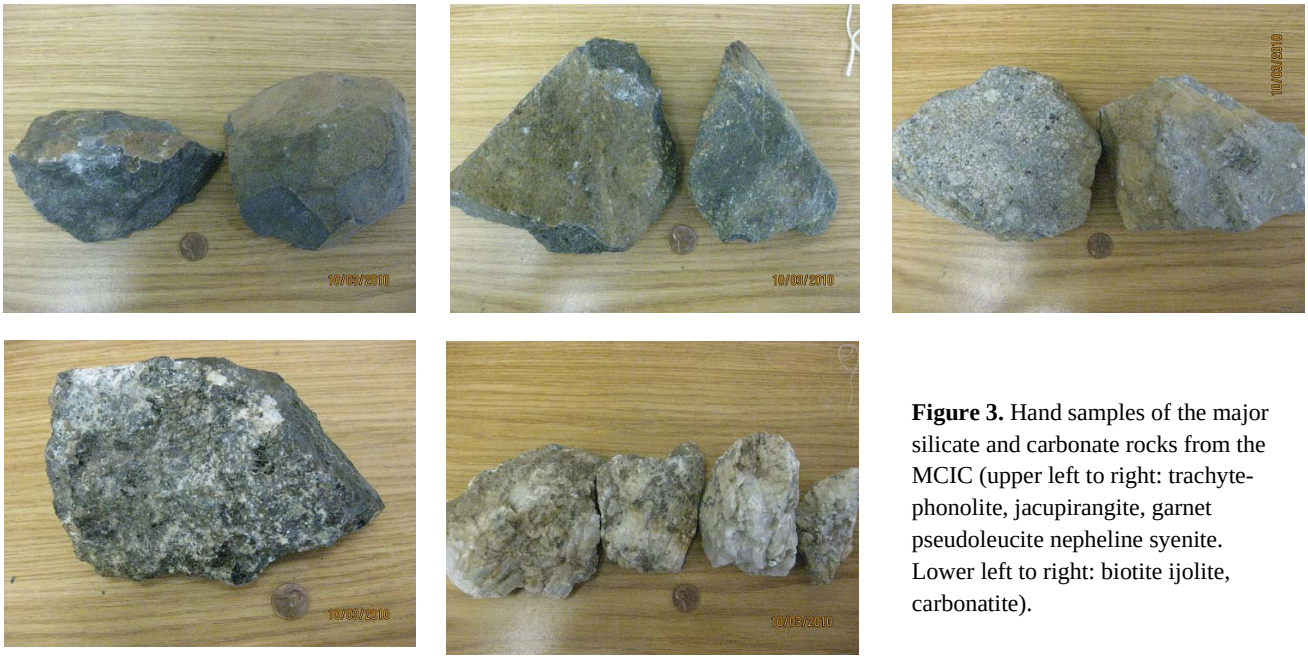

Figure 3. Hand samples of the major silicate and carbonate rocks from the MCIC (upper left to right: trachyte-phonolite, jacupirangite, garnet pseudoleucite nepheline syenite. Lower left to right: biotite ijolite, carbonatite).

The MCIC has been the subject of several past studies due in part to the rare rock types, and to the economic deposits located throughout the intrusions. It has been mined for calcite and magnetite, and is rich in Ti-bearing minerals. It conforms to the characteristic geometry and igneous associations of carbonatite complexes (Wooley, 1989) and is thus a useful source of sampling for geochemical analysis of carbonatites and associated rocks.

6. Models and calculations

6.1 Temperature modeling

For the portion of this study dealing with volatile fugacities, a multi-step calculation process was required to determine HF and HCl fugacities in various MCIC compositional stages (represented by the various rock types sampled from the MCIC). First, modeling of the temperature of crystallization was necessary for fugacity calculations. Temperature modeling was initially accomplished by calculation of apatite saturation temperatures (AST). AST values were determined using the models of Piccoli and Candela (1994), Watson (1979), and Hammouda et al. (2010), depending on the bulk rock composition. The Piccoli and Candela model was used for silicate rocks with 45-70% SiO_2 (peraluminous to slightly peralkaline), the Watson model was used for peralkaline silicate rocks, and the Hammouda model was used for carbonatites. This was somewhat problematic, as the silicate rocks of the MCIC are highly peralkaline, and in some cases contain well under 45 weight % SiO_2, rendering both the Piccoli and Candela and Watson models less accurate. This ended up yielding ASTs in the range of 900-1200^o C, which were excessively high considering the nature of the igneous system (see discussion of geothermometry later in this section). Because of this, fugacities for silicate rocks calculated assuming the high ASTs were several orders of magnitude lower than those calculated with alternate methods (described later in this section). AST values calculated using the Hammouda model also were problematic, again yielding fugacity values that were several orders of magnitude lower than those calculated with alternate temperature derivations (i.e. constant temperature modeling).

Fugacity ratios of f_{HF}/f_{H2O} and f_{HCl}/f_{H2O} for all rock types calculated with AST models tended to range from ~$1x10^{-10}$ to ~$1x10^{-12}$, which is a much lower range than previously reported values derived from similar calculations, which were on the order of ~$1x10^{-7}$-$1x10^{-8}$ (Andersen

Piccoli and Candela, 1994 (silicate rocks, C=wt %)

$$\boldsymbol{T(K) = \frac{26400 \times CSiO_2 - 4800}{12.4 \times CSiO_2 - \ln(CP_2O_5) - 3.97}}$$

Watson, 1979 (peralkaline rocks, D=K_d of P_2O_5)

$$\boldsymbol{T(K) = \frac{1.02 \times 10^4}{lnD - 4.69}}$$

Hammouda et al., 2010 (carbonatites)

$$\boldsymbol{T(K) = \frac{1000}{\frac{\ln(P_2O_{5melt}) - 0.0018 \times CaO_{melt}^{\,2-0.2368CaO_{melt}+6.6004}}{0.0034 \times CaO_{melt} - 4.9036}}}$$

Figure 4. Equations used to calculate AST.

and Austrheim, 1991).

An alternate approach is to assume the temperature to be constant throughout all rock types. A temperature of 700° C was used (determined from information provided by Howard and Eby, personal communication, 2010), which yielded more reasonable fugacity ranges (from ~$1x10^{-6}$ to ~$1x10^{-8}$, assuming the Andersen and Austrheim range of values to be applicable). This assumed temperature is corroborated by past oxygen isotope geothermometry on various minerals from several carbonatite complexes, including the MCIC, which yielded temperatures of 700-760 C for the MCIC (Haynes et al., 2003).

6.2 Pressure conditions

Pressure assumptions were also needed for fugacity calculations. Pressure was assumed to be 700 bars, based on calculation of original emplacement depth through exhumation rates (Howard, personal communication, 2010, and Eby, personal communication, 2010).

6.3 Fugacity modeling

HF and HCl fugacities were calculated using equations derived by Piccoli and Candela (1994). The variables required for the calculations were temperature, pressure, and mole fraction ratios of apatite end members (apatite-(CaF)=FAp, apatite-(CaCl)=CAp, apatite-(CaOH)=HAp). Temperatures and pressures were determined using the methods and sources described above.

Calculated fugacities of HF and HCl showed a systematic decrease from the outer, older rocks of the MCIC to the youngest, innermost rocks (carbonatite). The initial hypothesis for the project stated that a systematic decrease in HCl fugacity would be accompanied by an increase in HF fugacity. However, calculated fugacities both decreased as the rocks decreased in age (toward the core), with HF fugacities decreasing at a more rapid rate than HCl. These patterns were seen when a constant-temperature model was considered (variations in temperatures and the merits of assumed temperature ranges used in models are discussed in the previous section), wherein the AST of the complex was assumed to be constant throughout all rock types at 700° C.

$$\frac{f_{HCl}^{aq}}{f_{H_2O}^{aq}} = \frac{X_{CAp}^{Ap}}{X_{HAp}^{Ap}} \times \frac{1}{10^{0.04661 + \frac{2535.8}{T} - \frac{0.0303 \times (P-1)}{T}}}$$

$$\frac{f_{HF}^{aq}}{f_{H_2O}^{aq}} = \frac{X_{FAp}^{Ap}}{X_{HAp}^{Ap}} \times \frac{1}{10^{0.18219 + \frac{5301.1}{T} + \frac{0.0036 \times (P-1)}{T}}}$$

Figure 5. Fugacity ratio model equations (from Piccoli and Candela, 1994).

7. Results: MCIC apatite geochemistry

Composition of apatite from the MCIC rocks varies significantly between each rock type, however, there are certain compositional properties that are consistent throughout the samples. Apatite from all rock types tended to be high in Sr, Si, and S, and very low in Cl, generally near

or below the detection limit (~0.001 mole percent). All are enriched in LREE, though the degree of enrichment varies through the rock types (discussed below).

	MCIC-1	1σ	MCIC-2	1σ	MCIC-3	1σ	MCIC-4	1σ	MCIC-5A	1σ	MCIC-5B	1σ
F	2.871	0.686	3.442	0.354	1.517	0.111	2.148	0.152	1.079	0.13	**1.02**	0.11
Cl	0.011	0.005	0.005	0.004	0.013	0.005	0.023	0.009	0.01	0.01	**0.01**	0.00
Na2O	0.059	0.053	0.127	0.069	0.025	0.042	0.033	0.036	0.085	0.13	**0.06**	0.03
FeO	0.498	0.43	0.109	0.14	0.035	0.041	0.202	0.454	0.036	0.04	**0.03**	0.03
P2O5	40.211	0.781	40.959	0.859	40.459	0.883	39.907	1.016	37.71	1.47	**37.86**	0.80
SO3	0.302	0.251	0.016	0.012	0.262	0.046	0.666	0.581	0.99	0.21	**1.10**	0.15
SrO	0.208	0.205	3.111	0.833	0.635	0.244	0.68	0.061	0.289	0.03	**0.30**	0.03
MnO	0.055	0.04	0.101	0.051	0.026	0.028	0.032	0.031	0.014	0.02	**0.01**	0.03
SiO2	0.447	0.778	0.064	0.202	0.261	0.133	0.622	0.626	0.82	0.76	**1.41**	0.29
CaO	53.893	1.543	53.329	1.423	54.912	0.872	54.221	1.055	54.633	0.68	**53.33**	0.89

Figure 6. Table of average major element concentrations in apatite from all MCIC samples

7.1 Trace elements

The focus of the trace element analysis was to determine REE content in apatite in orfer to evaluate differentiation. REE have been used as a proxy for geochemical evolution of magmas (Walker et al., 1986). Enrichment in REE is characteristic of carbonatites, including those of the MCIC (Wooley, 1989). Systematic changes in REE concentrations in apatite from various rock types of the MCIC may correspond with particular modes of geochemical evolution. A progressive enrichment in REE from the oldest to youngest rocks may indicate a fractional crystallization origin, while differing concentrations that correspond with location (though, with the MCIC, trends in composition tend to follow the same path in both locational and temporal contexts) may indicate multiple episodes of magmatism from a parental source, rather than a

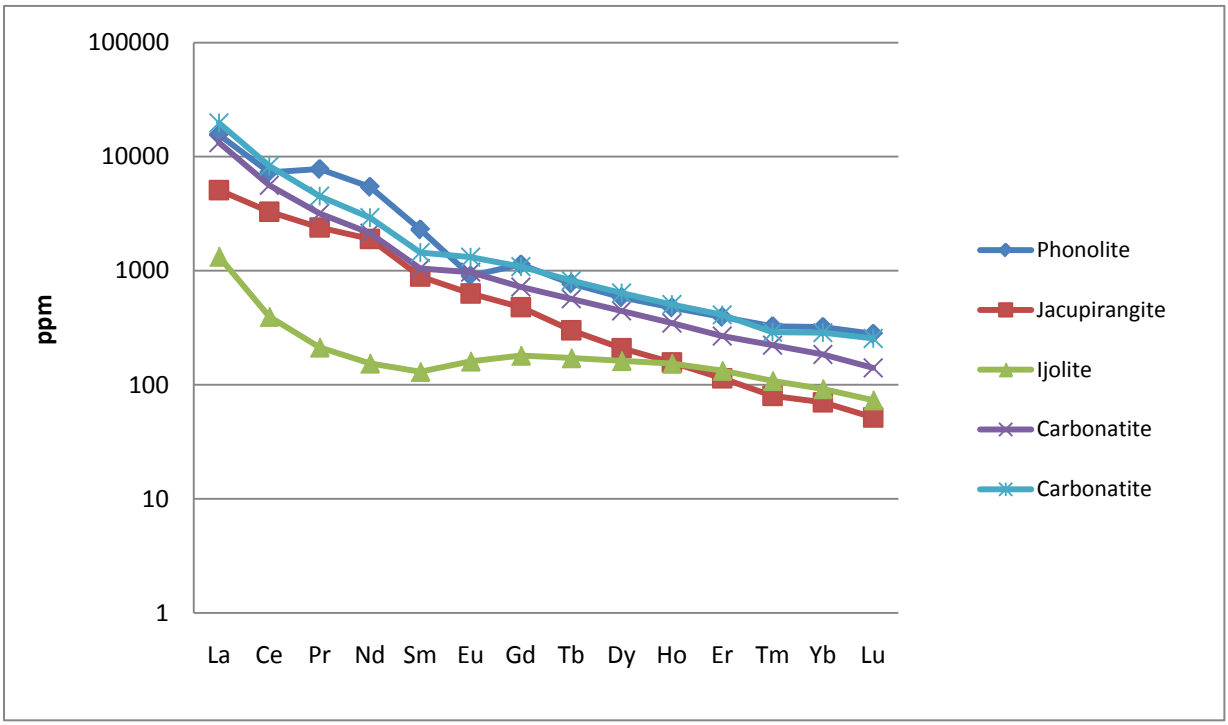

Figure 7. Chondrite-normalized REE showing abnormal kinks within LREE for apatite in all MCIC rock types. (values=averages of all apatite analyses in each rock type)

single cooling body.

REE concentrations were evaluated in apatite from 4 of the 5 MCIC rocks (phonolite, ijolite, jacupirangite, and carbonatite). The syenite sample was extensively altered, and, though it was possible to analyze grains using EPMA, the grains were too small for reliable ICP-MS analysis. Bulk chemical composition of the phonolite is similar to that of the syenite (Erickson and Blade, 1963), and so the syenite apatite compositions can be reasonably assumed to be similar to those in the phonolite, thus effectively representing all compositions within the MCIC sample types.

	ΣLREE	ΣHREE	ΣREE	LREE/HREE
MCIC-1	51974	6620.5	58595	7.8505
MCIC-4	14027	2299.6	16327	6.0998
MCIC-3	1727.6	1010.9	2738.5	1.7090
MCIC-5avg	10238	544.80	10782	18.792

Figure 8. Average REE concentrations for apatite in MCIC rocks (ppm). Rocks listed in order of decreasing age.

Trace and REE concentrations were analyzed using LA-ICP-MS, and yielded total REE concentrations (sum of all REE from La-Lu) ranging from ~500 ppm to multiple weight percent. Erickson and Blade (1963) reported whole-rock La concentrations in all MCIC rocks ranging from ~0.000*n*-0.*n* (*n*=1-9), so it can be plausibly assumed that total REE within the rock types were likely within the same measured order of magnitude concentration as those reported for whole-rock concentrations. There were a few exceptions, notably the whole-rock La concentration of the ijolite; however, analyses of REE-bearing mineral separates from this rock type yielded concentrations of >10% La in most cases. As modal abundances of these high-La minerals in the ijolite were >20% (Erickson and Blade, 1963), it is reasonable to assume that there is an appreciable concentration of REE within the whole rock. Assuming these concentrations, REE in apatite (total concentration as well as LREE/HREE fractionation) can be realistically assumed to be a function of other REE-bearing phases within the rock type.

7.1.1 REE in apatite in specific rock types and influence of mineralogy on concentrations

Trachyte-phonolite: REE-bearing phases in this rock include garnet, titanite, and apatite, with apatite and titanite being the two most abundant minerals in the phonolite (~1 modal % each). Apatite analyzed from the phonolite had the highest REE concentrations (LREE, HREE and total REE) of any of the rock types. Erickson and Blade (1963) considered the phonolite to be one of the oldest of the MCIC rock types, and by their logic (assuming geometry of the complex is correlated with relative age), the phonolite was the oldest rock type analyzed for REE

as part of this study. Thus, it may be possible that these high REE concentrations are reflections of an initially REE-rich magma that has undergone little fractionation due to cooling/crystallization.

Jacupirangite: The jacupirangite contains a large number of REE-bearing phases, the most abundant being apatite, garnet, perovskite and titanite, indicating that REE fractionation may not have occurred on a significant level if the magma had undergone cooling and fractional crystallization (or if another episode of magmatism feeding from the same original magma source had occurred). REE concentrations in apatite were still lower than those in the phonolite (total REE ppm was lower by a factor of ~5). REE-bearing phases make up >10% of the jacupirangite, however, which suggests that whole-rock REE concentrations may be similar to, or even greater than, those of the phonolite.

Biotite ijolite: REE concentrations in apatite within the ijolite were significantly lower than those of the jacupirangite, by a factor of ~8 within LREE, HREE and total REE. This is likely due to very high abundance of garnet in the ijolite (~20 modal %), which likely led to the majority of REE partitioning into garnet. Apatite and perovskite are also present, however, both of these minerals exist at a modal abundance of ~2% each. Thus, REE may still be high in the total rock, but much lower in the apatite due to the presence of abundant garnet.

Carbonatite: The main REE-bearing phase in the carbonatite is apatite, with lesser amounts of perovskite. REE concentrations in apatite as measured by LA-ICP-MS show a sharp increase in comparison to the older rock, the ijolite (as considered by Erickson and Blade, 1963). This may be due to the lack of significant amounts of other phases that take in REE. The LREE/HREE ratio was the highest of all the rock types, which is a chemical signature common to carbonatites (Wooley, 1989).

Considering this, it appears that whole-rock REE concentrations are high throughout all MCIC rock types, but there is nonetheless some decrease overall from the oldest to youngest rocks. The overall high concentrations throughout all rock types indicate that the original source magma for all MCIC rocks was high in REE, and, in spite of the variations in phase abundances within the rock types, it is likely that the differing REE concentrations (and LREE/HREE ratios) may indicate some type of progressive differentiation as well.

7.2 Volatiles

Volatile contents of apatite were determined using EPMA. F and Cl were measured directly, and OH content was calculated using stoichiometric relationships. Fluorine content of apatite decreased, and OH increased, from the outer to inner units of the MCIC (as the rocks decreased in age). Apatite was assumed to be the main F-bearing phase, minimizing the need to consider other minerals when considering F partitioning within the MCIC rock types. This was confirmed by EPMA analysis of biotite contained within the ijolite sample (since micas, as the main hydrous phase in the MCIC rocks other than apatite, could potentially take in halogens in solution with H_2O). Biotite analyzed showed F and Cl levels at or below detection limits. Cl levels were close to the detection limit in apatite, as well, indicating that the system likely contained low levels of Cl overall. The F content in apatite varied from 3.44 to 1.02 wt%, with a systematic decrease in F content as the rocks decreased in age.

7.2.1 Fugacities

Fugacity ratios for HF and HCl (average values shown below) were based on F and Cl concentrations in apatite composition (determined by EPMA analysis for F and Cl concentrations in apatite, and using stoichiometry (for the OH concentration), assuming a filled halogen site). The fugacities calculated ranged over ~2 orders of magnitude, and showed a systematic decrease in both HF and HCl fugacity as the rocks decreased in age (marginal rocks to core rocks). f_{HF}/f_{H2O} ratios started at the same order of magnitude as the f_{HCl}/f_{H2O} ratios, but decreased more rapidly from the oldest to youngest rocks of the MCIC. f_{HF}/f_{H2O} and f_{HCl}/f_{H2O} values both averaged around $1x10^{-5}$ for the syenite and phonolite. In the jacupirangite, f_{HCl}/f_{H2O} was ~$1x10^{-5}$, and f_{HF}/f_{H2O} was ~$1x10^{-6}$. There was an additional order of magnitude decrease in both fugacity ratios in the ijolite and carbonatite, with an order of magnitude difference between f_{HF}/f_{H2O} ($1x10^{-7}$) and f_{HCl}/f_{H2O} ($1x10^{-6}$). Overall, this represented an overall drop of 1 order of magnitude in the f_{HCl}/f_{H2O} ratios from the oldest to youngest rocks, and an overall drop of 2 orders of magnitude in f_{HF}/f_{H2O} as the rocks decreased in age. Though this second drop disagrees with the hypothesis (decreasing f_{HCl}/f_{H2O} will be accompanied by increasing f_{HF}/f_{H2O}), both of these trends in fugacities may represent an overall systematic change in volatile concentrations in the magma over time, as the rocks of the MCIC formed.

	f_{HCl}/f_{H2O}	f_{HF}/f_{H2O}
MCIC-2 (Syenite)	2.6E-05	1.6E-05
MCIC-1 (Phonolite)	3.3E-05	1.6E-05
MCIC-4 (Jacupirangite)	1.4E-05	1.6E-06
MCIC-3 (Ijolite)	5.7E-06	8.1E-07
MCIC-5A (Carbonatite)	2.9E-06	5.0E-07
MCIC-5B (Carbonatite)	3.2E-06	4.5E-07

Figure 9. Average fugacity ratios for MCIC rocks.

8. Methods

8.1 Petrography

Six thin sections were made from the five sampled rock types (two sections were made for the carbonatite, due to heterogeneous distribution of minerals within the sample), and were examined using a petrographic microscope to identify phases and determine petrographic relationships.

Initial phase identification was performed to confirm mineral presences listed by Erickson and Blade (1963). Phase identification also served to locate appropriate crystals for subsequent EPMA analysis. Maps of all sections were created, and later modified to include information and new identifications gathered from EPMA work.

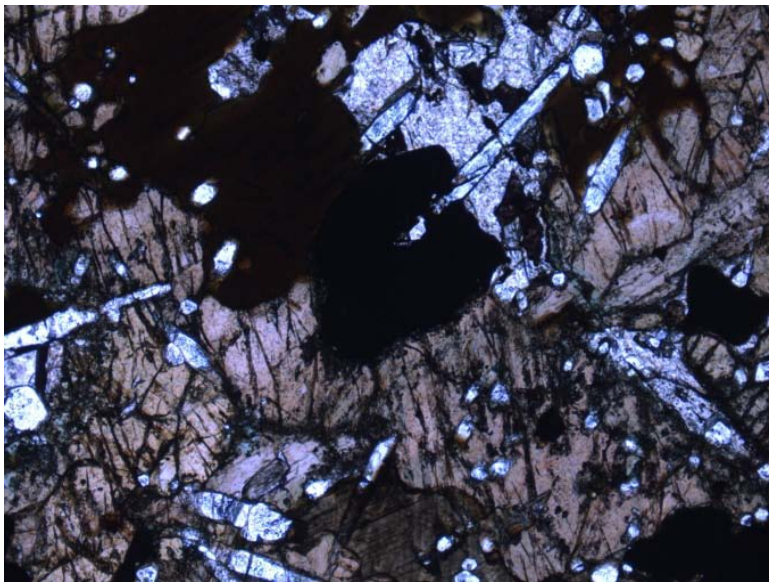

Figure 10. Thin section of jacupirangite showing varying morphologies of apatite (elongate, equant hexagonal), indicating multiple populations of apatite within the same rock type.

Particular care was taken to identify variations in apatite crystal habit, presence of inclusions (or the existence of apatite as an inclusion), and proximity to other hydrous minerals (due to the potential for halogen exchange). Nearly all of the rock types possessed multiple populations of apatite, which were distinguished by bimodal (or, in some cases, more) distribution of typical habits and associations.

8.2 Electron probe microanalysis

Apatite was analyzed for major and minor element composition using a JXA-8900 SuperProbe. Backscatter electron imaging was used to identify phase relationships, followed by energy dispersive spectroscopy and wavelength dispersive spectroscopy to identify phases by chemical composition and measure elemental concentrations, respectively. The following analytical conditions were employed: an accelerating voltage of 15 kV, beam diameter of 10-20 μm, and a cup current of 10 nA. Between10 and15 apatite crystals were analyzed per sample, and other phases (biotite and kimzeyite) were also analyzed in select samples. Apatite was chosen based on petrographic observations of apatite habits and phase relationships. Standards used are listed in Appendix 11.

8.3 Laser ablation-inductively coupled plasma mass spectrometry

Apatite from five thin sections (phonolite, ijolite, jacupirangite, and two carbonatite sections) was analyzed for trace element composition using laser ablation-inductively coupled plasma mass spectrometry (LA-ICP-MS). Between 5 and 12 grains were analyzed using a single collector Element 2 ICP-MS. Analytical conditions were: a laser beam width of between 55 and 6 μm (spot size or line width) and laser pulse frequency of 7 Hz. Elements analyzed on the LA-ICP-MS were Sc, Ti, V, As, Se, Sr, Y, Zr, Nb, Ba, La, Ce, Pr, Nd, Sm, Eu, Gd, Tb, Dy, Ho, Er, Tm, Yb, Lu, Hf, Ta, Pb, Th, and U. Measurements were normalized to Ca. Standards used are listed in Appendix 11.

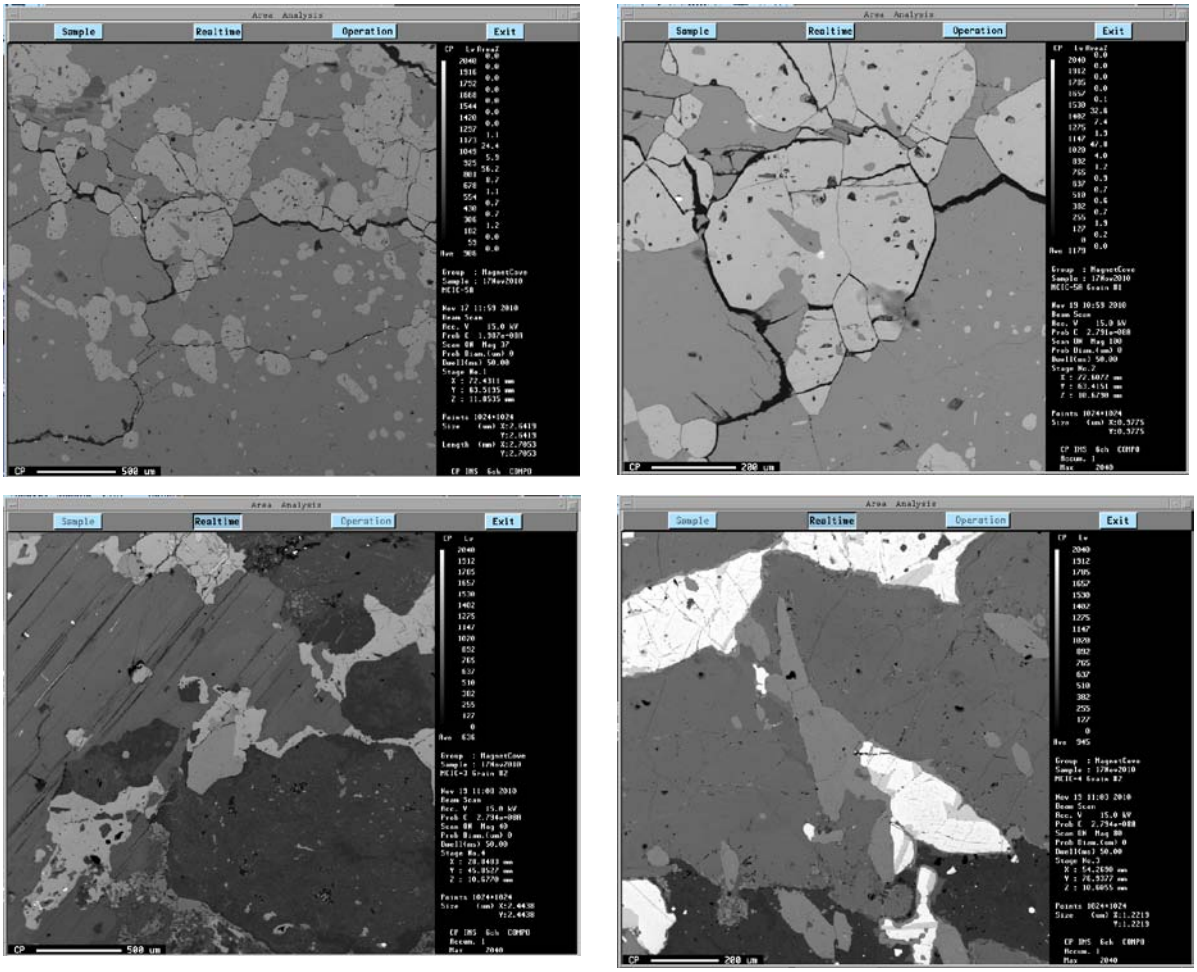

Figure 11. BSE sample images: Upper left: carbonatite with apatite in calcite, upper right: enlarged image of the same carbonatite containing apatite in calcite with magnetite and apatite inclusions, lower left: apatite within diopside and unknown Ca-Al silicate with perovskite reaction rim, lower right: elongate apatite within diopside with magnetite and ilmenite at lower right portion of apatite crystal.

9. Limitations and assumptions

A variety of issues could have potentially presented complications for the successful completion of this project. As part of this work, I assumed that diffusion of the volatiles within apatite, and between volatile-bearing phases, did not change since the crystallization of these phases, and that the volatile concentrations are indicative of those upon crystallization of the phase. It has been reported in the literature (Stormer et al., 1993) that there is difficulty in making accurate measurements of volatile concentrations in apatite, and that measured concentrations are, in part, a function of crystallographic orientation (anisotropy) of the apatite. Several of the more salient issues will be dealt with below.

9.1 Halogen diffusion

Detailed petrography of the samples in thin section allowed determination of phase relationships. In many rocks, minerals contain crystalline inclusions, melt inclusions, and fluid inclusions. The first type of inclusion may potentially be problematic if it is apatite within another mineral that shares certain chemical characteristics. If apatite is included in another mineral that also takes in volatiles, there may be a diffusion relationship between the two that has altered the original F/Cl/OH ratio that existed at the time the apatite formed. For the MCIC rocks, the primary culprit in this issue is phlogopite, another phase common in carbonatites that can take in fluorine, chlorine and water. If diffusion has occurred between the apatite and host phlogopite crystal, then the halogen measurements in that apatite are not reliable indicators of the conditions in the magma at the time the apatite crystallized.

To address this problem, apatite inclusions within minerals that cannot have diffusion relationships (i.e. minerals that do not contain volatiles) were be analyzed for halogen content, and these measurements were compared with those of minerals like phlogopite.

9.2 Crystal anisotropy effect on EPMA measurements

EPMA analysis was the primary mode of measurement of volatiles in apatite. In some cases, the particular orientation of apatite plays a role in the apparent chlorine and fluorine concentration (Stormer et al., 1993). If apatite in a thin section is oriented such that its c-axis is perpendicular to the section, the electron beam from the analyzer may cause anisotropic diffusion of F from the beam on the crystal. This effect is a function of time the beam interacts with the sample. Steps were taken to reduce these effects, including: analyzing the volatiles first in the analytical protocol; using a low cup current (10 nA), and using a wide beam (10-20 μm).

9.3 Accuracy, precision, and error analysis

To address accuracy and precision for analyses from the EPMA, standard X-ray counting statistics were employed to evaluate the uncertainty due to counting statistics. Replicate measurements were made on select samples (where possible) to determine the precision of the analyses. Secondary standards (e.g. synthetic apatite) were measured as unknowns to assess the accuracy. In all cases, standard error propagation techniques were employed.

Accuracy and precision for LA-ICP-MS analysis were accounted for similarly to the methods used for EPMA analysis. Some crystals were subjected to multiple analyses to

determine precision of analysis, and standards were used to assess accuracy. A list of standards used for EPMA and LA-ICP-MS analysis is provided in Appendix 11.

10. Discussion and conclusions

Geochemical data from apatite from the MCIC yielded information about changes in halogen fugacity and fractionation of REE through the cooling history and differentiation of the magma that ultimately formed the MCIC. Overall, fugacities (represented by f_{HF}/f_{H2O} and f_{HCl}/f_{H2O}) for both HF and HCl decreased from the older to younger rocks of the MCIC, representing a gradual decrease in HF and HCl concentrations over the time the MCIC formed. The f_{HF}/f_{H2O} decreased at a more rapid rate than the f_{HCl}/f_{H2O} values. This is in disagreement with the original hypothesis, which stated that f_{HF}/f_{H2O} would increase, while f_{HCl}/f_{H2O} would decrease.

The trace element concentrations in apatite varied significantly between rock types. LREE, HREE and total REE concentrations were initially very high in the oldest rock (totaling several weight percent), and decreased as the relative ages of the rocks decreased, up until the youngest rock type, the carbonatite. The transition between the silicate and carbonate rocks was characterized by a sudden jump in REE concentrations in apatite. Apatite and whole-rock REE concentrations were compared to determine if the values seen were due to mineral fractionation (fractional crystallization, i.e. changing magma composition over time), changes in mineral partitioning (constant source magma over time, with or without multiple separate episodes of magmatism), or both.

However, when considering whole-rock REE along with phases present in rock types, it is important to note that REE levels appear to be fairly high throughout all the rock types, with a similar concentration of total REE partitioned into various minerals, depending on the rock type. This may indicate a high-REE magma with concentrations that persisted throughout the cooling of the magma, and were reflected in whole-rock information combined with modal abundances of all REE-bearing phases in the MCIC rocks.

REE concentrations in apatite appear to be mainly a function of its abundance in comparison with other REE-bearing minerals in each rock type. All rocks in the MCIC have a fairly high level of REE, at least in the hundreds of ppm (Erickson and Blade, 1963). However, phases that can contain REE vary significantly between rock types. The primary phases in the MCIC that contain REE are apatite, perovskite, titanite, and garnet (the MCIC is the type locality of kimzeyite, a Ti-rich garnet that can take in unusually high levels of REE). Modal abundances of these minerals vary significantly between the rock types. All rocks contain appreciable apatite, as well as fairly abundant perovskite (between ~1 and 24 modal percent and $\leq$ 1 modal percent, respectively). Garnet abundance varies significantly, with silicate rock types containing up to 20% garnet. Of note is the fact that in the carbonatite, the only phase present at significant levels that contains REE is apatite. Unlike the silicate rocks, REE in the carbonatite are forced to partition nearly exclusively into apatite, which is the likely cause of the sudden increase in REE concentrations in apatite in the carbonatite. This overall pattern of decrease (as well as the sudden increase in the carbonatite, possibly) suggests that there may be some type of fractional crystallization that occurred, that gradually depleted the magma of REE. The initial

concentrations of REE in apatite in the phonolite, the oldest rock, were high even in comparison with those in the carbonatite. This, coupled with the fact that apatite is essentially the only REE-bearing phase in the carbonatite, suggests that initial REE levels in the earliest stages of crystallization of the MCIC were higher (>50,000 ppm in the apatite alone), and decreased due to fractionation until the whole-rock concentration was much lower (as may be reflected by the REE concentrations in the carbonatite apatite, which are ~10,000 ppm).

Overall, it is likely that the formation of the MCIC was complex, and involved more than one mechanism of differentiation. Information gathered from apatite distributed throughout the MCIC suggests both fractional crystallization and a constant-source magma that may have periodically recharged the shallow intrusion chamber that makes up the bulk of the MCIC rocks. Fugacities and REE concentrations in apatite indicate that some long-term fractionation of a single magma occurred, while comparison of whole-rock REE concentrations, abundance of REE-bearing phases including apatite, and REE within apatite from each rock type indicates that a single, parental magma may have recharged a shallower magma chamber and crystallized out at various times. However, the fact that major elements do vary significantly in whole-rock data from the MCIC rock types, it is unlikely that this process was particularly dominant. The MCIC likely formed from differentiation of magma in a shallow intrusion that was periodically recharged with minor amounts of a parental magma from a deeper source.

Acknowledgements

First and foremost, I would like to thank my thesis advisor, Dr. Phil Piccoli, for his guidance, assistance, and advice throughout this project. I would also like to thank all of my professors who provided advice for this project, in particular, Dr. Phil Candela, Dr. Jay Kaufman, Dr. Sarah Penniston-Dorland, and Dr. Rich Walker. I also owe thanks to Mike Howard of the Arkansas Geological Survey, who collected the samples and provided information for this project. I also thank Dr. Roberta Rudnick, for providing additional samples, and Dr. Bill McDonough, for providing samples and for fostering my initial interest in carbonatites. I owe thanks to Dr. Richard Ash, who patiently worked with me on the ICP-MS analyses for this project. I thank, of course, my fellow seniors, for their unwavering moral support (there you go, Amanda). And, finally, I thank my parents for their support, and their long-sufferingly listening to me talk about carbonatites for the past several semesters.

References

Andersen, T., Austrheim, H., 1991, *Temperature-HF fugacity trends during crystallization of calcite carbonatite magma in the Fen complex, Norway*, Mineralogical Magazine, vol. 55, p. 81-94

Barker, D.S., 1989, *Field relations of carbonatites*, Carbonatites, ch. 3, p. 38-69

Bühn, B., Rankin, A.H., Schneider, J., Dulski, P., 2002, *The nature of orthomagmatic, carbonatitic fluids precipitating REE, Sr-rich fluorite: fluid-inclusion evidence from the Okorusu fluorite deposit, Namibia*, Chemical Geology, vol. 186, p. 75-98

Conway, C.M., Taylor, H.P., 1969, *$^{18}O/^{16}O$ and $^{13}C/^{12}C$ Ratios of Coexisting Minerals in the Oka and Magnet Cove Carbonatite Bodies*, Journal of Geology, vol. 77, no. 5, p. 618-626

Dalou, C., Koga, K.T., Hammouda, T., Poitrasson, F., 2009, *Trace element partitioning between carbonatitic melts and mantle transition zone minerals: Implications for the source of carbonatites*, Geochimica et Cosmochimica Acta, vol. 73, p. 239-255

Erickson, R.L., Blade, L.V., 1963, *Geochemistry and Petrology of the Alkalic Igneous Complex at Magnet Cove, Arkansas*, United States Geological Survey Professional Paper 425

Fischer, T.P., Burnard, P., Marty, B., Hilton, D.R., Füri, E., Palhol, F., Sharp, Z.D., Mangasini, F., 2009, *Upper-mantle volatile chemistry at Oldoinyo Lengai volcano and the origin of carbonatites*, Nature, vol. 459, p. 77-80

Gaillard, F., Malki, M., Iacono-Marziano, G., Pinchavant, M., Scaillet, B., 2008, *Small Amount of Carbonatite Melts Explains High Electrical Conductivity in the Asthenosphere*, Science, vol. 322, p. 1363-1365

Hamilton, E.I., Deans, T., 1963, *Isotopic Composition of Strontium in some African Carbonatites and Limestones and in Strontium Minerals*, Nature, vol. 198, p. 776-777

Hammouda, T., Laporte, D., 2000, *Ultrafast mantle impregnation by carbonatite melts*, Geology, vol. 28, no. 3, p. 283-285

Hammouda , T., Chantel, J., Devidal, J-L., 2010, *Apatite solubility in carbonatitic liquids and trace element partitioning between apatite and carbonatite at high pressure*, Geochimica et Cosmochimica Acta (in review)

Haynes, E.A., Moecher, D.P., Spicuzza, M.J., *Oxygen isotope composition of carbonates, silicates, and oxides in selected carbonatites: constraints on crystallization temperatures of carbonatite magmas*, Chemical Geology, vol. 193, p. 43-57

Howard, J.M., Chandler, A., 2007, *Magnet Cove: A synopsis of its geology, lithology, and mineralogy*, AGES Brochure Series 004, p. 1-11

Jago, B.C., Gittins, J., 1991, *The role of fluorine in carbonatite magma evolution*, Nature, vol. 349, p. 56-58

Keller, J., Klaudius, J., Kervyn, M., Ernst, G.G.J., Mattsson, H.B., 2010, *Fundamental changes in the activity of the natrocarbonatite volcano Oldoinyo Lengai, Tanzania*, Bulletin of Volcanology, vol. 72, p. 893-912

Kervyn, M., Ernst, G.G.J., Keller, J., Vaughan, R.G., Klaudius, J., Pradal, E., Belton, F., Mattsson, H.B., Mbede, E., Jacobs, P., 2010, *Fundamental changes in the activity of the natrocarbonatite volcano Oldoinyo Lengai, Tanzania, II. Eruptive behaviour during the 2007-2008 explosive eruptions*, Bulletin of Volcanology, vol. 72, p. 913-931

Krafft, M., Keller, J., 1989, *Temperature Measurements in Carbonatite Lava Lakes and Flows from Oldoinyo Lengai, Tanzania*, Science, vol. 245, no. 4914, p. 168-170

Piccoli, P., Candela, P., 1994, *Apatite in felsic rocks: A model for the estimation of initial halogen concentrations in the Bishop Tuff (Long Valley) and Tuolumne Intrusive Suite (Sierra Nevada batholith) magmas*, American Journal of Science, vol. 294, p. 92-135

Piccoli, P.M., Candela, P.A., 2002, *Apatite in Igneous Systems*, Phosphates: Geochemical, Geobiological and Materials Importance, Reviews in Mineralogy and Geochemistry, vol. 48, p. 1-27

Pinkerton, H., Norton, G.E., Dawson, J.B., Pyle, D.M., 1991, *Field Observations and Measurements of the Physical Properties of Oldoinyo Lengai Alkali Carbonatite Lavas, November 1988*, IAVCEI Proceedings in Volcanology 4, Carbonatite Volcanism: Oldoinyo Lengai and the Petrogenesis of Natrocarbonatites, p.23-36

Powell, J.L., Hurley, P.M., Fairbarn, H.W., 1962, *Isotopic Composition of Strontium in Carbonatites*, Nature, vol. 196, p. 1085-1086

Santos, R.V., Clayton, R.N., 1995, *Variations of oxygen and carbon isotopes in carbonatites: A study of Brazilian alkaline complexes*, Geochimica et Cosmochimica Acta, vol. 59, no. 7, p. 1339-1352

Stormer, J.C., Pierson, M.L., Tacker, R.C., 1993, *Variation of F and Cl X-ray intensity due to anisotropic diffusion in apatite during electron microprobe analysis*, American Mineralogist, vol. 78, p. 641-648

Walker, R.J., Hanson, G.N., Papike, J.J., O'Neil, J.R., Laul, J.C., 1986, *Internal evolution of the Tin Mountain pegmatite, Black Hills, South Dakota*, The American Mineralogist, vol. 71, p. 440-459

Watson, E.B., *Apatite saturation in basic to intermediate magmas*, 1979, Geophysical Research Letters, vol. 6, p. 937-940

Wooley, A.R., Kempe, D.R.C., 1989, *Carbonatites: Nomenclature, average chemical compositions, and element distribution*, Carbonatites, ch. 1, p. 1-14

Zaitsev, A.N., Keller, J., 2006, *Mineralogical and chemical transformation of Oldoinyo Lengai natrocarbonatites, Tanzania*, Lithos, vol. 91, p. 191-207

Appendix 1

List of figures

Appendix 2

Magnet Cove Igneous Complex sample mineralogy (detailed)

Phases identified through use of EPMA are in bold.

Trachyte-phonolite: Feldspar (sodic orthoclase, albite/andesine), **nepheline**, analcime, sodalite, **pyroxene (diopside-hegenbergite, aegirine-diopside)**, biotite, garnet, hornblende, titanite, **magnetite**-ilmenite, pyrite, pyrrhotite, **apatite**, fluorite

Garnet pseudoleucite nepheline syenite: Pseudoleucite (myrmeketic orthoclase and nepheline), feldspar (sodic orthoclase), Ti-garnet, pyroxene (diopside-hedenbergite, aegirine-augite), apatite, nepheline

Carbonatite: **Calcite**, **Nb-perovskite**, **kimzeyite (Zr-garnet)**, **apatite** (residual and primary), **magnetite**

Jacupirangite: >50% **pyroxene**, **magnetite**-ilmenite, **apatite**, biotite, **titanite**, garnet, **perovskite**

Biotite ijolite: Nepheline, **pyroxene (diopside)**, Ti-garnet, **apatite**, biotite, **magnetite**

All data is from USGS Professional Paper 425 (Erickson and Blade, 1963)

Appendix 3

Simplified geologic map of the Magnet Cove Igneous Complex with sample locations (after Ausburn, 2006)

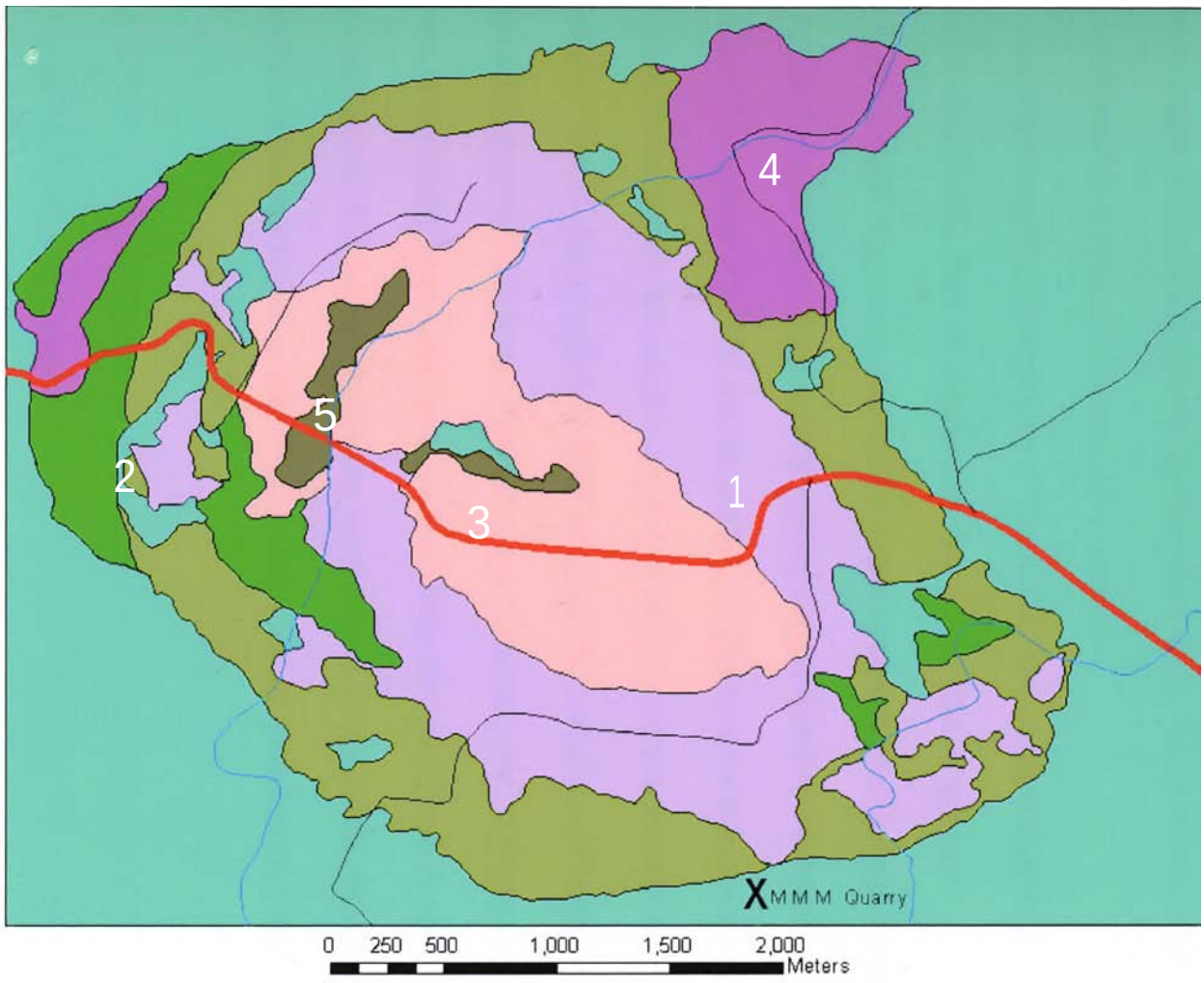

1) Trachyte-phonolite (sample location coordinates: 34.45376, -92.85434)
2) Garnet pseudoleucite nepheline syenite (sample location coordinates: 34.45530, -92.88400)
3) Biotite ijolite (sample location coordinates: 34.45248, -92.86485)
4) Jacupirangite (sample location coordinates: 34.46941, -92.84909)
5) Carbonatite (sample location coordinates: 34.45753, -92.87541)

Appendix 4

MCIC Sample Bulk Chemistry (Data from Erickson and Blade, 1963)

Garnet pseudoleucite nepheline syenite																				
Sample	SiO2	Al2O3	Fe2O3	FeO	MnO	MgO	CaO	BaO	Na2O	K2O	H2O-	H2O+	TiO2	CO2	P2O5	SO3	Cl	F	S
MC-111	49.43	20.17	4.00	1.71	0.32	0.64	5.08	0.27	8.30	6.19	0.10	1.73	0.63	0.96	0.13	0.13	0.08	0.20	0.03
MC-121	47.31	20.10	3.57	2.62	0.30	0.89	6.67	0.36	7.98	6.50	0.10	1.42	0.88	1.07	0.21	0.01	0.04	0.19	0.06
Avg	48.37	20.14	3.79	2.17	0.31	0.77	5.88	0.32	8.14	6.35	0.10	1.58	0.76	1.02	0.17	0.07	0.06	0.20	0.05
Jacupirangite																			
Sample	SiO2	Al2O3	Fe2O3	FeO	MnO	MgO	CaO	BaO	Na2O	K2O	H2O-	H2O+	TiO2	CO2	P2O5	SO3	Cl	F	S
MC-173	35.42	9.21	8.94	7.17	0.29	7.77	20.83	0.00	1.47	0.62	0.11	1.05	4.05	0.11	2.23	0.12	0.02	0.17	0.38
Trachyte-phonolite																			
Sample	SiO2	Al2O3	Fe2O3	FeO	MnO	MgO	CaO	BaO	Na2O	K2O	H2O-	H2O+	TiO2	CO2	P2O5	SO3	Cl	F	S
MC-170	52.60	22.18	0.29	3.83	0.27	0.33	3.67	0.29	5.61	7.41	0.10	1.61	0.71	0.00	0.07	0.11	0.00	0.36	1.02
MC-227	50.48	20.98	2.29	5.16	0.29	1.65	5.11	0.18	5.96	3.39	0.11	0.99	2.21	0.31	0.37	0.01	0.00	0.35	0.36
MC-171	49.62	19.13	1.04	5.59	0.23	1.68	6.52	0.14	6.93	4.81	0.07	0.63	1.97	0.05	0.38	0.10	0.25	0.22	1.57
Avg	50.90	20.76	1.21	4.86	0.26	1.22	5.10	0.20	6.17	5.20	0.09	1.08	1.63	0.12	0.27	0.07	0.08	0.31	0.98
Biotite ijolite																			
Sample	SiO2	Al2O3	Fe2O3	FeO	MnO	MgO	CaO	BaO	Na2O	K2O	H2O-	H2O+	TiO2	CO2	P2O5	SO3	Cl	F	S
MC-216	35.46	18.60	7.90	3.27	0.25	4.16	12.66	0.10	6.34	3.07	0.33	3.46	2.47	0.17	1.08	0.03	0.00	0.16	0.97
Carbonatite																			
Sample	SiO2	Al2O3	Fe2O3	FeO	MnO	MgO	CaO	BaO	Na2O	K2O	H2O-	H2O+	TiO2	CO2	P2O5	SO3	Cl	F	S
L-304	1.90	0.33	0.42	0.32	0.26	1.05	53.37	0.00	0.00	0.16	0.04	0.12	0.10	39.41	2.00	0.02	0.00	0.15	0.09

Appendix 5

Elemental concentrations in MCIC apatite (All values listed as weight %)

MCIC-1 (Trachyte-phonolite)

F	Cl	Na2O	FeO	P2O5	SO3	SrO	MnO	SiO2	CaO	La2O3	Ce2O3	Pr2O3	Nd2O3	Sm2O3	Total	Comment
3.3655	0.0111	0.0097	1.2072	40.0234	0.7752	0.1973	0.0806	0.4894	54.2812	0.1597	0.3115	0.0326	0.2183	0.0041	99.7472	MCIC-1 Phonolite Grain #2 core
3.3504	0.0102	0.0310	0.5775	40.2771	0.4766	0.2152	0.1296	0.6458	54.4659	0.2659	0.3448	0.0160	0.2627	0	99.6558	MCIC-1 Phonolite Grain #2 core
3.2827	0.0019	0.1187	0.7264	39.8331	0.3141	0.0726	0.0570	0.6471	53.2162	0.6529	1.0571	0.1692	0.4889	0	99.2553	MCIC-1 Phonolite Grain #2 rim
3.4641	0.0078	0.0560	0.3420	39.7836	0.2094	0.0549	0.0275	0.6225	54.0259	0.8027	1.5268	0	0.4736	0	99.9365	MCIC-1 Phonolite Grain #2 rim
3.2636	0.0126	0.0319	0.2508	38.3385	0.1149	0.1485	0.0540	0.1337	56.5269	0.1331	0.2098	0	0.2627	0.0893	98.1935	MCIC-1 Phonolite Grain #4 core
2.9985	0.0147	0.0308	0.3758	41.0379	0.1441	0.1725	0.0662	0.0928	57.0312	0.1504	0.0944	0.1937	0.2029	0	101.3400	MCIC-1 Phonolite Grain #4 core
3.4058	0.0205	0.0375	0.4259	40.5337	0.0898	0.1459	0.0717	0.3901	56.9186	0	0.2703	0	0.1536	0.1174	101.1422	MCIC-1 Phonolite Grain #4 rim
3.4071	0.0123	0.0754	1.4502	39.5317	0.7801	0.0970	0.0630	0.2251	55.5489	0.4143	0.6793	0.1289	0.2021	0.0647	101.2426	MCIC-1 Phonolite Grain #4 rim
3.1922	0	0.0601	0.7171	39.4598	0.0103	0.0367	0.0489	0.5542	54.5213	0.7051	1.2778	0.3779	0.4636	0	100.0808	MCIC-1 Phonolite Grain #5 small
3.2691	0.0135	0.0923	1.0102	39.3146	0.4109	0.1257	0.0833	0.4715	53.6560	0.5652	1.0573	0.2257	0.2468	0	99.1627	Line 1 MCIC-1 Phonolite Grain #6 Trav
3.1517	0.0127	0.1209	0.9778	39.6265	0.6184	0.0687	0.0588	0.7048	52.8831	0.9002	1.3399	0.3709	0.5135	0	100.0179	Line 2 MCIC-1 Phonolite Grain #6 Trav
3.0270	0.0182	0.1803	0.7384	37.6408	0.3703	0.0238	0	4.5792	50.2300	0.4519	1.2237	0.0160	0.2580	0	97.4791	Line 3 MCIC-1 Phonolite Grain #6 Trav
3.1924	0.0176	0.0110	1.8370	39.6815	1.2778	0.0535	0	0.5099	52.4256	0.8143	1.2630	0.0888	0.4408	0.0894	100.3543	Line 4 MCIC-1 Phonolite Grain #6 Trav
3.1939	0.0139	0.1774	0.3023	40.3456	0.2390	0.0565	0.0998	0.3167	53.6955	0.5239	1.0367	0.0812	0.4076	0	99.1422	Line 5 MCIC-1 Phonolite Grain #6 Trav
2.8831	0.0095	0.0242	0.3783	40.9025	0.1621	0.0772	0.0000	0.0118	54.4503	0.1603	0.3396	0.1949	0.1247	0.1345	98.6371	MCIC-1 Phonolite Grain #8 Core
2.9082	0.0099	0.0078	0.6635	40.8918	0.3519	0.0996	0.0314	0	55.2033	0.3468	0.7597	0.3406	0.0895	0.1057	100.5829	MCIC-1 Phonolite Grain #8 Core
2.9118	0.0104	0.1143	0.4158	41.1053	0.1950	0.1110	0.0098	0	54.7921	0.2643	0.6046	0.0000	0.1871	0.0443	99.5375	MCIC-1 Phonolite Grain #8 Rim
3.0602	0.0159	0.1565	0.3478	41.2827	0.1706	0.1292	0.1173	0.0696	53.2019	0.3155	0.7889	0.1439	0.2404	0.2569	99.0052	MCIC-1 Phonolite Grain #8 Rim
2.9838	0.0156	0.0575	0.1902	40.1881	0.1868	0.1308	0.1159	0.2928	51.1073	0.4027	0.7077	0.2313	0.2056	0	95.5564	MCIC-1 Phonolite Grain #9 Core
3.0147	0.0108	0.0297	0.1652	40.2880	0.1049	0.1090	0.0903	0.1859	51.8274	0.3058	0.8335	0.1995	0.3325	0	96.2256	MCIC-1 Phonolite Grain #9 Core
3.0000	0.0009	0.0000	0.4620	40.6589	0.2319	0.0917	0.0375	0.2890	52.6202	0.5932	0.9517	0.0955	0.3369	0	98.1061	MCIC-1 Phonolite Grain #9 rim
3.0559	0.0055	0.1151	0.3545	40.4490	0.1796	0.1354	0	0.2745	51.9003	0.7676	0.6718	0.0559	0.2538	0	96.9311	MCIC-1 Phonolite Grain #9 rim
3.1827	0.0123	0.1213	0.5361	40.7071	0.2887	0.1949	0.0702	0.2550	53.5622	0.4102	0.5127	0	0.1369	0	98.6475	MCIC-1 Phonolite Grain #10 Core
3.4676	0.0092	0.0240	0.6346	40.0226	0.1967	0.1253	0.0478	0.4513	52.8099	0.5581	0.6117	0.0158	0.3708	0.0999	97.9833	MCIC-1 Phonolite Grain #10 Core
2.9585	0.0047	0.0468	0.3052	40.3702	0.1154	0.1374	0.0672	0.1864	53.2192	0.5592	0.4597	0	0.1613	0.0559	97.4004	MCIC-1 Phonolite Grain #10 rim
3.7431	0.0075	0.0568	0.4202	40.1894	0.1824	0.1457	0.1385	0.2857	54.0632	0.4619	1.0443	0	0.1902	0.1238	99.4751	MCIC-1 Phonolite Grain #10 rim

MCIC-2 (Garnet pseudoleucite nepheline syenite)

F	Cl	Na2O	FeO	P2O5	SO3	SrO	MnO	SiO2	CaO	La2O3	Ce2O3	Pr2O3	Nd2O3	Sm2O3	Total	Comment
3.1468	0.0006	0.0836	0.1149	41.0077	0.0088	3.6602	0.0567	0	51.8036	0	0.2855	0.1270	0	0	98.9704	MCIC-2 Syenite Grain #1
3.4227	0.0035	0.0086	0.0415	40.9631	0.0109	2.1194	0.1400	0	53.2738	0.3602	0.6504	0.0399	0.2115	0	99.8036	MCIC-2 Syenite Grain #2
3.3218	0.0037	0.1694	0	40.7763	0.0425	3.8718	0.1082	0	51.4195	0.3858	0.6692	0.2241	0.0589	0.1163	99.7681	MCIC-2 Syenite Grain #3
3.3072	0.0140	0.1727	0.0746	38.9950	0.0254	3.7926	0.1686	0	51.4524	0.1055	0.5498	0	0	0	97.2621	MCIC-2 Syenite Grain #4
3.8811	0.0040	0.0847	0	41.6350	0.0110	2.2186	0.1052	0	54.6759	0	0.4553	0	0.1474	0.1367	101.7198	MCIC-2 Syenite Grain #5
2.9614	0.0023	0.1441	0.0249	41.2017	0.0283	3.5283	0.1588	0	54.1619	0.3073	0.5559	0	0.0442	0.0885	101.9601	MCIC-2 Syenite Grain #6
3.2440	0.0047	0.0832	0.0992	40.1091	0.0106	2.7447	0	0.6397	53.6820	1.0238	1.2814	0.0081	0.1028	0	101.6663	MCIC-2 Syenite Grain #7
3.3084	0.0049	0.0865	0.0249	41.9305	0.0032	1.6915	0.0859	0	55.7378	0.0882	0.0673	0	0.1181	0	101.7531	MCIC-2 Syenite Grain #8
3.7015	0.0088	0.2149	0.2809	41.4123	0.0049	3.7503	0.0710	0	53.8488	0.1750	0.2004	0.1279	0.0050	0.2364	102.4775	MCIC-2 Syenite Grain #9
4.1220	0.0039	0.2241	0.4294	41.5631	0.0146	3.7343	0.1182	0	53.2336	0.3499	0.6935	0	0.0490	0.1201	102.9191	MCIC-2 Syenite Grain #10

MCIC-3 (Biotite ijolite, part 1)

F	Cl	Na2O	FeO	P2O5	SO3	SrO	MnO	SiO2	CaO	La2O3	Ce2O3	Pr2O3	Nd2O3	Sm2O3	Total	Comment
1.4931	0.0135	0	0	40.9495	0.2669	0.5902	0	0.3075	55.3643	0	0	0.0159	0	0.1169	98.4862	MCIC-3 Apt1 core
1.4555	0.0141	0	0	40.8582	0.2384	0.6002	0.0394	0.2955	54.9016	0	0.0610	0.1860	0.0200	0.0568	98.1107	MCIC-3 Apt1 core
1.3798	0.0067	0.0412	0	40.6341	0.2371	0.6438	0.0247	0.2164	53.9293	0.2854	0.1907	0	0.0099	0.0938	97.1105	MCIC-3 Apt1 Rim adj pyx
1.5849	0.0121	0.0067	0	40.4018	0.2181	0.6668	0.0704	0.2468	53.4366	0	0	0	0	0	95.9743	MCIC-3 Apt1 Rim adj pyx
1.6624	0.0131	0.0200	0.0672	40.6923	0.2447	0.6003	0	0.2464	53.8493	0	0	0	0.0649	0	96.7577	MCIC-3 Apt1 Rim adj CaAlSi
1.5705	0.0147	0.0267	0.0587	40.7482	0.2599	0.596	0.0481	0.2994	54.9143	0.0443	0.0746	0.0891	0.0349	0	98.1149	MCIC-3 Apt1 Rim adj CaAlSi
1.5321	0.0154	0.0105	0.0084	40.6306	0.2872	0.559	0.0246	0.2368	54.2603	0	0	0.2430	0.0397	0.1098	97.3089	MCIC-3 Apt2 Core
1.5243	0.0131	0.0306	0	41.0073	0.2569	0.5548	0.0326	0.3276	53.7313	0.3024	0	0	0.1441	0	97.2802	MCIC-3 Apt2 Core
1.546	0.0156	0	0	41.0515	0.2395	0.5901	0	0.2353	54.1524	0	0	0	0	0.1953	97.3713	MCIC-3 Apt2 Rim adj pyx
1.4876	0.0171	0.0334	0.0837	40.7086	0.2537	0.5634	0.0215	0.2248	53.8982	0.0176	0.1695	0.0728	0.1043	0	97.026	MCIC-3 Apt2 Rim adj pyx
1.6474	0.0111	0	0.0670	40.5612	0.2259	0.5421	0	0.3211	54.3794	0.0176	0.1354	0	0.164	0	97.3762	MCIC-3 Apt2 Rim adj CaAlSi
1.6133	0.0111	0	0	40.78	0.2288	0.5316	0	0.3729	54.3851	0	0.0948	0.0403	0.0247	0.0773	97.4782	MCIC-3 Apt2 Rim adj CaAlSi
1.5672	0.0126	0	0.0502	40.1696	0.2769	0.6576	0.0510	0.3847	55.0325	0.2932	0	0.0486	0.1043	0	97.9858	MCIC-3 Apt3 Core
1.5084	0.0186	0	0.0084	40.113	0.2507	0.6466	0.0351	0.3155	55.6027	0	0.0745	0	0.0149	0	97.9492	MCIC-3 Apt3 Core
1.611	0.016	0.0391	0.0168	40.5952	0.2665	0.5103	0	0.2594	55.115	0.1424	0.2167	0	0	0.0488	98.1553	MCIC-3 Apt3 Rim
1.6051	0.0099	0	0	40.5739	0.3245	0.5378	0.0394	0.3314	55.8738	0.0624	0	0.0811	0.0746	0.0202	98.8562	MCIC-3 Apt3 Rim
1.7265	0.0133	0.0029	0.0754	40.4098	0.2424	0.6242	0	0.3662	55.9732	0	0	0	0	0.0202	98.7243	MCIC-3 Apt4 Core
1.639	0.0086	0	0.0419	40.4821	0.2753	0.5521	0.0344	0.2769	56.0963	0.1776	0	0	0.0447	0.0366	98.9735	MCIC-3 Apt4 Core
1.6317	0.0144	0.0191	0.1089	40.604	0.2861	0.5319	0.0351	0.3587	56.2757	0.2224	0	0	0	0	99.3979	MCIC-3 Apt4 Rim
1.5899	0.0161	0	0	40.6338	0.2814	0.5492	0.0221	0.3953	56.3447	0.0091	0	0.0889	0	0.1383	99.3959	MCIC-3 Apt4 Rim
1.8022	0.0005	0.0362	0	41.473	0.1582	2.4773	0	0	55.3067	0.0533	0.0812	0	0	0	100.6296	MCIC-3 Apt5 Core
1.6329	0.0145	0	0.0336	40.6864	0.2623	0.589	0.0358	0.3202	57.0562	0.1512	0	0.1056	0.0648	0.1424	100.404	MCIC-3 Apt5 Core
1.5974	0.0231	0.0153	0.0336	40.6853	0.2743	0.5618	0	0.3794	56.7429	0	0	0.2193	0	0.0937	99.9483	MCIC-3 Apt5 Rim
1.6267	0.0124	0.0277	0	40.6589	0.248	0.7787	0.0327	0.2457	56.3237	0	0.0339	0.0327	0.0299	0.1305	99.4939	MCIC-3 Apt5 Rim
1.5544	0.017	0.0259	0.0084	40.7456	0.2425	0.6692	0.0383	0.4116	56.2218	0.2052	0.1022	0	0	0.0448	99.6287	MCIC-3 Apt6 (in Perovskite) Core
1.5506	0.0171	0.024	0.0505	40.7555	0.2185	0.5942	0.0402	0.3448	56.786	0	0.1706	0.1305	0	0.0204	100.046	MCIC-3 Apt6 (in Perovskite) Core
1.6954	0.0174	0.0452	0.0421	40.3771	0.1948	0.6512	0	0.332	55.4146	0.1609	0	0.2281	0	0.0081	98.4492	MCIC-3 Apt6 (in Perovskite) Rim
1.6391	0.0142	0.0125	0.0337	40.3154	0.2208	0.6352	0	0.3015	55.2838	0	0.1158	0.0572	0.03	0.0939	98.0598	MCIC-3 Apt6 (in Perovskite) Rim
1.3577	0.0305	0	0	30.5544	0.1766	1.3885	0	0	37.3129	0.1779	0.0542	0.0083	0	0.1020	70.5845	MCIC-3 Apt7 Core
1.4932	0.0119	0.0632	0	41.0891	0.1864	0.6554	0.0414	0.2298	52.4564	0.3037	0.0339	0.0571	0.03	0.0654	96.0856	MCIC-3 Apt7 Core
1.5047	0.0089	0.0315	0.0589	41.5418	0.1714	1.0276	0	0.0918	53.8973	0.0091	0.0887	0.0571	0	0.0245	97.8778	MCIC-3 Apt7 Rim
1.4204	0.0209	0.0239	0	40.9974	0.1772	0.6628	0.0594	0.2333	54.1758	0.0628	0	0.0977	0	0	97.3288	MCIC-3 Apt7 Rim
1.6637	0.0064	0.0587	0.1011	40.8216	0.1842	1.0685	0	0.0337	54.6683	0.1968	0.0613	0.1793	0	0	98.3418	MCIC-3 Apt8 Rim --> Core --> Rim
1.6256	0.0073	0.023	0.0421	41.0159	0.2397	1.4093	0	0.1018	54.0717	0.2141	0.1359	0	0.2095	0.0286	98.4385	MCIC-3 Apt8 Rim --> Core --> Rim
1.5567	0.0053	0.0518	0	40.5318	0.267	0.7412	0	0.3225	54.6612	0.0627	0.0409	0.2198	0.1100	0	97.9143	MCIC-3 Apt8 Rim --> Core --> Rim
1.4083	0.012	0.0153	0.0084	40.9473	0.2388	0.6224	0.0006	0.3626	55.3744	0	0	0	0	0.0736	98.468	MCIC-3 Apt8 Rim --> Core --> Rim
1.5023	0.0163	0.0374	0.0590	40.5982	0.2674	0.4129	0.0600	0.2773	55.3957	0	0.2864	0.0650	0	0.0164	98.3582	MCIC-3 Apt8 Rim --> Core --> Rim
1.3617	0.0139	0.0316	0	40.708	0.2303	0.6371	0.0093	0.2552	54.8471	0.1073	0.1158	0.1305	0	0	97.8715	MCIC-3 Apt8 Rim --> Core --> Rim
1.3825	0.01	0.0095	0	40.9407	0.2405	0.5651	0	0.2933	55.3387	0	0.0818	0	0.0150	0	98.2928	MCIC-3 Apt8 Rim --> Core --> Rim
1.4165	0.0094	0	0.0667	40.8851	0.2587	0.5313	0.0172	0.3464	55.2856	0.1151	0	0.2016	0.0246	0	98.5597	MCIC-3 Apt8 Rim --> Core --> Rim
1.2976	0.0091	0.0293	0	40.6323	0.3149	0.5187	0	0.4269	54.8546	0.0355	0.1950	0	0.0296	0	97.7951	MCIC-3 Apt9 Core
1.2776	0.0076	0.0340	0.0166	40.4638	0.3388	0.5284	0.0299	0.4249	54.9519	0.1146	0	0	0.1624	0	97.811	MCIC-3 Apt9 Core
1.317	0.0159	0	0.1077	41.0114	0.3026	0.6206	0.0103	0.3074	54.2305	0	0	0.2162	0.0787	0.0562	97.7164	MCIC-3 Apt9 Rim
1.326	0.0153	0.0038	0.0414	41.6217	0.2905	0.5898	0.0201	0.3472	54.1462	0.1491	0	0.0960	0	0.0441	98.1294	MCIC-3 Apt9 Rim

MCIC-3 Biotite ijolite, part 2)

F	Cl	Na2O	FeO	P2O5	SO3	SrO	MnO	SiO2	CaO	La2O3	Ce2O3	Pr2O3	Nd2O3	Sm2O3	Total	Comment
1.452	0.0099	0.0282	0.0248	40.9575	0.234	0.6875	0.0273	0.2462	54.6741	0	0.1136	0	0.103	0	97.9446	Line 1 MCIC 3 Apt 10 core-->rim-->core
1.3958	0.0194	0.0084	0	40.8684	0.2544	0.6566	0.0061	0.2715	55.1732	0	0.0936	0	0	0	98.1553	Line 2 MCIC 3 Apt 10 core-->rim-->core
1.4002	0.0177	0.0357	0	40.6006	0.2929	0.5693	0	0.2534	54.8988	0	0	0	0	0	97.4751	Line 3 MCIC 3 Apt 10 core-->rim-->core
1.4555	0.0092	0.0366	0.1240	40.9352	0.2394	0.3914	0	0.3155	54.819	0.0963	0.0534	0	0	0.0561	97.9167	Line 4 MCIC 3 Apt 10 core-->rim-->core
1.3825	0.0121	0.0037	0.0909	40.5543	0.2678	0.6246	0.0680	0.3263	54.513	0	0.0602	0	0	0.1282	97.4469	Line 5 MCIC 3 Apt 10 core-->rim-->core
1.3544	0.0109	0.0019	0.0165	40.4367	0.2995	0.5750	0.0103	0.3162	54.7039	0	0	0	0.005	0.1124	97.2699	Line 6 MCIC 3 Apt 10 core-->rim-->core
1.3601	0.0099	0.0216	0	40.6245	0.2825	0.6133	0.0400	0.3494	54.4901	0	0.0534	0.0321	0	0	97.3021	Line 7 MCIC 3 Apt 10 core-->rim-->core
1.3899	0.0194	0.0169	0.0165	40.9969	0.2997	0.5633	0.0121	0.2886	54.3685	0	0	0	0	0.1203	97.5026	Line 8 MCIC 3 Apt 10 core-->rim-->core
1.4065	0.0201	0.0376	0	41.0548	0.2849	0.5879	0.0860	0.2998	54.4503	0.1485	0.0801	0.1354	0.1565	0.176	98.3278	Line 9 MCIC 3 Apt 10 core-->rim-->core
1.3973	0.0182	0.0141	0.0908	41.2232	0.259	0.5787	0	0.2984	54.2937	0	0.0469	0.0799	0.0978	0	97.8057	Line 10 MCIC 3 Apt 10 core-->rim-->core
1.5293	0.0166	0.0113	0.0413	40.556	0.2461	0.6121	0.0661	0.2963	54.1114	0	0.1202	0.0479	0	0	97.007	MCIC-3 Apt11 Core
1.5754	0.0143	0.0187	0	40.9222	0.2815	0.5781	0	0.2872	54.746	0.0352	0	0	0	0	97.7922	MCIC-3 Apt11 Core
1.5472	0.0158	0.0366	0.2064	40.7162	0.2819	0.518	0.0194	0.3207	54.4207	0	0	0	0.0391	0	97.467	MCIC-3 Apt11 Rim
1.5718	0.0220	0	0.0991	40.8805	0.2378	0.5142	0	0.2344	54.6121	0.0089	0	0	0.0932	0	97.6073	MCIC-3 Apt11 Rim
1.3294	0.0192	0.0206	0.0413	40.7605	0.3462	0.5433	0.1164	0.3044	53.2189	0	0	0	0	0.0481	96.1844	MCIC-3 Apt12 Core
1.3463	0.0107	0.0468	0.0165	40.717	0.3182	0.5515	0.0218	0.3171	53.3022	0	0.1533	0	0.0244	0.0799	96.3364	MCIC-3 Apt12 Core
1.3698	0.0237	0.0337	0.0990	40.5354	0.3542	0.5605	0.0987	0.3939	53.8765	0	0.1201	0.0478	0	0	96.9313	MCIC-3 Apt12 Rim
1.4267	0.0175	0	0	40.9071	0.3296	0.5729	0.0121	0.3491	53.0538	0.0436	0.1604	0	0.0050	0.0120	96.2852	MCIC-3 Apt12 Rim
1.5425	0.0070	0	0.0334	39.4437	0.2759	0.5501	0.0092	0.3321	55.6338	0	0	0.1371	0.1389	0	97.4527	MCIC-3 Apt13 Core
1.6176	0.0100	0.0506	0.0084	39.7905	0.2286	0.6868	0	0.1845	55.8054	0.1507	0.1149	0	0.0744	0.0163	98.0554	MCIC-3 Apt13 Core
1.4859	0.0138	0.1038	0	40.5223	0.3056	0.5885	0.0839	0.5937	55.0007	0.3544	0.0742	0	0.0496	0.0486	98.5964	MCIC-3 Apt13 Rim
1.4874	0.0077	0.0323	0	41.0448	0.2615	0.6842	0.0067	0.4943	54.9843	0.1593	0.2429	0	0	0.0405	98.8179	MCIC-3 Apt13 Rim
1.5339	0.0152	0.0248	0	37.033	0.2027	0.6183	0.0643	0.1664	55.0493	0.0090	0.2161	0	0.0199	0	94.3037	MCIC-3 Apt14 Core
1.5282	0.0114	0.0019	0.0667	37.2886	0.2694	0.5496	0	0.2755	54.9222	0.0266	0.0810	0	0	0.0566	94.4317	MCIC-3 Apt14 Core
1.5473	0.0148	0.0247	0.1584	37.6268	0.2832	0.5502	0	0.2585	54.6467	0	0.0271	0	0.0644	0	94.5474	MCIC-3 Apt14 Rim
1.5355	0.0178	0.0124	0.0333	37.8944	0.2456	0.6779	0.0275	0.2884	54.6561	0.2388	0.1619	0	0.0543	0.089	95.2825	MCIC-3 Apt14 Rim
1.4916	0.0159	0.0057	0.0166	40.8598	0.2162	0.6141	0.0697	0.2603	55.9312	0.2030	0	0	0	0.1534	99.206	MCIC-3 Apt15 Core
1.5548	0.0183	0.0637	0	40.0345	0.2418	0.5813	0.0452	0.2875	54.6067	0.2559	0.0808	0.1366	0.0741	0	97.3224	MCIC-3 Apt15 Core
1.7609	0.0053	0.0780	0.0749	40.2847	0.4413	0.4411	0	0.5394	55.8877	0.2385	0.0473	0.2173	0	0	99.2738	MCIC-3 Apt15 Rim
1.4963	0.0105	0.0265	0.0583	41.6664	0.1718	0.8136	0.0434	0.0822	55.897	0	0.0538	0.0724	0.0050	0	99.7649	MCIC-3 Apt15 Rim
1.684	0.0157	0.3483	0.0361	38.3074	0.3045	0.6472	0.0057	0	56.0515	0.1515	0.0350	0.1457	0	0.0803	97.1003	MCIC-3 Ijo Grain#1 Apt with Rxn rim c
1.5737	0.0139	0.0511	0.0209	38.7825	0.2025	0.6471	0.0576	0	55.5237	0	0	0.2562	0.0453	0	96.5089	MCIC-3 Ijo Grain#1 Apt with Rxn rim c
1.5726	0.0070	0	0.0539	39.0532	0.2777	0.5762	0	0	55.8236	0.3196	0.1398	0	0.2164	0.1177	97.4941	MCIC-3 Ijo Grain#1 Apt with Rxn rim r
1.6389	0.0102	0.0569	0	38.5468	0.2287	0.7005	0.0728	0	55.1732	0	0.1819	0	0.0655	0	95.983	MCIC-3 Ijo Grain#1 Apt with Rxn rim r
1.4755	0.0079	0.0284	0	40.4926	0.3100	0.5406	0.0176	0	55.4204	0.1242	0.0491	0.2221	0	0	98.0653	MCIC-3 Ijo Grain#2 Apt Part Rxn rim c
1.4859	0.0126	0	0.0659	40.6504	0.3088	0.5216	0.0214	0	54.9686	0.1422	0.2170	0.0426	0.0552	0	97.8638	MCIC-3 Ijo Grain#2 Apt Part Rxn rim c
1.5576	0.0026	0	0.0299	40.6539	0.3141	0.5378	0.0464	0	54.6214	0.0357	0	0.2651	0.0553	0	97.4635	MCIC-3 Ijo Grain#2 Apt Part Rxn rim +ri
1.5361	0.0140	0	0.0809	40.7895	0.3066	0.5592	0.0276	0	54.5794	0	0.0768	0.1538	0	0.0461	97.5201	MCIC-3 Ijo Grain#2 Apt Part Rxn rim +ri
1.5791	0.0171	0	0	40.6936	0.2620	0.5439	0.0238	0	54.8949	0.1241	0.0701	0.2138	0.0806	0	97.8343	MCIC-3 Ijo Grain#2 Apt Part Rxn rim -ri
1.5149	0.0092	0	0.0389	40.3222	0.3076	0.5496	0.0941	0	54.9151	0.1423	0.0911	0	0.0353	0	97.3804	MCIC-3 Ijo Grain#2 Apt Part Rxn rim -ri

MCIC-4 (Jacupirangite)

F	Cl	Na2O	FeO	P2O5	SO3	SrO	MnO	SiO2	CaO	La2O3	Ce2O3	Pr2O3	Nd2O3	Sm2O3	Total	Comment
1.8340	0.0504	0.0725	0.0329	38.8524	0.8440	0.6778	0.0641	0.6587	52.8176	0.2184	0.2728	0.0081	0.1661	0	95.7863	MCIC-4 Apt5 Core
2.1513	0.0364	0.0122	0.0576	39.5653	0.9343	0.6938	0.0514	0.6486	54.6067	0	0	0	0.0586	0.1678	98.0701	MCIC-4 Apt5 Core
2.0970	0.0300	0	0	40.4232	0.5230	0.7549	0.0175	0.4067	54.3072	0.1573	0.0132	0	0	0	97.8404	MCIC-4 Apt5 Rim
2.1664	0.0221	0.0094	0.1151	41.5741	0.2044	0.7624	0.0061	0.0353	54.4261	0.1481	0.1197	0.0319	0.0489	0.0878	98.8407	MCIC-4 Apt5 Rim
2.2270	0.0234	0.0319	0.1152	39.8685	0.6039	0.7437	0	0.7898	55.0743	0	0.1797	0.0716	0.0146	0	98.8007	MCIC-4 Apt6 Core
2.0634	0.0122	0	0.0576	40.1969	0.5990	0.7131	0.0410	0.7025	54.9902	0.0435	0.1266	0.0320	0.1171	0	98.8236	MCIC-4 Apt6 Core
2.2687	0.0155	0.0198	0	40.0029	0.5972	0.7469	0.0700	0.8414	54.8199	0.1397	0.3260	0	0.1121	0	99.0014	MCIC-4 Apt6 Rim
2.1022	0.0148	0.017	0.0986	39.471	0.6097	0.7115	0	0.7619	55.3777	0.0873	0.4452	0	0.3410	0.0676	99.2172	MCIC-4 Apt6 Rim
1.8063	0.0281	0.0565	1.0678	35.4963	1.4092	0.4960	0.0434	3.7910	50.1292	0	0.1063	0	0.2286	0.0758	93.9677	MCIC-4 Apt7
2.0788	0.0252	0.0161	0.0166	41.0046	0.2388	0.6956	0.0267	0.2113	53.1882	0.2898	0.3686	0	0	0.0482	97.3276	MCIC-4 Apt7
1.998	0.0367	0.0305	0.0916	40.2525	0.4636	0.6508	0.0073	0.4250	53.7391	0.2029	0.3232	0	0.1431	0.0969	97.6117	MCIC-4 Apt7
2.0591	0.0214	0.0534	0.1082	40.6284	0.2782	0.7408	0.0745	0.2527	53.6667	0.0704	0.5318	0.0482	0.0592	0.0685	97.7897	MCIC-4 Apt7
2.1112	0.0221	0.0418	0.0832	39.7493	0.5598	0.6738	0.0574	0.5989	53.9268	0	0.2019	0.0564	0.1184	0.1211	97.4282	MCIC-4 Apt8 Core
2.1565	0.0180	0.0295	0	39.7930	0.6327	0.6960	0.0605	0.6362	53.6396	0.2911	0.0674	0	0.1776	0.0768	97.3628	MCIC-4 Apt8 Core
2.2769	0.0192	0.0600	0.0499	40.2397	0.7213	0.6651	0.0616	0.4704	53.4618	0.2817	0.3225	0	0.0789	0	97.7461	MCIC-4 Apt8 Rim
2.2164	0.0185	0.0029	0.0997	39.9964	0.7106	0.6413	0.0025	0.5525	53.4662	0.3526	0.1411	0	0.1774	0	97.4408	MCIC-4 Apt8 Rim
2.5466	0.0230	0.0248	0.1747	38.9696	0.3350	0.7049	0	0.3051	54.6792	0.1414	0.1886	0	0	0.1654	97.1808	MCIC-4 Apt9 Core
2.4056	0.0421	0.0437	0.0997	40.6496	0.3645	0.7415	0.1	0.2839	55.1823	0.0354	0.1142	0	0.1086	0.0605	99.2093	MCIC-4 Apt9 Core
2.3923	0.0118	0.0086	0.1828	40.7102	0.3742	0.7646	0.0341	0.4790	54.5264	0.1760	0.2688	0	0.1233	0.0484	99.0906	MCIC-4 Apt9 Rim
2.4468	0.0102	0.0105	0.1412	41.0077	0.2822	0.7689	0.0208	0.2919	54.8691	0.1495	0.3091	0.1926	0.1182	0	99.5863	MCIC-4 Apt9 Rim
2.0602	0.0200	0.0152	0.0831	40.3551	0.3786	0.6443	0.0286	0.6190	54.319	0.3346	0.4837	0	0.0689	0	98.5384	MCIC-4 Apt10 Acic Rnd
2.0172	0.0151	0.0325	0.3903	39.2349	1.0279	0.6673	0.0226	1.1712	53.4616	0.2375	0.6171	0.1602	0.1919	0	98.3947	MCIC-4 Apt10 Acic Rnd
2.0371	0.0196	0.0096	0.2162	39.3566	0.8806	0.6365	0.1270	1.1671	53.8582	0.5110	0.4703	0	0.2069	0	98.6347	MCIC-4 Apt10 Acic Rnd
2.0778	0.0250	0.0601	0.2495	38.8859	0.7647	0.6409	0.0305	1.3021	53.0907	0.1232	0.4909	0	0.1381	0.0767	97.0756	MCIC-4 Apt10 Acic Rnd
2.1443	0.0251	0.0067	0.0333	39.2859	0.6700	0.6362	0.0587	0.9618	53.9301	0.1499	0.5586	0.1206	0.0246	0.0727	97.77	MCIC-4 Apt11 Rnd Adj Sph
2.1567	0.0223	0.0124	0.0500	40.4800	0.2977	0.6965	0.0018	0.4507	54.0817	0.1766	0.4448	0	0.0691	0.0121	98.0394	MCIC-4 Apt11 Rnd Adj Sph
2.1916	0.0266	0.0504	0	40.2048	0.4662	0.6387	0.0220	0.5226	53.9846	0.1857	0	0	0.0941	0.0444	97.503	MCIC-4 Apt11 Rnd Adj Sph
2.1333	0.0231	0.0507	0.1168	40.3927	0.4847	0.6513	0	0.6247	54.4085	0	0.4317	0.0967	0.361	0.0728	98.9447	MCIC-4 Apt11 Rnd Adj Sph
2.2346	0.0258	0.0422	0.0835	39.9675	0.5222	0.5949	0.0411	0.7210	55.0528	0.2391	0.4254	0	0.1435	0.0323	99.1793	MCIC-4 Apt12 Rnd Adj Perovskite
2.2492	0.0387	0.0830	0.6257	39.7197	1.1325	0.6538	0.0471	0.9132	54.6021	0.3711	0.3437	0	0.4350	0.0769	100.3359	MCIC-4 Apt12 Rnd Adj Perovskite
2.1755	0.0174	0.0308	0.0501	40.3499	0.5216	0.5753	0	0.6826	54.3111	0.2656	0.4931	0.2019	0.3319	0	99.087	MCIC-4 Apt12 Rnd Adj Perovskite
2.1049	0.0153	0.0215	2.6659	38.7463	3.6841	0.6375	0.0073	0.6507	52.4402	0.0702	0.5104	0.0883	0.2266	0.0242	101.0036	MCIC-4 Apt12 Rnd Adj Perovskite
2.1898	0.0105	0.0010	0.0501	40.1249	0.5233	0.5790	0	0.6967	54.7986	0.5310	0.2904	0.0968	0.1880	0.0202	99.176	MCIC-4 Apt12 Rnd Adj Perovskite
2.2481	0.0278	0.0918	0.0332	38.4644	1.2027	0.6400	0	0	55.1438	0.1969	0.183	0.0088	0.0252	0.0127	97.3255	MCIC-4 Jac Grain#1 Apt in Neph c
1.8401	0.0295	0.8317	0.0211	33.6482	0.9479	0.3310	0	0	47.3461	0.2231	0	0.258	0	0.0845	84.7798	MCIC-4 Jac Grain#1 Apt in Neph c
2.2623	0.0227	0	0.0933	40.3384	0.7837	0.6729	0.0012	0	55.2364	0.3301	0.3933	0.2832	0	0	99.46	MCIC-4 Jac Grain#1 Apt in Neph r
0.5156	2.6706	7.8027	1.1505	11.8630	0.134	0	0	0	20.0129	0.0173	0	0	0.0249	0	43.3717	MCIC-4 Jac Grain#1 Apt in Neph r
2.0194	0.0119	0	0.1234	40.6568	0.1848	0.7622	0.0630	0	55.7759	0.1247	0.2036	0.0685	0.0858	0.017	99.2441	MCIC-4 Jac Grain#2 Elongate Apatite
1.9923	0.0137	0.1943	0.0662	40.7650	0.1921	0.7421	0.0435	0	55.1625	0.0712	0.2951	0	0.0555	0	98.7516	MCIC-4 Jac Grain#2 Elongate Apatite
1.9387	0.0142	0	0.1383	40.6960	0.2937	0.7370	0	0	55.8611	0.2139	0.2389	0.2059	0.1312	0	99.6495	MCIC-4 Jac Grain#2 Elongate Apatite

MCIC-5A (Carbonatite, part 1)

F	Cl	Na2O	FeO	P2O5	SO3	SrO	MnO	SiO2	CaO	La2O3	Ce2O3	Pr2O3	Nd2O3	Sm2O3	Total	Comment
1.0435	0.0087	0.059	0.0575	38.8016	0.8373	0.2994	0	0.9782	53.3656	0.2611	0.4313	0.0081	0.073	0.0518	95.8348	MCIC-5A Grain #1 Apt in Kimz
1.0261	0.0103	0.1200	0	36.0936	1.1727	0.277	0.0644	2.0096	53.7766	0.2522	0.4113	0.0081	0.1118	0.0041	94.9035	MCIC-5A Grain #1 Apt in Kimz
1.1014	0.0066	0.1063	0.1558	36.6845	1.1647	0.2796	0	1.8461	54.1126	0.4869	0.3052	0	0.1263	0	95.9109	MCIC-5A Grain #1 Apt in Kimz
1.1758	0.0129	0.0047	0.1395	38.5410	0.997	0.2981	0	1.2681	54.9887	0.2351	0.3585	0.0795	0	0.1034	97.7044	MCIC-5A Grain #2 Apt in Kimz
1.1389	0.0021	0.0234	0	38.9583	1.0851	0.3212	0.0529	1.2330	54.5893	0.3736	0.4769	0.1187	0.0341	0	97.9275	MCIC-5A Grain #2 Apt in Kimz
1.2242	0.0084	0.0563	0.0164	38.0526	1.201	0.3207	0.0024	1.5666	54.7938	0.3997	0.5234	0	0.0291	0.1232	97.8005	MCIC-5A Grain #2 Apt in Kimz
1.1850	0.0094	0.1039	0.0164	37.0542	1.0904	0.2761	0	2.0307	55.2609	0.1997	0.3846	0.1107	0.0583	0.1986	97.4780	MCIC-5A Grain #3 Apt in Kimz
1.2135	0.0051	0.1350	0.0246	36.9333	1.0876	0.2432	0	2.0295	55.2256	0.0172	0.6561	0	0.2624	0.0636	97.3846	MCIC-5A Grain #3 Apt in Kimz
1.1330	0.0083	0.0781	0.0818	37.1828	1.1100	0.3036	0	2.0604	55.9459	0.2343	0.5825	0.2452	0.2328	0	98.7198	MCIC-5A Grain #3 Apt in Kimz
1.1918	0.0150	0.0600	0.0654	39.0808	0.956	0.3339	0	1.3183	55.6467	0.399	0.4365	0.3082	0	0.2339	99.5404	MCIC-5A Grain #4 Apt in Kimz/Boundary
1.1932	0.0135	0.0141	0	39.5454	0.7746	0.31	0	0.9873	55.0465	0.4165	0.5293	0	0.0873	0	98.4124	MCIC-5A Grain #4 Apt in Kimz/Boundary
1.2324	0.0064	0.1124	0.0572	38.0754	1.0519	0.2416	0	1.7691	55.3173	0.3548	0.3633	0.1027	0.2905	0.1228	98.5775	MCIC-5A Grain #4 Apt in Kimz/Boundary
1.0912	0.0143	0.1178	0.0898	36.9133	1.1428	0.2655	0.0126	2.114	55.0789	0.2946	0.5614	0.0554	0	0	97.2889	MCIC-5A Grain #4 Apt in Kimz/Boundary
1.1531	0.0022	0.0665	0.0489	38.3391	1.0265	0.2903	0	1.4246	55.1136	0.5536	0.4551	0.1575	0.0531	0.1305	98.3287	MCIC-5A Grain #4 Apt in Kimz/Boundary
1.0784	0.0061	0.1346	0	37.1085	1.0889	0.2804	0	1.9445	54.8539	0.4155	0.4028	0.1893	0.0096	0.0356	97.0927	MCIC-5A Grain #4 Apt in Kimz/Boundary
1.1290	0.0096	0.0606	0	37.3881	1.1063	0.2457	0.0162	1.9361	54.5952	0.2686	0.2643	0.0791	0.1502	0.0316	96.8031	MCIC-5A Grain #4 Apt in Kimz/Boundary
1.1795	0.0053	0.0589	0	38.6896	0.9225	0.2674	0.0420	1.2090	54.9856	0.1472	0.6944	0	0.0969	0.0159	97.8165	MCIC-5A Grain #5 Core
1.1600	0.0133	0.1265	0	37.5429	1.0135	0.2569	0	1.6605	54.9887	0.3732	0.3243	0.1422	0.1213	0	97.2320	MCIC-5A Grain #5 Core
1.0954	0.0135	0.0766	0	38.7881	0.9067	0.2924	0.0522	1.3322	55.2256	0.1472	0.5224	0.1265	0.0777	0.2022	98.3946	MCIC-5A Grain #5 Rim
1.1716	0.0125	0.0918	0.0579	38.2052	0.9954	0.3093	0	1.6179	55.2843	0.2543	0.4485	0	0.1275	0	98.0802	MCIC-5A Grain #5 Rim
1.0025	0.0035	0.0399	0	39.2284	0.7561	0.3131	0	1.1489	54.3095	0.4490	0.3424	0.0722	0.1477	0.0242	97.4145	MCIC-5A Grain #6 Core
0.9649	0.0032	0.0427	0.0249	39.5278	0.6406	0.3436	0.0244	0.9871	54.5222	0.4311	0.3823	0.1284	0.0788	0.0282	97.7233	MCIC-5A Grain #6 Core
0.8983	0.0023	0.0670	0.0083	37.8648	1.1353	0.3277	0.0304	1.6129	54.4365	0.7984	0.6021	0.2317	0.2354	0.0643	97.9367	MCIC-5A Grain #6 Rim
0.8764	0.0084	0.0795	0	38.8242	0.909	0.3239	0	1.1735	54.4656	0.3602	0.5028	0	0	0.0282	97.1808	MCIC-5A Grain #6 Rim
1.1729	0.0086	0.0647	0.0083	39.2968	0.7199	0.3016	0.0189	1.1462	54.6773	0.4125	0.7967	0	0.0834	0.0161	98.2281	MCIC-5A Grain #7 Core
1.2398	0.0045	0.0541	0.0248	39.4995	0.7406	0.2952	0	0.9637	55.2775	0.2544	0.6759	0.0158	0.1422	0	98.6651	MCIC-5A Grain #7 Core
1.2205	0.0119	0.0628	0.149	38.5903	0.7415	0.2686	0	1.1344	55.1892	0.4649	0.5954	0	0.1669	0	98.0789	MCIC-5A Grain #7 Rim
1.2714	0.0094	0.0248	0.0248	39.2411	0.6445	0.2851	0.0067	1.0617	55.3828	0.4827	0.5150	0.2557	0.1030	0	98.7713	MCIC-5A Grain #7 Rim
0.9629	0.008	0.0398	0	39.6670	0.6694	0.3225	0.0176	0.9416	55.7343	0.1670	0.3949	0.2558	0.2895	0	99.0631	MCIC-5A Grain #8 Acic Rnd
0.9543	0.0054	0.0522	0.0580	38.8535	0.7801	0.3079	0	1.2189	55.5158	0.5443	0.3214	0	0.1523	0	98.3612	MCIC-5A Grain #8 Acic Rnd
0.9089	0.0092	0.0521	0.0331	39.3936	0.8028	0.2832	0.0043	1.0567	55.1626	0.2017	0.7699	0.0960	0.0442	0.0682	98.5017	MCIC-5A Grain #8 Acic Rnd
0.9362	0.0139	0.0198	0	39.2784	0.6986	0.3395	0.0280	0.8507	54.8944	0.1932	0.281	0.1439	0.1325	0.0763	97.4892	MCIC-5A Grain #8 Acic Rnd
1.1154	0.0044	0.0455	0.0662	38.7686	1.0485	0.2872	0.0237	1.5078	55.2514	0.2804	0.4414	0.0959	0.2109	0.012	98.6888	MCIC-5A Grain #9 Rnd
1.2214	0.0077	0.0132	0.0745	40.4925	0.5707	0.3351	0	0.78	55.1694	0.2279	0.3746	0	0	0	98.7511	MCIC-5A Grain #9 Rnd
1.0899	0.0055	0.0742	0.0331	38.9999	0.8239	0.3012	0.0091	1.2639	54.9495	0.7449	0.4009	0	0.2401	0.0921	98.5682	MCIC-5A Grain #9 Rnd
0.9909	0.0239	0	0	38.3945	0.9049	0.2593	0.0216	0	54.6909	0.0717	0.5384	0.1469	0.0865	0	95.7069	Line 1 MCIC-5 Carb Grain 1 Trav (22.3um
1.2357	0.0141	0.1384	0.0303	37.1044	1.0119	0.2387	0.0012	0	54.5635	0.3237	0.2763	0.1127	0	0	94.5275	Line 2 MCIC-5 Carb Grain 1 Trav (22.3um
1.1088	0.0083	0	0	35.9252	1.0692	0.2475	0.0031	0	55.204	0.1889	0.4392	0.0950	0.1987	0	94.0192	Line 3 MCIC-5 Carb Grain 1 Trav (22.3um
1.0965	0.0053	0.0582	0.0394	35.9921	1.0203	0.2695	0.0350	0	54.763	0.6387	0.3968	0	0.0254	0	93.8773	Line 4 MCIC-5 Carb Grain 1 Trav (22.3um
1.2042	0.0149	0	0	36.5605	0.9883	0.2668	0.0305	0	54.4529	0.8347	0.5164	0.1555	0.1321	0.0171	94.6635	Line 5 MCIC-5 Carb Grain 1 Trav (22.3um
1.1896	0.006	0	0.0091	36.6522	1.047	0.3295	0	0	54.9834	0.2423	0.5656	0.2679	0.1474	0	94.9377	Line 6 MCIC-5 Carb Grain 1 Trav (22.3um
1.2344	0.006	0	0	36.5698	1.0698	0.3361	0.0031	0	54.4696	0.5016	0.7062	0	0.1118	0.1145	94.6018	Line 7 MCIC-5 Carb Grain 1 Trav (22.3um
1.0953	0.0093	0.6087	0.0061	37.2142	1.1462	0.3022	0.0216	0	54.0872	0.2421	0.5650	0.0259	0.071	0	94.9316	Line 8 MCIC-5 Carb Grain 1 Trav (22.3um
1.1957	0.0127	0	0.0664	38.2206	1.0171	0.3117	0	0	54.5262	0.5811	0.5074	0.2754	0.1977	0.0889	96.4946	Line 9 MCIC-5 Carb Grain 1 Trav (22.3um
1.0495	0.0077	0	0.0815	37.8433	1.0855	0.3047	0.0373	0	54.2262	0.7059	0.5630	0.2669	0.1367	0.0084	95.873	Line 10 MCIC-5 Carb Grain 1 Trav (22.3u

MCIC-5A (Carbonatite, part 2)

F	Cl	Na2O	FeO	P2O5	SO3	SrO	MnO	SiO2	CaO	La2O3	Ce2O3	Pr2O3	Nd2O3	Sm2O3	Total	Comment
1.2822	0.0189	0	0	37.4409	1.0663	0.2609	0.0045	0	54.4269	0.3398	0.5075	0.0945	0.2029	0	95.1012	MCIC-5 Carb Grain#2 c
1.2737	0.0028	0	0	37.6768	0.9646	0.3209	0.0551	0	54.0017	0.4833	0.4443	0	0.3043	0	94.9906	MCIC-5 Carb Grain#2 r
0.8421	0.0091	0	0	34.9531	1.2862	0.2497	0.0677	0	53.9136	0.4478	0.4236	0.0171	0.2793	0	92.1327	MCIC-5 Carb Grain#3 Acic End
0.851	0.0124	0.5423	0.0574	34.4288	1.2667	0.2708	0	0	53.7482	0.2594	0.6911	0.2326	0.2383	0.0297	92.2676	MCIC-5 Carb Grain#3 Acic Mid
0.8832	0.0045	0	0.0182	34.8802	1.2776	0.2167	0.0418	0	53.4555	0.5379	0.5013	0.1294	0.1676	0.0339	91.775	MCIC-5 Carb Grain#3 Acic Mid
0.9076	0.0132	0	0.0666	37.1547	1.105	0.2201	0	0	52.8328	0.1167	0.6147	0	0.2082	0	92.8546	MCIC-5 Carb Grain#3 Acic Mid
0.7363	0.0196	0.365	0.1179	32.84	1.1736	0.2558	0	0	53.9896	0.4031	0.7623	0.2156	0.0661	0.0552	90.6857	MCIC-5 Carb Grain#4 Apt incld w/i Kimz
0.8932	0.0224	0.3961	0.0968	36.179	1.1781	0.272	0.0057	0	55.177	0.1076	0.3814	0.2241	0.0710	0.0763	94.6996	MCIC-5 Carb Grain#4 Apt incld w/i Kimz
1.0645	0.0085	0	0	38.0506	0.7948	0.299	0	0	53.9469	0.2864	0.5221	0.0088	0.2031	0	94.7346	MCIC-5 Carb Grain#5 Apt in Diop Mess c
0.9467	0.019	0.1092	0	38.6192	0.6539	0.325	0	0	53.4378	0.3401	0.3811	0.0517	0.1422	0.0338	94.6569	MCIC-5 Carb Grain#5 Apt in Diop Mess c
1.0412	0.0078	0	0.0876	38.2637	0.7768	0.3412	0.0215	0	53.0027	0.2056	0.4793	0	0.0609	0	93.8482	MCIC-5 Carb Grain#5 Apt in Diop Mess r
1.0463	0	0	0	37.8215	0.7889	0.3287	0.0083	0	53.2584	0.3311	0.5357	0.0604	0.2281	0.0170	93.984	MCIC-5 Carb Grain#5 Apt in Diop Mess r
0.9618	0.0174	0	0.0725	36.1721	1.6877	0.2604	0.0259	0	54.6505	0.4390	0.3950	0	0	0.0298	94.3033	MCIC-5 Carb Grain#6 Apt in Perov c
0.6928	0.0182	0	0.0302	29.2167	1.6695	0.2120	0	0	51.0362	0.5290	0.3107	0	0.0356	0.0509	83.5061	MCIC-5 Carb Grain#6 Apt in Perov c
0.9419	0.0111	0.0577	0	35.7740	1.2080	0.2480	0.064	0	54.4889	0.0630	0.4314	0.3796	0.0305	0.0425	93.3416	MCIC-5 Carb Grain#6 Apt in Perov r
0.9039	0.0135	0.4771	0.0936	36.3529	1.3778	0.2671	0	0	54.5473	0.3667	0.5288	0	0.1521	0.0254	94.7226	MCIC-5 Carb Grain#6 Apt in Perov r

MCIC-5B (Carbonatite)

F	Cl	Na2O	FeO	P2O5	SO3	SrO	MnO	SiO2	CaO	La2O3	Ce2O3	Pr2O3	Nd2O3	Sm2O3	Total	Comment
0.8439	0.0130	0.0464	0	38.0889	1.1761	0.3112	0	1.3478	52.6896	0.3333	0.6558	0.0480	0.0442	0	95.2401	MCIC-5B Grain #1 Acic Core
0.8829	0.0071	0.0095	0.0910	38.6515	1.0627	0.3385	0	1.1512	52.8049	0.6664	0.4882	0.0959	0.1521	0	96.0286	MCIC-5B Grain #1 Acic Core
0.9121	0.0078	0.0332	0.0910	38.6080	1.0039	0.3256	0	1.2980	52.1328	0.3682	0.6149	0.0479	0.2109	0.0963	95.3648	MCIC-5B Grain #1 Acic Rim
0.8975	0.0087	0.0548	0	39.2748	0.9869	0.3468	0.1186	1.0569	52.2024	0.3952	0.4019	0	0.0295	0	95.3942	MCIC-5B Grain #1 Acic Rim
0.9253	0.0132	0.0982	0.0166	36.4262	1.1500	0.2818	0.0846	1.7194	52.8692	0.6064	0.6836	0	0.0540	0.0562	94.5922	MCIC-5B Grain #2 Core
0.9379	0.0115	0.0276	0.0249	37.8119	0.9878	0.3393	0	1.0002	52.8361	0.2814	0.6173	0	0.2902	0	94.7687	MCIC-5B Grain #2 Core
1.0389	0.0019	0.0610	0.0166	37.6564	1.0432	0.2796	0	1.1975	52.0299	0.7389	0.3756	0.0722	0.0590	0	94.1329	MCIC-5B Grain #2 rim
1.0335	0.0092	0.0486	0.0332	37.1415	1.3406	0.3521	0	1.5802	52.4714	0.5538	0.6907	0.0721	0.1180	0.1248	95.1324	MCIC-5B Grain #2 rim
0.9093	0.0093	0	0.0748	38.6649	1.0982	0.3246	0.0018	1.0986	52.6901	0.3347	0.3428	0.0882	0	0.0162	95.2686	MCIC-5B Grain #3 Core
0.9283	0.0092	0.0735	0	38.0869	1.2029	0.2660	0	1.3654	52.5513	0.6163	0.4902	0.1685	0.1527	0.0442	95.5625	MCIC-5B Grain #3 Core
0.8565	0.0132	0.0572	0.0665	38.7649	1.0312	0.2930	0.0433	1.3087	52.3918	0.3870	0.5907	0.2407	0.1722	0	95.8534	MCIC-5B Grain #3 Rim
0.9072	0.0025	0.0219	0.0249	38.0726	1.0745	0.2957	0	1.3576	52.1969	0.5458	0.4162	0	0.2461	0	94.7794	MCIC-5B Grain #3 Rim
1.1738	0.0092	0.0540	0.0083	39.2020	0.7883	0.3359	0	0.8694	53.6186	0.0439	0.0069	0.2009	0.3452	0.0926	96.2527	MCIC-5B Grain #3 Rim
1.1761	0.0088	0.0946	0	37.2197	1.0749	0.2592	0	1.7291	54.6877	0.6433	0.5644	0	0.0937	0.0242	97.0786	MCIC-5B Grain (#4)
1.1715	0.0095	0.0733	0	37.2968	1.0177	0.3163	0	1.6112	53.6916	0.3173	0.4839	0.0482	0.1871	0	95.7291	MCIC-5B Grain (#4)
1.1439	0.0120	0.0769	0	37.4956	1.4030	0.2880	0	1.707	54.636	0.3175	0.2288	0	0.1775	0.0443	97.0462	MCIC-5B Grain (#4)
0.9923	0.0117	0.0481	0.0412	37.9419	0.9409	0.2492	0.0496	1.4685	54.4229	0.4190	0.4062	0	0.21	0	96.7811	MCIC-5B Grain (#4)
1.1348	0.0043	0.0710	0	36.9561	1.2857	0.2651	0	1.6448	54.0482	0.7545	0.6878	0.2135	0.1941	0.0198	96.8009	MCIC-5B Grain (#5)
1.1605	0.0122	0.0756	0	38.5982	0.9834	0.2773	0	1.2119	54.4136	0.1822	0.4696	0	0.0533	0.0159	96.9623	MCIC-5B Grain (#5)
1.0873	0.0124	0.0122	0.0244	38.4106	0.9243	0.3138	0.0060	1.3063	54.3190	0.5527	0.3752	0	0.3041	0	97.1878	MCIC-5B Grain (#5)
1.1088	0.0064	0.0513	0	37.6200	0.9471	0.3236	0	1.3787	54.3099	0.3454	0.5331	0	0.1737	0	96.3297	MCIC-5B Grain (#5)
1.0805	0.0138	0.0578	0.0163	37.0091	1.3364	0.3296	0	1.643	54.0222	0.2674	0.0986	0.5655	0.1446	0	96.1269	MCIC-5B Grain (#6)
1.1205	0.0078	0.0475	0	37.5425	1.2565	0.2880	0	1.4764	53.8014	0.5691	0.2103	0	0.0868	0.0828	96.0161	MCIC-5B Grain (#6)
1.0789	0.0131	0.1040	0.0325	36.1648	1.2110	0.2675	0.0322	2.1838	53.9588	0.2329	0.4606	0	0.0674	0.1143	95.4646	MCIC-5B Grain (#6)
1.0996	0.0040	0.0834	0.0569	37.9043	1.0399	0.2791	0.0143	1.623	53.5202	0.8609	0.1642	0.2670	0.2793	0	96.7322	MCIC-5B Grain (#6)

Appendix 6

Plots of concentrations (mole %) of major elements in apatite in MCIC rock types

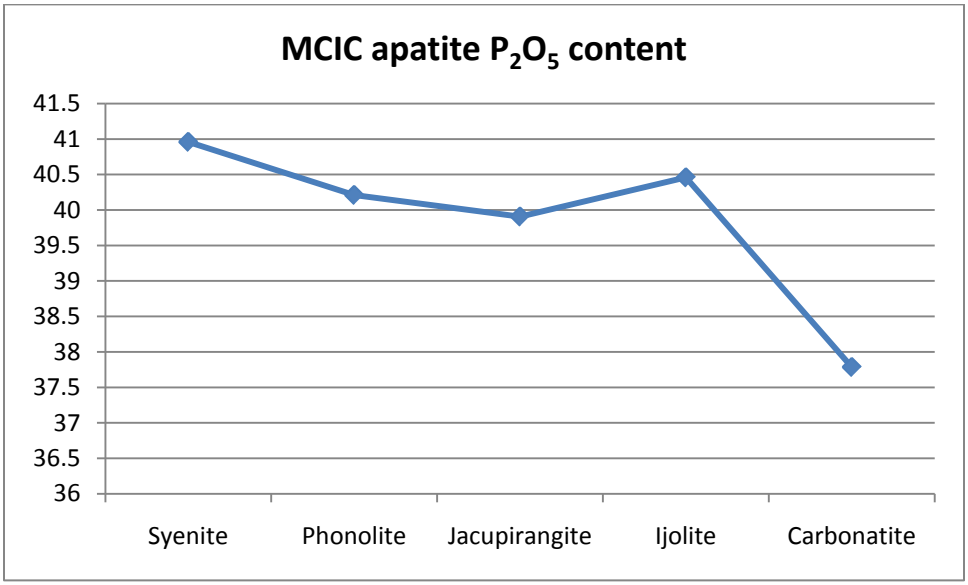

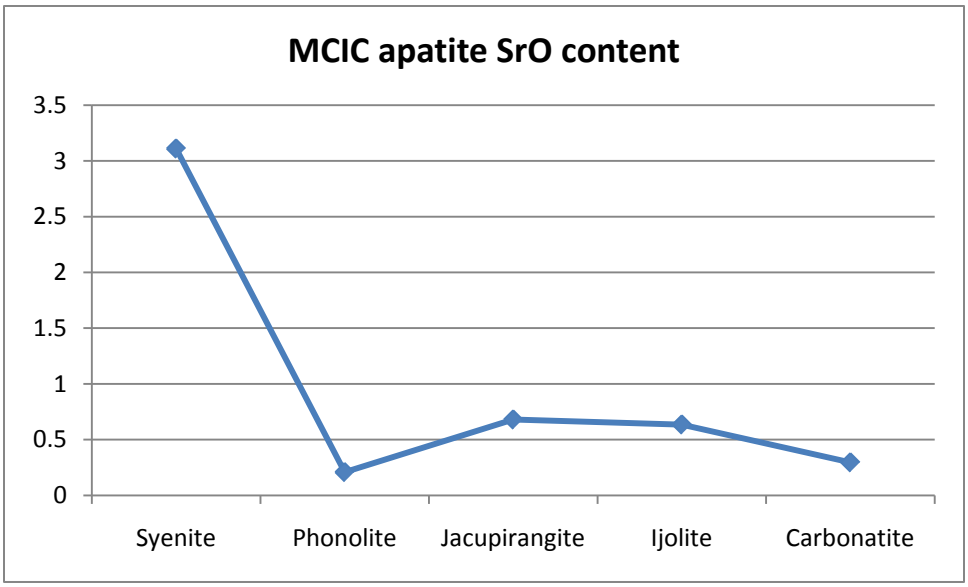

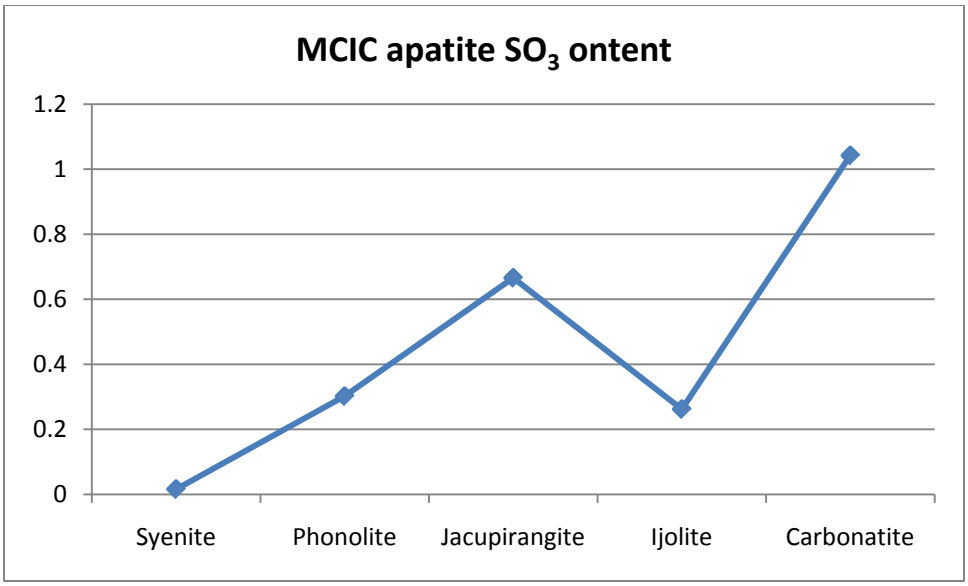
MCIC apatite SO3 ontent
1.2
1
0.8
0.6
0.4
0.2
0
Syenite
Phonolite
Jacupirangite
Ijolite
Carbonatite

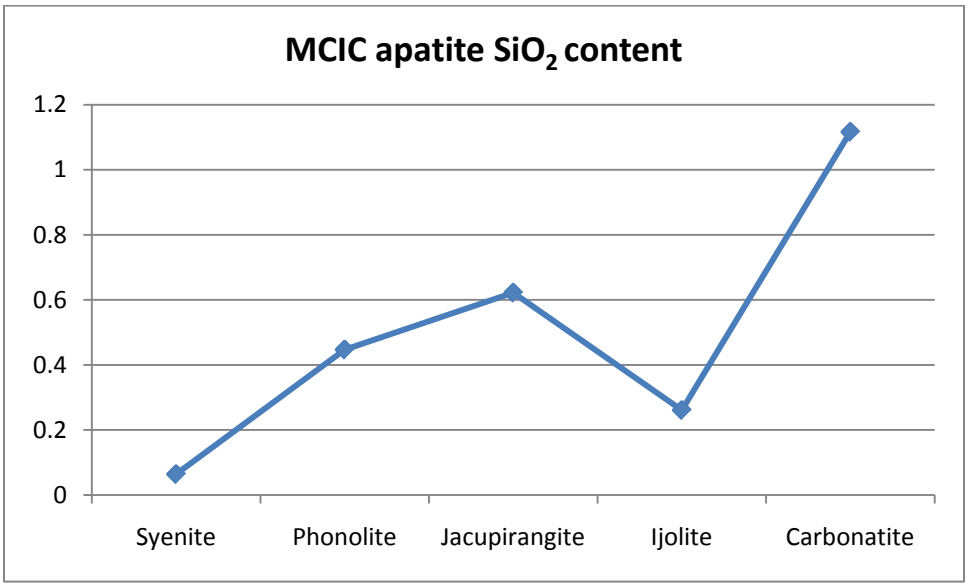
MCIC apatite SiO2 content
1.2
1
0.8
0.6
0.4
0.2
0
Syenite
Phonolite
Jacupirangite
Ijolite
Carbonatite

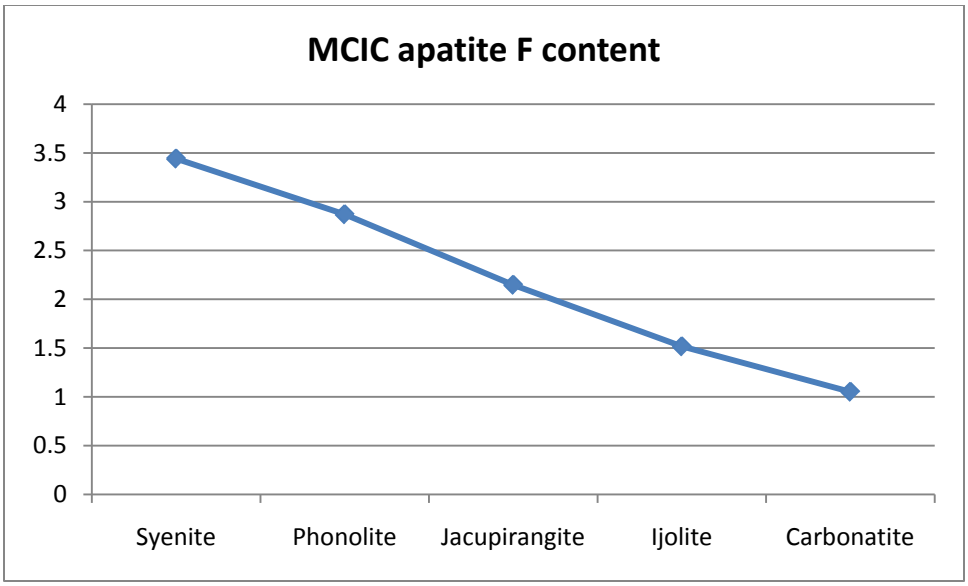
MCIC apatite F content
4
3.5
3
2.5
2
1.5
1
0.5
0
Syenite
Phonolite
Jacupirangite
Ijolite
Carbonatite

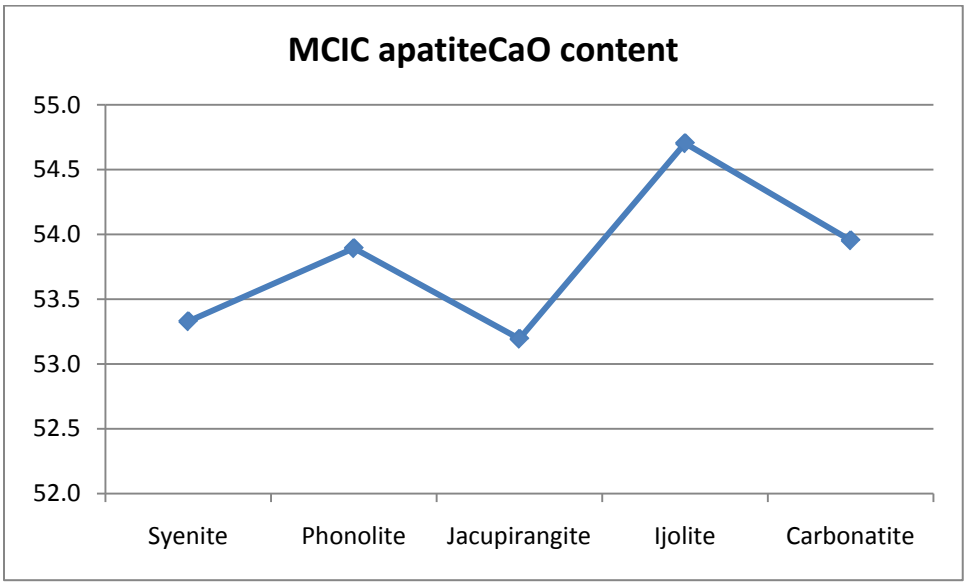
MCIC apatiteCaO content
55.0
54.5
54.0
53.5
53.0
52.5
52.0
Syenite
Phonolite
Jacupirangite
Ijolite
Carbonatite

Appendix 7

Plots of halogen composition of apatite from MCIC rock types

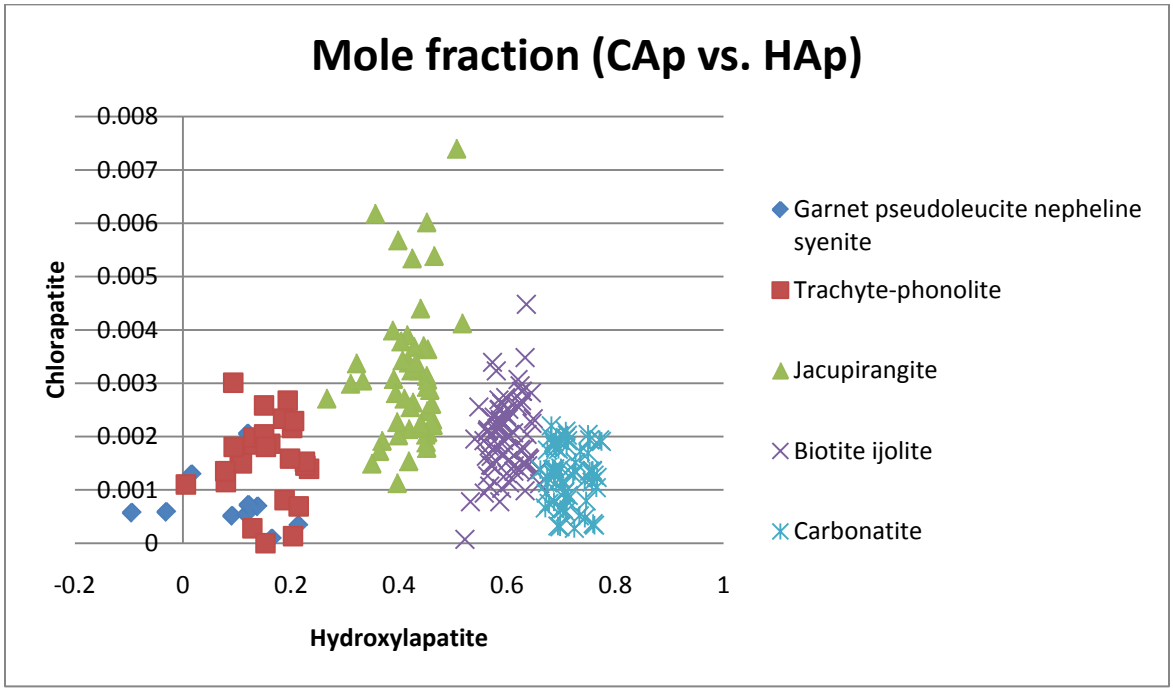

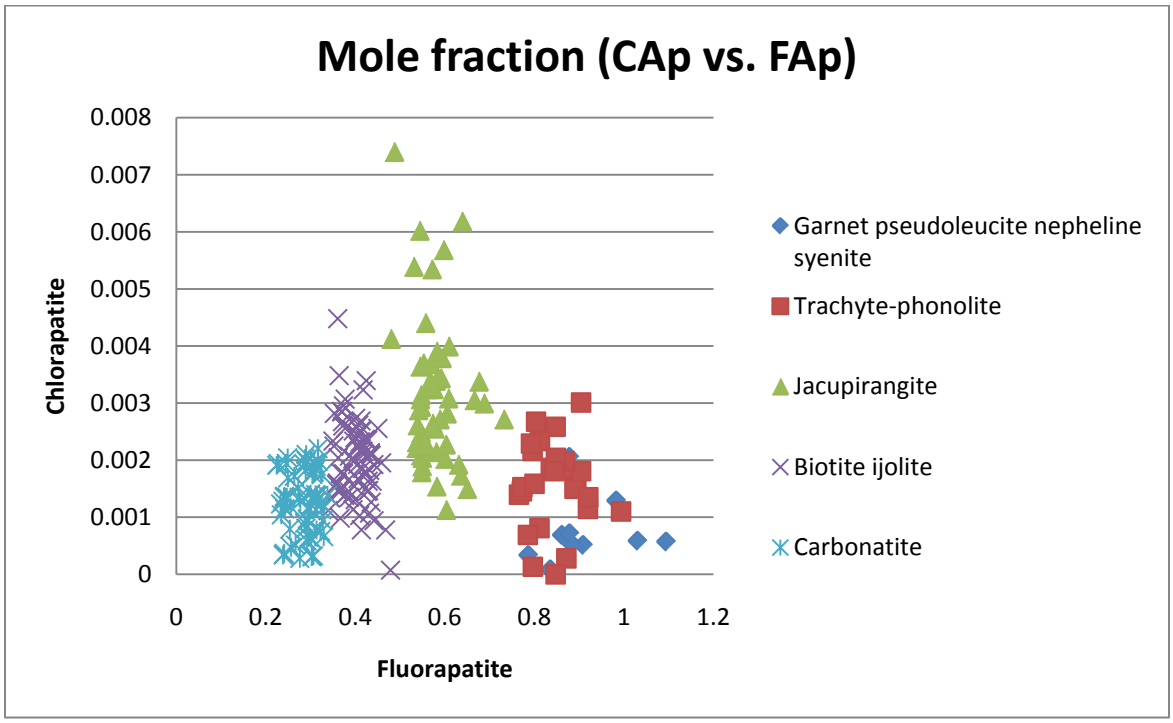

A**ppendix 8 (LA-ICP-MS results)**

LA-ICP-MS Results (MCIC-1: Trachyte-phonolite)

LAM-ICP-MS RESULTS - DETECTION LIMIT FILTERED

MCIC-1 (Trachyte-phonolite)

04/01/11

Isotopic mass		CaO 43	Sc 45	TiO2 47	TiO2 49	V 51	As 75	Se 77	Sr 88	Y 89	Zr 90	Nb 93	Ba 137	La 139	Ce 140	Pr 141	U 238	Peak secs	Abitn yield	Comments
		wt%	ppm	wt%	wt%	ppm	ppm	ppm	ppm	ppm	ppm	ppm	ppm	ppm	ppm	ppm	ppm			
Chondrite		1.30	5.90	0.08	0.08	54.30	1.81	21.40	7.26	1.56	3.86	0.25	2.41	0.25	0.64	0.10				
Det. limit		0.03	0.19	0.00	0.00	0.10	0.80	2.17	0.09	0.02	0.02	0.01	0.10	0.01	0.01	0.01				
std-1		11.4	444.02	<0.24	0.07	435	310	106	504.20	456.14	448.64	422.38	417.08	460.13	448.25	435.51	33.2	40.4	85%	NIST 610 40um 7Hz 66% 2.08Jcm-2
std-2		11.4	438.17	<0.37	0.08	448	325	112	490.60	443.64	431.14	416.41	431.12	454.66	447.35	424.08	5.0	40.4	62%	NIST 610 60um 7Hz 66% 2.22Jcm-2
Ap01a03		11.4	28.87	4.97	2.54	308	<2.35	<5.02	380	22	153	15.52	122.61	15.69	37.28	5.0	40.4	44.0	264%	BHVO 2g 55um 7Hz 66% 2.10Jcm-2
Ap01a04		56	143.95	24.03	12.54	1501	<14.41	<31.52	1846	109	736	74.57	570.60	74.03	171.51	23.7	44.0	55%		BHVO 2g 55um 7Hz 66% 2.16Jcm-2
Ap01a05	05	55.60	<6.75	<0.62	0.02	193	70	<32.99	1243.5	780	6.75	1.15	9.79	2797.71	2591.98	613.32	31.8	38%		MCIC-1 Apt4 25um 7Hz 66% 2.07Jcm-2
Ap01a06	06	55.60	<20.68	<3.05	<0.02	189	<90.30	<153.38	1368.6	692	9.23	0.56	6.67	2689.79	4589.42	487.49	17.3	11%		MCIC-1 Apt4 12um 7Hz 66% 2.18Jcm-2
Ap01a07	07	55.60	<24.13	<2.17	<0.03	412	114	<205.77	970.9	1112	10.98	1.53	<16.96	5729.07	8071.22	1001.63	24.5	10%		MCIC-1 Apt3 12um 7Hz 66% 2.13Jcm-2
Ap01a08	08	55.60	<5.61	<0.58	0.01	386	88	<50.60	1449.1	1087	16.86	1.10	<6.70	4307.50	2251.47	871.70	41.9	36%		MCIC-1 Apt2 25um 7Hz 66% 2.23Jcm-2
Ap01a09	09	56	<19.15	<2.19	<0.02	346	107	<140.10	1133.5	1137	17.64	<3.58	<9.78	5365.56	8246.85	842.92	23.8	11%		MCIC-1 Apt1 12um 7Hz 66% -Jcm-2
Ap01a10		56	<5.14	<0.53	0	324	90	<55.12	1236.6	705	11.30	0.81	11.60	2868.82	2202.73	676.82	44.8	37%		MCIC-1 Apt9 25um 7Hz 66% 2.02Jcm-2
Ap01a11		56	<14.40	<2.30	<0.03	325	<73.07	<203.25	1977.1	469	17.47	0.49	23.49	2840.67	5240.98	490.66	18.8	11%		MCIC-1 Apt9 12um 7Hz 66% -Jcm-2
Ap01a12		56	<7.94	<0.82	0	298	74	<59.01	1262.0	403	10.22	0.63	9.22	2070.51	1440.00	543.62	46.2	34%		MCIC-1 Apt10 12um line 7Hz 66% 2.18Jcm-2
Ap01a13		56	<17.17	<2.06	<0.02	308	<56.36	<167.64	1146	305	7.3	0.53	<21.30	2478.07	2805.48	519.272	45.5	11%		MCIC-1 Apt10 6um line 7Hz 66% 2.07Jcm-2
Ap01a14		55.60	<5.79	<0.49	0.06	308	114	37	1104	564	8.7	3.28	66.32	2249.84	1844.30	736.655	39.0	48%		MCIC-1 Apt10 25um 7Hz 66% -Jcm-2
Ap01a15		55.6	<15.50	<2.24	0.03	652	232	<174.95	1189	1213	15.5	3.84	19.57	7653.38	10053.22	1110.214	17.3	11%		MCIC-1 Apt5 12um 7Hz 66% 2.13Jcm-2
Ap01a16		55.6	<20.06	<1.97	<0.02	370	144	<198.46	798	984	9.7	0.68	9.15	4742.73	6407.85	1111.26	12.3	15%		MCIC-1 Apt6 12um 7Hz 66% -Jcm-2
Ap01a17	17	11.4	30.71	4.68	2.65	311	<1.71	<4.58	375	23	154.0	15.20	116.92	15	35.5	4.9	44.0	376%		BHVO 2g 12um 7Hz 66% 2.22Jcm-2
Ap01a18		11.4	30.83	4.54	2.67	316	<2.09	<4.91	379	23	159.1	15.66	116.09	15	35.7	4.7	39.7	357%		BHVO 2g 35um 7Hz 66% -Jcm-2
std-3		11.40	452.02	<0.17	0.07	444.71	327.05	109.78	497.61	448.64	438.19	414.30	424.05	454.27	449.92	428.64	31.0	123%		NIST 610 40um 7Hz 66% -Jcm-2
std-4		11.40	430.15	<0.16	0.07	438.69	307.76	108.23	497.19	451.16	441.62	424.52	424.15	460.53	445.68	430.96	28.9	130%		NIST 610 60um 7Hz 66% -Jcm-2

LAM-ICP-MS RESULTS - DETECTION LIMIT FILTERED

MCIC-1 (Trachyte-phonolite)

04/01/11

Isotopic mass		Nd 146	Sm 147	Eu 151	Gd 157	Tb 159	Dy 163	Ho 165	Er 166	Tm 169	Yb 172	Lu 175	Hf 178	Ta 181	Pb 208	Th 232	U 238	Peak secs	Abitn yield	Comments
		ppm	ppm	ppm	ppm	ppm	ppm	ppm	ppm	ppm	ppm	ppm	ppm	ppm	ppm	ppm	ppm			
Chondrite		0.47	0.15	0.06	0.20	0.04	0.25	0.06	0.17	0.03	0.17	0.03	0.11	0.01	2.53	0.03	0.01			
Det. limit		0.02	0.03	0.01	0.05	0.00	0.01	0.00	0.01	0.00	0.01	0.00	0.01	0.00	0.03	0.00	0.00			
std-1		433.70	453.55	462.12	422.46	449.35	436.01	456.89	432.46	428.20	471.27	440.45	415.15	378.04	411.25	470.01	469.76	33.2	85%	NIST 610 40um 7Hz 66% 2.08Jcm-2
std-2		427.89	447.44	460.08	417.33	436.22	416.95	441.88	419.51	411.97	451.69	428.93	420.26	375.15	415.36	431.10	444.38	40.4	62%	NIST 610 60um 7Hz 66% 2.22Jcm-2
Ap01a03		24.8	6.15	2	5.79	0.87	4.83	0.89	2.20	0.27	1.94	0.25	4.11	0.96	1.72	1.15	0.40	40.4	264%	BHVO 2g 55um 7Hz 66% 2.10Jcm-2
Ap01a04		113.2	29.0	10	28.72	4.15	22.79	4.28	10.96	1.38	8.91	1.29	18.81	4.31	7.67	5.74	2.16	44.0	55%	BHVO 2g 55um 7Hz 66% 2.16Jcm-2
Ap01a05	05	2084.27	299.72	45.82	207.89	27.29	140.77	26.96	64.37	8.75	51.42	7.41	<0.55	0.01	3.82	33.01	5.09	31.8	38%	MCIC-1 Apt4 25um 7Hz 66% 2.07Jcm-2
Ap01a06	06	1672.69	244.47	45.72	174.70	22.67	134.40	23.28	59.50	8.68	49.62	7.68	0.20	0.00	3.24	17.56	2.20	17.3	11%	MCIC-1 Apt4 12um 7Hz 66% 2.18Jcm-2
Ap01a07	07	3426.32	446.72	52.57	319.68	41.69	201.07	36.68	92.49	10.30	65.75	8.58	0.00	0.08	3.24	95.50	10.35	24.5	10%	MCIC-1 Apt3 12um 7Hz 66% 2.13Jcm-2
Ap01a08	08	2983.99	427.32	70.32	275.55	36.28	191.48	34.61	87.16	12.24	79.82	10.70	0.03	0.04	3.93	83.77	9.13	41.9	36%	MCIC-1 Apt2 25um 7Hz 66% 2.23Jcm-2
Ap01a09	09	2789.96	387.73	61.87	252.63	34.06	200.92	36.84	87.64	12.01	90.80	10.64	0.28	<0.57	3.45	85.31	10.68	23.8	11%	MCIC-1 Apt1 12um 7Hz 66% -Jcm-2
Ap01a10		2510.73	384.57	64.17	254.03	31.85	159.94	28.09	63.87	7.98	48.95	6.44	0.07	0.02	3.71	77.37	10.04	44.8	37%	MCIC-1 Apt9 25um 7Hz 66% 2.02Jcm-2
Ap01a11		1983.93	276.56	58.04	151.40	18.33	94.39	14.73	38.81	5.17	32.62	4.28	0.18	0.07	4.00	63.66	5.26	18.8	11%	MCIC-1 Apt9 12um 7Hz 66% -Jcm-2
Ap01a12		1864.23	260.89	41.95	142.93	15.92	81.50	14.56	33.09	4.17	26.08	3.13	0.12	<0.38	7.22	44.27	6.92	46.2	34%	MCIC-1 Apt10 12um line 7Hz 66% 2.18Jcm-2
Ap01a13		1662.64	226.23	39.90	140.72	15.82	67.73	11.88	29.56	3.72	24.08	3.15	0.15	0.04	10.92	31.61	6.09	46.5	11%	MCIC-1 Apt10 6um line 7Hz 66% 2.07Jcm-2
Ap01a14		2719.54	380.61	55.06	231.68	27.54	136.76	26.21	64.60	8.23	51.95	6.59	0.17	0.08	3.11	69.95	9.05	39.0	48%	MCIC-1 Apt10 25um 7Hz 66% -Jcm-2
Ap01a15		3530.48	424.58	33.08	286.35	33.94	159.86	33.52	81.71	10.11	60.25	8.90	0.00	0.04	3.48	235.55	18.10	17.3	11%	MCIC-1 Apt5 12um 7Hz 66% 2.13Jcm-2
Ap01a16		3679.43	487.21	60.10	333.74	42.21	212.74	36.07	80.08	8.72	53.63	7.76	0.00	0.00	4.87	269.78	43.00	12.3	15%	MCIC-1 Apt6 12um 7Hz 66% -Jcm-2
Ap01a17	17	23.8	5.7	2	5.16	0.86	4.95	0.88	2.27	0.27	1.81	0.25	3.97	0.86	1.65	1.15	0.40	44.0	376%	BHVO 2g 12um 7Hz 66% 2.22Jcm-2
Ap01a18		23.3	6.2	2	5.36	0.81	4.73	0.89	2.20	0.27	1.83	0.24	3.94	0.91	1.71	1.18	0.41	39.7	357%	BHVO 2g 35um 7Hz 66% -Jcm-2
std-3		429.36	452.51	465.69	426.63	439.89	429.55	447.45	421.85	416.82	464.56	440.95	420.32	380.64	423.05	451.55	475.35	31.0	123%	NIST 610 40um 7Hz 66% -Jcm-2
std-4		432.24	448.48	456.50	413.15	445.72	423.43	451.36	430.17	423.39	458.42	428.43	415.07	372.55	403.51	449.65	438.75	28.9	130%	NIST 610 60um 7Hz 66% -Jcm-2

LA-ICP-MS Results (MCIC-3: Biotite ijolite)

LAM-ICP-MS RESULTS - DETECTION LIMIT FILTERED

MCIC-3 (Biotite ijolite) 04/01/11

		CaO	Sc	TiO2	TiO2	V	As	Se	Sr	Y	Zr	Nb	Ba	La	Ce	Pr	Peak	Abitn	Comments
Isotopic mass		43	45	47	49	51	75	77	88	89	90	93	137	139	140	141	secs	yield	
		wt%	ppm	wt%	wt%	ppm	ppm	ppm	ppm	ppm	ppm	ppm	ppm	ppm	ppm	ppm			
Chondrite		1.30	5.90	0.08	0.08	54.30	1.81	21.40	7.26	1.56	3.86	0.25	2.41	0.25	0.64	0.10			
Det. limit		0.02	0.18	0.01	0.00	0.08	0.68	2.15	0.11	0.01	0.04	0.01	0.12	0.01	0.01	0.01			
std-1		11.4	443.19	<0.37	0.07	440	318	111	497.72	455.00	446.25	422.73	417.58	461.00	450.42	435.51	36.1	139%	NIST 610 40um 74% 7Hz -Jcm-2
std-2		11.4	439.01	<0.78	0.07	444	317	107	497.08	444.80	433.54	416.07	430.63	453.81	445.19	424.09	43.3	90%	NIST 610 40um 74% 7Hz 2.49Jcm-2
Fe09c03	03	11.4	31.89	8.84	2.63	314	<1.87	<8.80	392	24	172	16.69	124.34	16.73	37.79	5.2	39.7	254%	BHVO 55um 74% 7Hz 2.28Jcm-2
Fe09c04	04	11	32.02	7.95	2.59	315	<2.18	<13.61	393	23	167	15.63	128.06	16.08	37.65	5.3	31.0	252%	BHVO 55um 74% 7Hz 2.10Jcm-2
Fe09c05	05	55.00	<3.72	<1.16	<0.01	843	<20.69	<23.76	5278.4	275	16.70	0.22	70.06	379.05	279.47	22.10	46.9	41%	MCIC-3 Ap1-1 25um 74% 7Hz -Jcm-2
Fe09c06	06	55.00	<9.17	<1.22	<0.00	915	<15.64	<34.43	5493.0	329	21.57	0.17	76.20	323.77	323.18	22.07	44.0	37%	MCIC-3 Ap1-2 25um 74% 7Hz -Jcm-2
Fe09c07	07	55.00	<8.31	<1.70	<0.01	921	<17.22	<61.05	4753.4	338	13.92	0.29	53.93	296.01	228.02	19.76	39.7	33%	MCIC-3 Ap2 25um 74% 7Hx -Jcm-2
Fe09c08	08	55.00	<7.15	<1.59	<0.01	763	<12.56	<94.69	4093.6	248	14.81	<0.75	67.44	295.40	210.60	17.77	36.1	39%	MCIC-3 Ap3-1 25um 74% 7Hz 2.07Jcm-2
Fe09c09	09	55	<4.20	<0.98	<0.01	825	<10.42	<50.87	4793.3	295	13.13	0.11	63.66	257.42	180.80	13.94	28.9	46%	MCIC-3 Ap3-2 25um 74% 7Hz -Jcm-2
Fe09c10	10	55	<6.00	<1.65	<0.00	936	<17.61	<95.97	5258.6	343	20.26	0.37	59.09	326.29	268.18	22.36	37.5	30%	MCIC-3 Ap4 25um 74% 7Hz -Jcm-2
Fe09c11	11	55	<7.09	<1.74	<0.01	843	<20.16	<28.87	5111.6	242	15.61	0.20	54.08	249.22	189.19	17.15	47.6	34%	MCIC-3 Ap5 25um 74% 7Hz -Jcm-2
Fe09c12	12	55	<4.41	<1.68	<0.01	967	<20.23	<52.41	4987.8	356	22.17	0.20	66.27	330.62	260.09	22.73	41.9	33%	MCIC-3 Ap6 25um 74% 7Hz 2.41Jcm-2
Fe09c13	13	55	<5.01	<1.45	<0.01	852	<16.11	<37.10	5253	348	15.7	0.33	79.31	299.45	222.82	19.240	27.4	41%	MCIC-3 Ap7 25um 74% 7Hz -Jcm-2
Fe09c14	14	55.00	<4.44	<1.75	<0.01	951	<19.78	<24.08	5485	323	17.3	0.28	72.60	319.46	243.69	20.104	40.4	34%	MCIC-3 Ap8 25um 74% 7Hz -Jcm-2
Fe09c15	15	55.0	<5.03	<1.56	<0.01	950	23	<53.17	5587	297	18.1	0.22	64.34	389.12	282.81	23.990	41.1	31%	MCIC-3 Ap9 25um 74% 7Hz -Jcm-2
Fe09c16	16	55.0	<6.78	<1.85	<0.01	871	62	<51.44	5947	325	18.0	0.39	76.11	446.75	337.91	24.89	39.7	31%	MCIC-3 Ap10 25um 74% 7Hz -Jcm-2
Fe09c17	17	11.4	31.42	4.06	2.66	319	<2.05	<5.58	392	24	163.9	15.54	126.54	16	36.7	5.0	44.0	253%	BHVO 55um 74% 7Hz 2.22Jcm-2
Fe09c18	18	11.4	32.33	3.88	2.61	313	<2.60	<6.40	395	24	170.0	15.76	131.71	17	36.9	5.2	44.0	243%	BHVO 55um 74% 7Hz -Jcm-2
std-3		11.40	434.49	<0.68	0.07	443.17	314.81	109.78	492.56	452.65	443.19	417.21	426.69	457.19	444.09	425.15	43.3	76%	NIST 610 40um 74% 7Hz -Jcm-2
std-4		11.40	447.72	<0.56	0.08	440.23	319.98	108.22	502.24	447.15	436.60	421.59	421.50	457.61	451.51	434.45	40.4	95%	NIST 610 40um 74% 7Hz -Jcm-2

LAM-ICP-MS RESULTS - DETECTION LIMIT FILTERED

MCIC-3 (Biotite ijolite) 04/01/11

		Nd	Sm	Eu	Gd	Tb	Dy	Ho	Er	Tm	Yb	Lu	Hf	Ta	Pb	Th	U	Peak	Abitn	Comments
		146	147	151	157	159	163	165	166	169	172	175	178	181	208	232	238	secs	yield	
		ppm	ppm	ppm	ppm	ppm	ppm	ppm	ppm	ppm	ppm	ppm	ppm	ppm	ppm	ppm	ppm			
Chondrite		0.47	0.15	0.06	0.20	0.04	0.25	0.06	0.17	0.03	0.17	0.03	0.11	0.01	2.53	0.03	0.01			
Det. limit		0.05	0.09	0.03	0.07	0.01	0.03	0.01	0.02	0.01	0.03	0.01	0.01	0.00	0.03	0.00	0.00			
std-1		432.49	451.45	463.24	424.94	450.26	431.85	455.10	435.02	424.83	467.14	438.87	423.53	380.83	414.67	453.10	454.04	36.1	139%	NIST 610 40um 74% 7Hz -Jcm-2
std-2		429.12	449.55	458.96	414.86	435.34	421.14	443.69	416.97	415.36	455.86	430.53	411.87	372.36	411.93	448.10	460.16	43.3	90%	NIST 610 40um 74% 7Hz 2.49Jcm-2
Fe09c03	03	25.9	6.31	2	6.13	0.88	5.20	1.02	2.40	<0.33	1.89	0.26	4.43	0.86	1.53	1.26	0.41	39.7	254%	BHVO 55um 74% 7Hz 2.28Jcm-2
Fe09c04	04	24.9	6.5	2	6.63	0.89	5.12	0.96	2.28	0.32	2.36	0.22	4.64	0.92	2.14	1.11	0.46	31.0	252%	BHVO 55um 74% 7Hz 2.10Jcm-2
Fe09c05	05	78.12	18.06	9.25	34.45	5.90	36.60	7.39	19.05	2.43	14.99	1.71	0.15	<0.24	1.30	0.76	1.80	46.9	41%	MCIC-3 Ap1-1 25um 74% 7Hz -Jcm-2
Fe09c06	06	82.12	20.49	9.40	35.49	6.65	40.20	8.30	19.64	2.77	14.63	2.07	0.12	0.00	0.46	0.73	2.35	44.0	37%	MCIC-3 Ap1-2 25um 74% 7Hz -Jcm-2
Fe09c07	07	75.09	24.79	10.99	48.48	7.81	51.40	10.68	28.42	3.30	18.81	2.60	0.73	0.03	0.41	0.31	1.76	39.7	33%	MCIC-3 Ap2 25um 74% 7Hx -Jcm-2
Fe09c08	08	57.12	17.38	8.23	27.36	5.04	32.35	6.87	16.88	1.84	11.15	1.72	0.00	0.00	<1.06	0.26	1.44	36.1	39%	MCIC-3 Ap3-1 25um 74% 7Hz 2.07Jcm-2
Fe09c09	09	51.90	14.11	7.82	27.89	5.68	37.92	7.94	20.47	2.94	15.54	1.80	0.00	0.00	<0.51	0.20	1.35	28.9	46%	MCIC-3 Ap3-2 25um 74% 7Hz -Jcm-2
Fe09c10	10	76.22	20.23	9.98	41.50	6.65	43.18	10.05	24.70	2.99	16.19	1.70	0.25	0.00	<5.92	0.59	1.81	37.5	30%	MCIC-3 Ap4 25um 74% 7Hz -Jcm-2
Fe09c11	11	62.20	16.13	7.72	32.11	5.12	33.59	7.16	18.83	2.17	12.61	1.29	0.18	0.01	0.47	0.38	1.38	47.6	34%	MCIC-3 Ap5 25um 74% 7Hz -Jcm-2
Fe09c12	12	83.27	23.49	11.35	41.97	7.27	47.69	10.13	25.46	3.33	17.07	1.96	0.14	0.00	0.38	0.94	2.26	41.9	33%	MCIC-3 Ap6 25um 74% 7Hz 2.41Jcm-2
Fe09c13	13	67.67	18.62	9.00	37.59	6.43	40.86	8.70	22.60	2.69	15.09	2.25	0.08	0.00	<0.45	0.42	1.50	27.4	41%	MCIC-3 Ap7 25um 74% 7Hz -Jcm-2
Fe09c14	14	75.81	21.03	9.34	37.54	7.02	45.05	9.51	22.33	2.81	15.92	1.76	0.07	0.00	0.53	0.59	2.25	40.4	34%	MCIC-3 Ap8 25um 74% 7Hz -Jcm-2
Fe09c15	15	81.89	21.77	10.18	38.08	6.70	42.02	8.92	24.45	2.90	14.94	1.65	0.00	<0.29	0.87	0.70	2.18	41.1	31%	MCIC-3 Ap9 25um 74% 7Hz -Jcm-2
Fe09c16	16	84.26	24.37	8.38	38.81	6.93	42.59	8.73	21.95	3.08	14.83	1.82	0.00	0.00	0.68	0.80	1.90	39.7	31%	MCIC-3 Ap10 25um 74% 7Hz -Jcm-2
Fe09c17	17	24.2	5.9	2	6.25	0.87	5.32	0.98	2.44	0.30	1.86	0.26	4.55	1.00	1.41	1.30	0.41	44.0	253%	BHVO 55um 74% 7Hz 2.22Jcm-2
Fe09c18	18	24.4	6.1	2	5.90	0.95	5.01	0.97	2.42	0.34	1.93	0.28	4.20	0.89	1.49	1.23	0.43	44.0	243%	BHVO 55um 74% 7Hz -Jcm-2
std-3		433.22	443.40	456.59	419.02	441.55	424.15	447.33	420.49	417.59	459.00	427.43	414.56	368.61	418.70	451.40	457.14	43.3	76%	NIST 610 40um 74% 7Hz -Jcm-2
std-4		428.38	457.60	465.61	420.78	444.05	428.85	451.48	431.51	422.61	464.00	441.98	420.84	384.61	407.91	449.80	457.06	40.4	95%	NIST 610 40um 74% 7Hz -Jcm-2

LA-ICP-MS Results (MCIC-4: Jacupirangite)

LAM-ICP-MS RESULTS - DETECTION LIMIT FILTERED

MCIC-4 (Jacupirangite) — **02/19/11**

Isotopic mass		CaO 43	Sc 45	TiO2 47	TiO2 49	V 51	As 75	Se 77	Sr 88	Y 89	Zr 90	Nb 93	Ba 137	La 139	Ce 140	Pr 141	Peak secs	Abltn yield	Comments
		wt%	ppm	wt%	wt%	ppm	ppm	ppm	ppm	ppm	ppm	ppm	ppm	ppm	ppm	ppm			
Chondrite		1.30	5.90	0.08	0.08	54.30	1.81	21.40	7.26	1.56	3.86	0.25	2.41	0.25	0.64	0.10			
Det. limit		0.06	0.59	0.02	0.00	0.24	2.12	4.99	0.24	0.09	0.08	0.02	0.26	0.04	0.04	0.03			
std-1		11.4	441.70	<0.61	0.07	427	305	109	483.30	444.08	435.77	414.52	404.64	447.43	434.28	414.11	46.2	127%	NIST 610 40um 74% 7Hz 2.42Jcm-2
std-2		11.4	440.50	<0.72	0.07	457	330	109	511.47	455.71	444.03	424.27	443.49	467.36	461.29	445.46	42.6	84%	NIST 610 40um 74% 7Hz 2.49Jcm-2
Fe09b03	03	55.0	165.34	21.30	11.92	1526	<20.58	<66.28	1894	117	800	77.56	605.71	76.20	176.32	23.1	42.6	33%	BHVO 40um 74% 7Hz -Jcm-2
Fe09b04	04	55	157.10	22.04	12.11	1549	<21.11	<36.01	1920	124	813	76.93	598.52	77.21	180.39	23.5	43.3	33%	BHVO 40um 74% 7Hz -Jcm-2
Fe09b05	05	55.00	<14.49	<2.10	<0.01	347	26	15	5540.1	177	12.33	0.50	5.08	771.21	1382.84	159.82	44.0	27%	MCIC-4 Ap1 25um 74% 7Hz -Jcm-2
Fe09b06	06	55.00	<9.92	<2.01	<0.02	314	<21.08	<85.42	6063.5	265	13.92	0.26	1.42	1569.40	2536.60	252.29	38.3	32%	MCIC-4 Ap2 25um 74% 7Hz -Jcm-2
Fe09b07	07	55.00	<7.12	<1.69	<0.00	387	<22.05	<27.24	5972.8	251	20.54	0.57	9.49	1206.27	2255.20	261.84	41.9	39%	MCIC-4 Ap3 25um 74% 7Hz 2.54Jcm-2
Fe09b08	08	55.00	<7.87	<1.55	0.01	358	34	<55.89	5804.0	243	16.50	0.16	11.50	1303.96	2142.14	231.98	30.3	44%	MCIC-4 Ap4 25um 74% 7Hz -Jcm-2
Fe09b09	09	55	<6.20	<1.87	0	382	<29.06	<61.32	5711.7	236	20.86	0.58	4.69	1098.31	1955.28	221.66	41.9	35%	MCIC-4 Ap5 25um 74% 7Hz -Jcm-2
Fe09b10	10	55	<7.31	<1.39	<0.00	297	<16.24	<45.01	5814.2	168	10.60	0.14	3.85	1041.41	1639.27	169.48	28.2	41%	MCIC-4 Ap6 25um 74% 7Hz -Jcm-2
Fe09b11	11	55	<6.64	<1.89	<0.00	359	<24.29	<40.98	5152.9	207	14.95	0.36	16.77	836.31	1546.00	187.15	42.6	35%	MCIC-4 Ap7 25um 74% 7Hz -Jcm-2
Fe09b12	12	55	<7.89	<1.85	0	364	<19.15	<64.49	6966.4	232	6.82	0.41	15.15	1286.16	1967.97	201.48	38.3	34%	MCIC-4 Ap8 25um 74% 7Hz -Jcm-2
Fe09b13	13	55	<3.94	<1.39	<0.01	383	<18.46	<32.50	5268	203	17.1	0.34	10.98	894.99	1738.04	217.049	24.5	39%	MCIC-4 Ap9 25um 74% 7Hx -Jcm-2
Fe09b14	14	55.00	16.73	153.85	69.19	1266	<22.01	42	1156	587	2870.4	4041.11	0.23	1554.99	3853.11	508.036	44.8	23%	MCIC-4 Sphene 25um 74% 7Hz -Jcm-2
Fe09b15	15	55.0	<9.75	<1.76	0.01	359	<19.76	<31.58	6042	372	19.2	0.30	6.18	2298.25	3623.94	396.628	45.5	35%	MCIC-4 Ap10 25um 74% 7Hz -Jcm-2
Fe09b16	16	55.0	<7.78	<1.46	<0.01	291	51	<53.31	5516	215	13.4	0.43	11.81	1409.64	2276.77	238.09	36.1	34%	MCIC-4 Ap11 25um 74% 7Hz -Jcm-2
Fe09b17	17	55.0	147.78	27.68	12.60	1471	<29.73	<40.27	1818	115	786.6	74.04	575.54	75	165.9	21.7	42.6	34%	BHVO 40um 74% 7Hz -Jcm-2
Fe09b18	18	55.0	159.71	28.35	12.72	1474	<15.02	<54.07	1795	119	829.6	72.18	550.53	75	167.3	22.7	41.9	33%	BHVO 40um 74% 7Hz -Jcm-2
std-3		11.40	447.15	<0.77	0.07	450.49	318.06	110.68	501.46	451.00	434.25	422.75	432.14	463.03	452.28	428.90	43.3	94%	NIST 610 40um 74% 7Hz 2.62Jcm-2
std-4		11.40	435.05	<0.72	0.07	432.92	316.74	107.33	493.35	448.80	445.55	416.06	416.09	451.78	443.34	430.69	44.0	94%	NIST 610 40um 74% 7Hz -Jcm-2

LAM-ICP-MS RESULTS - DETECTION LIMIT FILTERED

MCIC-4 (Jacupirangite) — **02/19/11**

Isotopic mass		Nd 146	Sm 147	Eu 151	Gd 157	Tb 159	Dy 163	Ho 165	Er 166	Tm 169	Yb 172	Lu 175	Hf 178	Ta 181	Pb 208	Th 232	U 238	Peak secs	Abltn yield	Comments
		ppm	ppm	ppm	ppm	ppm	ppm	ppm	ppm	ppm	ppm	ppm	ppm	ppm	ppm	ppm	ppm			
Chondrite		0.47	0.15	0.06	0.20	0.04	0.25	0.06	0.17	0.03	0.17	0.03	0.11	0.01	2.53	0.03	0.01			
Det. limit		0.15	0.15	0.13	0.21	0.02	0.09	0.01	0.08	0.03	0.14	0.01	0.06	0.01	0.08	0.02	0.00			
std-1		415.60	441.55	445.87	411.82	431.62	419.18	443.70	417.28	415.31	453.12	426.41	415.46	368.86	398.20	438.01	427.35	46.2	127%	NIST 610 40um 74% 7Hz 2.42Jcm-2
std-2		445.96	459.42	476.31	427.97	453.97	433.81	455.10	434.71	424.89	469.87	442.98	419.94	384.34	428.38	463.17	486.79	42.6	84%	NIST 610 40um 74% 7Hz 2.49Jcm-2
Fe09b03	03	115.9	28.66	10	30.19	4.16	25.70	4.63	13.33	1.44	10.04	1.51	21.02	4.59	7.97	6.02	2.12	42.6	33%	BHVO 40um 74% 7Hz -Jcm-2
Fe09b04	04	119.0	30.0	10	32.29	4.36	24.85	4.93	13.47	1.45	9.61	1.12	23.70	5.04	7.23	5.82	2.18	43.3	33%	BHVO 40um 74% 7Hz -Jcm-2
Fe09b05	05	676.39	106.86	29.09	80.46	7.90	41.36	6.24	14.46	1.57	7.86	0.82	0.09	0.02	7.79	27.80	4.77	44.0	27%	MCIC-4 Ap1 25um 74% 7Hz -Jcm-2
Fe09b06	06	966.71	135.72	34.93	102.06	13.29	59.31	9.14	21.58	2.58	13.82	1.78	0.00	0.00	7.98	78.17	14.86	38.3	32%	MCIC-4 Ap2 25um 74% 7Hz -Jcm-2
Fe09b07	07	1080.71	166.97	43.58	111.55	13.30	60.09	10.36	21.69	2.13	13.05	1.37	0.07	0.01	10.74	55.50	8.37	41.9	39%	MCIC-4 Ap3 25um 74% 7Hz 2.54Jcm-2
Fe09b08	08	965.27	139.31	40.45	106.35	12.46	57.40	9.46	19.88	2.57	13.06	1.44	<2.70	<0.23	10.16	36.54	3.62	30.3	44%	MCIC-4 Ap4 25um 74% 7Hz -Jcm-2
Fe09b09	09	893.11	147.06	40.42	104.60	11.40	59.26	9.04	18.86	2.14	<11.41	1.22	0.00	0.01	5.23	52.17	6.20	41.9	35%	MCIC-4 Ap5 25um 74% 7Hz -Jcm-2
Fe09b10	10	653.85	104.26	27.82	74.17	8.26	41.75	7.58	15.17	1.85	8.44	1.01	0.00	0.03	4.06	72.64	11.56	28.2	41%	MCIC-4 Ap6 25um 74% 7Hz -Jcm-2
Fe09b11	11	768.20	128.74	34.08	85.69	10.00	46.25	7.61	15.45	1.48	9.39	1.01	0.00	0.00	4.32	33.78	2.41	42.6	35%	MCIC-4 Ap7 25um 74% 7Hz -Jcm-2
Fe09b12	12	754.18	117.44	30.32	84.52	10.48	45.56	8.29	17.01	1.93	9.44	1.25	0.00	0.00	4.32	76.32	16.51	38.3	34%	MCIC-4 Ap8 25um 74% 7Hz -Jcm-2
Fe09b13	13	866.88	135.13	37.18	96.94	10.55	51.20	7.80	17.78	1.29	9.56	0.85	<1.05	0.04	5.65	42.82	5.50	24.5	39%	MCIC-4 Ap9 25um 74% 7Hx -Jcm-2
Fe09b14	14	2219.54	398.45	105.26	270.00	34.45	168.39	28.69	54.54	6.78	35.07	3.33	51.27	234.01	2.63	245.03	40.93	44.8	23%	MCIC-4 Sphene 25um 74% 7Hz -Jcm-2
Fe09b15	15	1399.09	200.56	53.77	139.57	16.09	77.45	13.79	28.35	3.08	19.49	2.22	0.13	0.02	7.22	112.18	19.19	45.5	35%	MCIC-4 Ap10 25um 74% 7Hz -Jcm-2
Fe09b16	16	889.83	123.44	31.28	88.71	10.12	45.48	8.49	17.83	1.88	11.54	1.46	0.09	0.06	8.43	66.81	7.13	36.1	34%	MCIC-4 Ap11 25um 74% 7Hz -Jcm-2
Fe09b17	17	112.8	26.6	9	26.68	3.90	23.91	3.88	11.66	1.30	9.33	1.47	23.10	4.90	7.12	5.07	1.81	42.6	34%	BHVO 40um 74% 7Hz -Jcm-2
Fe09b18	18	111.5	28.6	9	28.09	3.95	24.77	4.37	12.48	1.20	8.53	1.16	19.12	4.25	7.22	5.45	1.67	41.9	33%	BHVO 40um 74% 7Hz -Jcm-2
std-3		433.96	454.12	460.32	417.62	446.83	425.94	451.79	427.92	422.81	465.30	435.17	412.71	377.36	405.78	446.66	454.19	43.3	94%	NIST 610 40um 74% 7Hz 2.62Jcm-2
std-4		427.65	446.89	461.88	422.18	438.77	427.06	447.01	424.08	417.39	457.70	434.23	422.68	375.84	420.81	454.53	460.00	44.0	94%	NIST 610 40um 74% 7Hz -Jcm-2

LA-ICP-MS Results (MCIC-5A: Carbonatite)

LAM-ICP-MS RESULTS - DETECTION LIMIT FILTERED

MCIC-5A (Carbonatite) — **02/18/11**

Isotopic mass		CaO 43 wt%	Sc 45 ppm	TiO2 47 wt%	TiO2 49 wt%	V 51 ppm	As 75 ppm	Se 77 ppm	Sr 88 ppm	Y 89 ppm	Zr 90 ppm	Nb 93 ppm	Ba 137 ppm	La 139 ppm	Ce 140 ppm	Pr 141 ppm	Peak secs	Abitn yield	Comments
Chondrite		1.30	5.90	0.08	0.08	54.30	1.81	21.40	7.26	1.56	3.86	0.25	2.41	0.25	0.64	0.10			
Det. limit		0.04	0.22	0.01	0.00	0.63	0.72	2.41	0.78	0.34	0.16	0.04	0.17	0.56	0.57	0.16			
std-1		11.4	444.11	<1.21	0.07	439	327	101	497.85	454.38	442.87	413.38	419.47	459.66	444.91	439.01	47.6	70%	NIST610 40um 7Hz 74% 2.62Jcm-2
std-2		11.4	438.09	<1.19	0.07	445	307	117	496.95	445.43	436.94	425.41	428.72	455.14	450.68	420.62	33.2	70%	NIST610 40um 7Hz 74% 2.56Jcm-2
Fe09a03	03	11.4	30.23	17.84	2.46	307	<3.35	<6.56	382	24	164	15.45	123.14	15.76	35.21	4.9	49.8	352%	BHVO 55um 74% 7Hz 2.34Jcm-2
Fe09a04	04	11	30.08	14.95	2.48	308	<2.49	<9.41	383	24	165	15.68	120.11	16.00	34.64	4.8	54.1	356%	MCIC-5A Ap1 25um 74% 7Hz 2.34Jcm-2
Fe09a05	05	55.00	<14.57	<2.97	<0.01	1214	66	<80.33	3026.0	692	47.64	0.32	5.57	3490.60	3845.09	342.43	49.8	34%	MCIC-5A Ap2 25um 74% 7Hz 2.20Jcm-2
Fe09a06	06	55.00	<10.66	<2.13	<0.01	1232	78	<92.39	3038.3	635	63.92	2.01	5.81	3507.05	3945.01	330.17	49.1	39%	MCIC-5A Ap3 25um 74% 7Hz 2.15Jcm-2
Fe09a07	07	55.00	<11.93	<2.35	<0.01	1231	66	<93.50	3050.9	658	39.81	0.46	<4.13	3382.99	3860.82	327.07	51.3	36%	MCIC-5A Ap3 25um 74% 7Hz 2.20Jcm-2
Fe09a08	08	55.00	<31.80	<6.85	<0.07	997	<68.11	<263.44	3420.3	557	75.61	2.14	184.90	2979.08	3207.95	285.36	31.8	13%	MCIC-5A Ap4 15um 74% 7Hz -Jcm-2
Fe09a09	09	55	<8.65	<1.87	<0.01	1140	69	<83.23	2923.4	606	62.69	2.82	22.21	3131.12	3442.26	299.41	47.6	42%	MCIC-5A Ap5 25um 74% 7Hz 2.15Jcm-2
Fe09a11	11	55	<9.13	<2.49	<0.02	1186	62	<88.22	3099.1	676	76.52	0.94	4.21	3578.10	3886.52	335.90	53.4	36%	MCIC-5A Ap7 25um 74% 7Hz -Jcm-2
Fe09a12	12	55	1312	24	10	78	<36.69	<69.73	192.4	2306	0.05	11797.38	0.62	438.01	1295.24	192.36	49.8	23%	MCIC-5A Kim1 25um 74% 7Hz 2.24Jcm-2
Fe09a13	13	55	<6.52	<1.54	<0.01	<1.98	<13.98	<48.10	5086	8	<1.31	0.00	79.26	48.68	38.42	3.169	33.9	56%	MCIC-5A Cal 25um 74% 7Hz -Jcm-2
Fe09a14	14	55.00	<8.42	<2.39	<0.01	1037	58	<99.91	3238	475	28.0	1.62	20.09	2540.47	2734.68	230.628	52.0	37%	MCIC-5A Ap8 25um 74% 7Hz -Jcm-2
Fe09a15	15	55.0	<4.58	<2.17	<0.00	1283	70	<85.08	2985	574	44.2	1.81	18.98	3047.37	3335.38	281.467	53.4	40%	MCIC-5A Ap9 25um 74% 7Hz -Jcm-2
Fe09a16	16	55.0	<6.86	<2.01	<0.01	1291	62	<110.25	3184	686	53.1	0.20	6.68	3620.39	3938.72	323.32	54.1	43%	MCIC-5A Ap10 25um 74% 7Hz -Jcm-2
Fe09a17	17	11.4	31.07	4.81	2.54	312	<1.76	<7.10	383	24	164.0	15.77	119.82	16	34.4	5.0	54.1	491%	BHVO 55um 74% 7Hz 2.65Jcm-2
Fe09a18	18	11.4	30.84	4.58	2.53	314	<1.62	<9.21	391	25	169.1	15.76	128.05	16	35.9	5.1	54.9	451%	BHVO 55um 74% 7Hz 2.71Jcm-2
std-3		11.40	441.52	<0.69	0.08	440.41	322.66	111.87	500.69	455.17	438.92	425.62	420.74	460.15	450.99	433.28	54.1	129%	NIST610 40um 74% 7Hz -Jcm-2
std-4		11.40	440.68	<0.69	0.07	442.99	312.15	106.14	494.12	444.64	440.87	413.19	427.45	454.65	444.62	426.33	53.4	131%	NIST610 40um 74% 7Hz -Jcm-2

LAM-ICP-MS RESULTS - DETECTION LIMIT FILTERED

MCIC-5A (Carbonatite) — **02/18/11**

Isotopic mass		Nd 146 ppm	Sm 147 ppm	Eu 151 ppm	Gd 157 ppm	Tb 159 ppm	Dy 163 ppm	Ho 165 ppm	Er 166 ppm	Tm 169 ppm	Yb 172 ppm	Lu 175 ppm	Hf 178 ppm	Ta 181 ppm	Pb 208 ppm	Th 232 ppm	U 238 ppm	Peak secs	Abitn yield	Comments
Chondrite		0.47	0.15	0.06	0.20	0.04	0.25	0.06	0.17	0.03	0.17	0.03	0.11	0.01	2.53	0.03	0.01			
Det. limit		0.72	0.31	0.11	0.28	0.05	0.19	0.04	0.12	0.02	0.12	0.02	0.03	0.00	0.04	0.01	0.05			
std-1		430.47	455.23	462.35	419.09	446.39	430.16	452.83	431.77	420.62	461.51	440.21	428.62	376.99	408.26	454.18	466.10	47.6	70%	NIST610 40um 7Hz 74% 2.62Jcm-2
std-2		431.13	445.78	459.86	420.71	439.23	422.86	445.99	420.25	419.59	461.49	429.23	406.87	376.21	418.33	447.05	448.13	33.2	70%	NIST610 40um 7Hz 74% 2.56Jcm-2
Fe09a03	03	23.2	5.40	2	5.66	0.94	5.06	0.95	2.29	0.29	1.89	0.27	4.24	1.05	1.48	1.27	0.40	49.8	352%	BHVO 55um 74% 7Hz 2.34Jcm-2
Fe09a04	04	24.0	5.6	2	5.01	0.87	4.98	0.90	2.24	0.26	2.05	0.26	4.83	0.95	1.52	1.20	0.42	54.1	356%	MCIC-5A Ap1 25um 74% 7Hz 2.34Jcm-2
Fe09a05	05	1127.15	185.81	65.42	178.05	24.61	138.33	23.85	52.67	6.55	35.74	3.96	0.00	0.00	<1.13	<1.16	52.93	49.8	34%	MCIC-5A Ap2 25um 74% 7Hz 2.20Jcm-2
Fe09a06	06	1078.70	168.59	58.36	154.69	21.99	119.44	22.12	48.01	5.91	33.07	4.14	0.00	0.00	<1.71	0.31	63.37	49.1	39%	MCIC-5A Ap3 25um 74% 7Hz 2.15Jcm-2
Fe09a07	07	1115.46	169.12	61.75	164.32	23.96	120.83	21.65	48.41	6.09	30.99	3.76	0.92	0.01	0.97	0.51	42.03	51.3	36%	MCIC-5A Ap3 25um 74% 7Hz 2.20Jcm-2
Fe09a08	08	974.54	139.35	50.05	121.94	20.19	99.84	15.49	38.16	7.08	28.79	3.32	0.00	0.00	3.07	<2.37	42.07	31.8	13%	MCIC-5A Ap4 15um 74% 7Hz -Jcm-2
Fe09a09	09	971.26	161.48	56.72	139.47	20.67	110.70	19.13	40.68	5.08	29.70	3.06	0.00	0.00	1.24	0.56	41.22	47.6	42%	MCIC-5A Ap5 25um 74% 7Hz 2.15Jcm-2
Fe09a11	11	1071.31	180.94	57.88	161.82	22.47	116.98	21.62	49.21	6.18	32.66	4.03	0.17	0.00	2.66	0.44	54.18	53.4	36%	MCIC-5A Ap7 25um 74% 7Hz -Jcm-2
Fe09a12	12	953.79	304.37	137.46	384.42	71.12	479.19	92.40	231.46	30.54	179.82	21.20	1712.58	16.83	0.63	0.32	295.65	49.8	23%	MCIC-5A Kim1 25um 74% 7Hz 2.24Jcm-2
Fe09a13	13	7.32	1.41	<0.92	1.47	<0.58	1.33	0.28	<0.96	0.09	0.70	0.07	0.76	0.00	0.67	0.00	0.00	33.9	56%	MCIC-5A Cal 25um 74% 7Hz -Jcm-2
Fe09a14	14	762.43	120.96	42.38	107.17	16.17	85.07	14.36	34.66	3.43	21.44	2.75	<1.88	0.00	<5.90	0.48	30.27	52.0	37%	MCIC-5A Ap8 25um 74% 7Hz -Jcm-2
Fe09a15	15	944.91	149.60	54.27	138.11	19.39	102.35	18.00	39.52	5.11	27.50	3.42	0.00	0.00	1.41	0.56	38.90	53.4	40%	MCIC-5A Ap9 25um 74% 7Hz -Jcm-2
Fe09a16	16	1064.65	171.65	60.20	156.20	21.72	120.87	21.19	48.05	5.84	33.73	3.68	0.14	0.00	1.30	0.58	58.42	54.1	43%	MCIC-5A Ap10 25um 74% 7Hz -Jcm-2
Fe09a17	17	23.5	5.6	2	5.85	0.85	4.81	0.96	2.39	0.31	2.01	0.28	4.53	0.83	1.42	1.16	0.39	54.1	491%	BHVO 55um 74% 7Hz 2.65Jcm-2
Fe09a18	18	24.5	6.1	2	5.81	0.95	5.11	1.05	2.46	0.33	2.02	0.29	4.16	0.93	1.42	1.24	0.46	54.9	451%	BHVO 55um 74% 7Hz 2.71Jcm-2
std-3		433.42	453.40	454.82	420.23	446.59	426.02	447.81	432.75	421.69	464.73	441.54	425.21	379.07	413.06	459.40	461.31	54.1	129%	NIST610 40um 74% 7Hz -Jcm-2
std-4		428.19	447.61	467.36	419.57	439.03	426.97	450.98	419.27	418.52	458.28	427.90	410.24	374.14	413.54	441.86	452.91	53.4	131%	NIST610 40um 74% 7Hz -Jcm-2

LA-ICP-MS Results (MCIC-5B: Carbonatite)

LAM-ICP-MS RESULTS - DETECTION LIMIT FILTERED

MCIC-5B (Carbonatite)

04/01/11

		CaO	Sc	TiO2	TiO2	V	As	Se	Sr	Y	Zr	Nb	Ba	La	Ce	Pr	Peak	Abitn	Comments
Isotopic mass		43	45	47	49	51	75	77	88	89	90	93	137	139	140	141	secs	yield	
		wt%	ppm	wt%	wt%	ppm	ppm	ppm	ppm	ppm	ppm	ppm	ppm	ppm	ppm	ppm			
Chondrite		1.30	5.90	0.08	0.08	54.30	1.81	21.40	7.26	1.56	3.86	0.25	2.41	0.25	0.64	0.10			
Det. limit		0.04	0.41	0.01	0.00	5.40	1.20	2.79	0.19	0.05	0.11	0.03	0.33	0.02	0.01	0.01			
std-1	0:	11.4	442.58	<0.28	0.07	437	307	109	484.03	441.34	432.14	411.59	419.73	448.00	442.93	422.77	28.9	137%	NIST 610 40um 7Hz 74% -Jcm-2
std-2	0:	11.4	439.61	<0.71	0.07	446	328	109	510.94	458.57	447.75	427.30	428.53	466.93	452.74	436.91	41.1	69%	NIST 610 40um 7Hz 74% 2.62Jcm-2
Ma30a03		11.4	31.29	4.60	2.65	319	<2.62	<9.61	400	24	162	17.17	139.25	17.47	40.46	5.6	42.6	248%	BHVO 2g 55um 7Hz 74% 2.46Jcm-2
Ma30a04		56	148.79	22.32	12.61	1510	<13.84	<55.84	1908	112	783	79.85	654.88	85.61	191.26	26.3	42.6	55%	BHVO 2g 55um 7Hz 74% -Jcm-2
Ma30a06		55.60	<17.06	<2.25	<0.03	1385	60	<85.17	4044.9	1035	99.23	0.41	<29.16	6131.93	6631.52	549.39	42.6	24%	MCIC-5B apt2 30um 7Hz 74% 2.29Jcm-2
Ma30a07		55.60	<14.32	<1.90	<0.03	1282	75	<86.40	3740.7	912	63.64	<1.09	<22.95	4964.70	5366.83	440.78	38.3	25%	MCIC-5B apt3 30um 7Hz 74% 2.39Jcm-2
Ma30a08		55.60	<83.07	<9.61	<0.18	1373	<147.52	<519.73	2766.1	642	67.00	2.67	<47.39	3246.78	3604.70	282.21	17.3	6%	MCIC-5B apt6 30um 7Hz 74% 2.44Jcm-2
Ma30a09		56	<45.48	<5.55	<0.07	1434	<131.03	<271.55	3411.0	801	95.48	<2.62	<75.10	5421.87	6218.70	494.57	27.4	8%	MCIC-5B apt 4 40um 7Hz 74% 2.49Jcm-2
Ma30a10		56	<66.11	<7.52	<0.14	1330	109	<300.46	3744.2	853	75.96	<9.18	15.92	4566.50	4706.19	425.27	41.9	7%	MCIC-5B apt5 40um 7Hz 74% 2.29Jcm-2
Ma30a11		56	<15.81	<1.87	<0.03	1349	69	<136.70	3825.3	890	67.52	<3.72	<18.73	4733.14	5157.31	414.55	41.1	24%	MCIC-5B apt1 30um 7Hz 74% 2.02Jcm-2
Ma30a12		11	34	5	3	330	<3.73	<3.49	477.5	31	212.22	18.86	170.22	22.09	48.76	6.46	44.0	211%	BHVO 2g 55um 7Hz 74% 2.34Jcm-2
Ma30a13		11	35	5	3	323	<4.46	<7.43	473	32	213.6	20.01	171.72	22.83	50.03	6.882	33.9	224%	BHVO 2g 55um 7Hz 74% 2.34Jcm-2
std-3	1:	11.40	441.32	<0.41	0.07	423	251	102	463	423	419.1	398.29	377.49	423.71	411.33	406.640	39.7	118%	NIST 610 40um 7Hz 74% 2.62Jcm-2
std-4	1:	11.4	440.88	<0.59	0.08	461	387	116	533	478	461.0	440.80	471.51	491.68	484.90	453.277	39.7	76%	NIST 610 40um 7Hz 74% -Jcm-2

LAM-ICP-MS RESULTS - DETECTION LIMIT FILTERED

MCIC-5B (Carbonatite)

04/01/11

		Nd	Sm	Eu	Gd	Tb	Dy	Ho	Er	Tm	Yb	Lu	Hf	Ta	Pb	Th	Peak	Abitn	Comments
		146	147	151	157	159	163	165	166	169	172	175	178	181	208	232	secs	yield	
		ppm	ppm	ppm	ppm	ppm	ppm	ppm	ppm	ppm	ppm	ppm	ppm	ppm	ppm	ppm			
Chondrite		0.47	0.15	0.06	0.20	0.04	0.25	0.06	0.17	0.03	0.17	0.03	0.11	0.01	2.53	0.03			
Det. limit		0.05	0.06	0.03	0.21	0.01	0.02	0.01	0.03	0.01	0.01	0.01	0.02	0.01	0.11	0.01			
std-1	0:	427.22	448.94	449.77	414.84	444.61	428.86	442.41	422.28	416.01	449.15	430.02	410.75	369.30	399.76	438.47	28.9	137%	NIST 610 40um 7Hz 74% -Jcm-2
std-2	0:	434.42	452.08	472.58	425.03	440.96	424.10	456.51	429.79	424.27	474.11	439.49	424.83	383.96	427.00	463.01	41.1	69%	NIST 610 40um 7Hz 74% 2.62Jcm-2
Ma30a03		25.8	6.35	2	5.58	0.90	5.32	1.01	2.26	0.30	2.33	0.29	4.35	0.96	1.63	1.28	42.6	248%	BHVO 2g 55um 7Hz 74% 2.46Jcm-2
Ma30a04		125.1	33.7	11	25.75	4.17	25.57	4.91	11.07	1.62	9.68	1.24	22.35	4.87	8.10	6.14	42.6	55%	BHVO 2g 55um 7Hz 74% -Jcm-2
Ma30a06		1741.44	291.01	97.63	262.73	37.50	197.93	36.10	77.76	9.56	54.58	6.71	0.22	0.00	<2.94	0.94	42.6	24%	MCIC-5B apt2 30um 7Hz 74% 2.29Jcm-2
Ma30a07		1443.40	240.44	82.43	224.86	30.84	169.56	29.85	69.22	7.78	49.44	5.27	0.24	<0.83	<3.30	0.92	38.3	25%	MCIC-5B apt3 30um 7Hz 74% 2.39Jcm-2
Ma30a08		947.44	133.33	53.46	176.09	20.10	110.21	18.93	48.27	3.71	34.53	7.27	7.16	0.18	<15.13	<1.62	17.3	6%	MCIC-5B apt6 30um 7Hz 74% 2.44Jcm-2
Ma30a09		1515.64	224.19	73.50	244.06	35.09	179.42	31.82	77.80	7.51	47.30	7.16	0.00	0.00	<10.55	1.45	27.4	8%	MCIC-5B apt 4 40um 7Hz 74% 2.49Jcm-2
Ma30a10		1287.30	221.18	77.16	204.53	30.45	154.09	25.90	66.87	8.28	49.68	5.98	0.00	0.00	<11.98	<2.20	41.9	7%	MCIC-5B apt5 40um 7Hz 74% 2.29Jcm-2
Ma30a11		1367.22	223.56	73.85	218.35	30.30	160.73	29.20	68.71	7.58	48.06	6.42	0.40	0.00	<3.46	0.65	41.1	24%	MCIC-5B apt1 30um 7Hz 74% 2.02Jcm-2
Ma30a12		32.96	7.26	2.64	7.94	1.27	7.19	1.34	3.31	0.49	3.12	0.47	7.80	1.07	1.89	1.86	44.0	211%	BHVO 2g 55um 7Hz 74% 2.34Jcm-2
Ma30a13		31.76	7.73	2.49	8.17	1.20	8.33	1.41	3.96	0.47	3.00	0.48	7.80	1.21	1.86	2.02	33.9	224%	BHVO 2g 55um 7Hz 74% 2.34Jcm-2
std-3	1:	404.76	422.22	435.41	393.28	410.99	394.23	411.21	387.27	376.83	402.57	378.23	347.63	346.54	373.51	387.69	39.7	118%	NIST 610 40um 7Hz 74% 2.62Jcm-2
std-4	1:	457.20	479.10	487.20	446.99	475.18	459.38	488.47	465.69	464.51	522.15	493.14	490.59	406.95	453.64	515.58	39.7	76%	NIST 610 40um 7Hz 74% -Jcm-2

Appendix 9

LA-ICP-MS Results: Chondrite-normalized apatite REE concentration plots

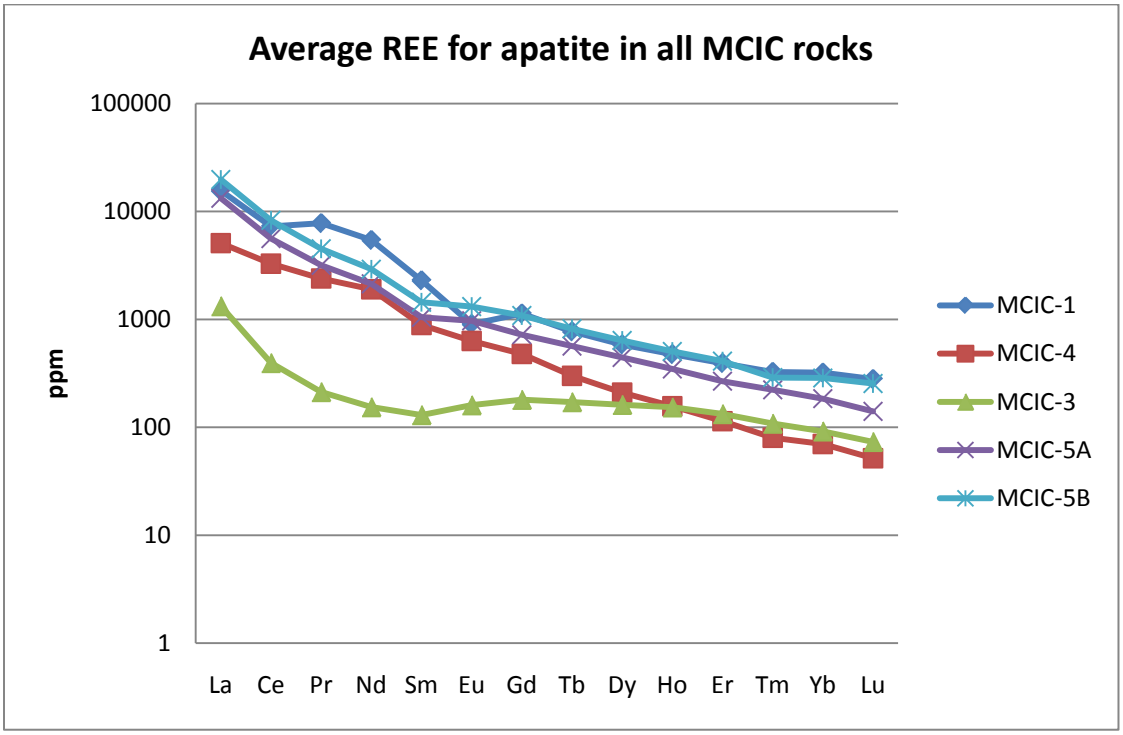

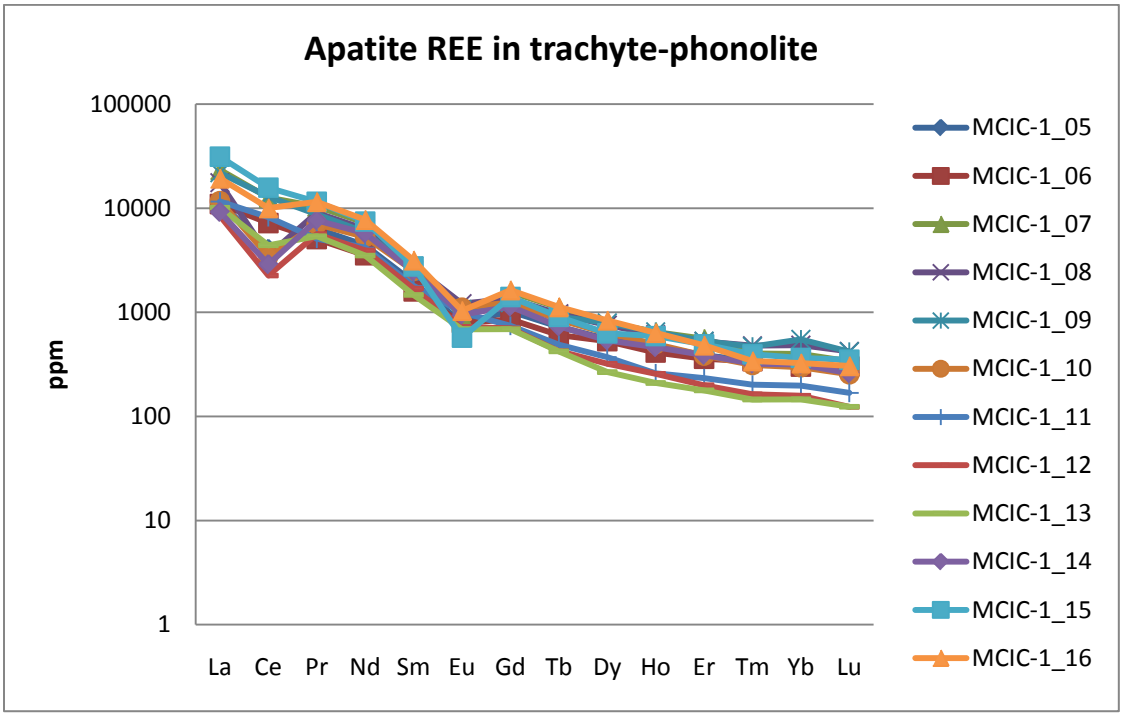

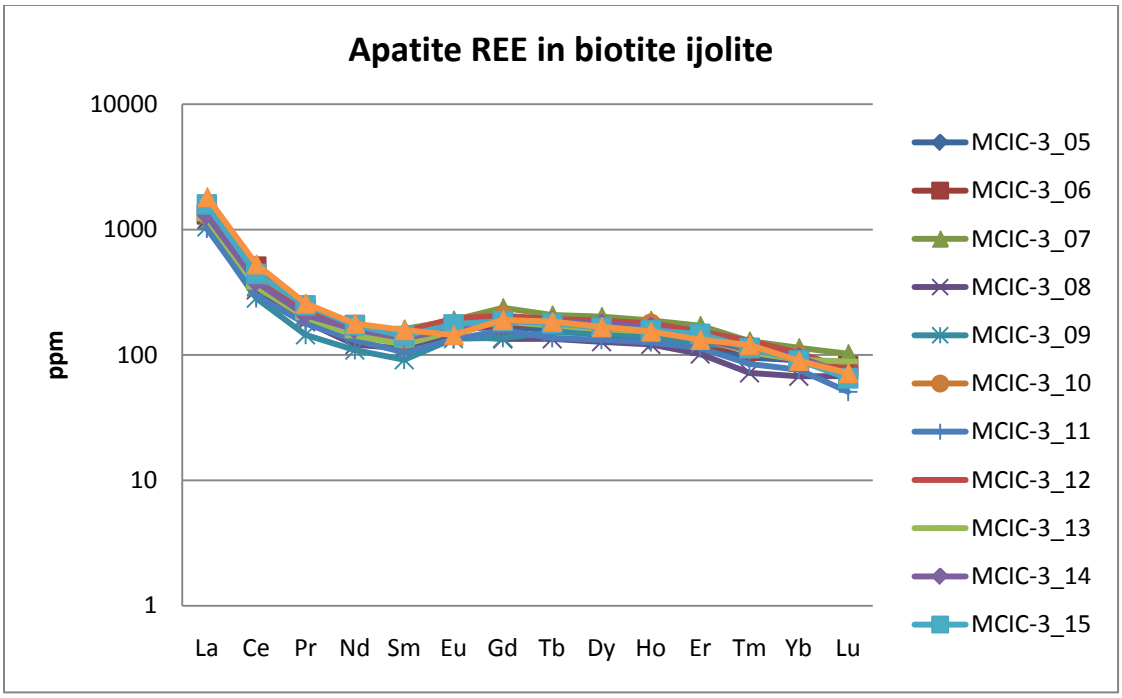
Apatite REE in biotite ijolite
10000
1000
100
10
1
ppm
La Ce Pr Nd Sm Eu Gd Tb Dy Ho Er Tm Yb Lu
MCIC-3_05
MCIC-3_06
MCIC-3_07
MCIC-3_08
MCIC-3_09
MCIC-3_10
MCIC-3_11
MCIC-3_12
MCIC-3_13
MCIC-3_14
MCIC-3_15

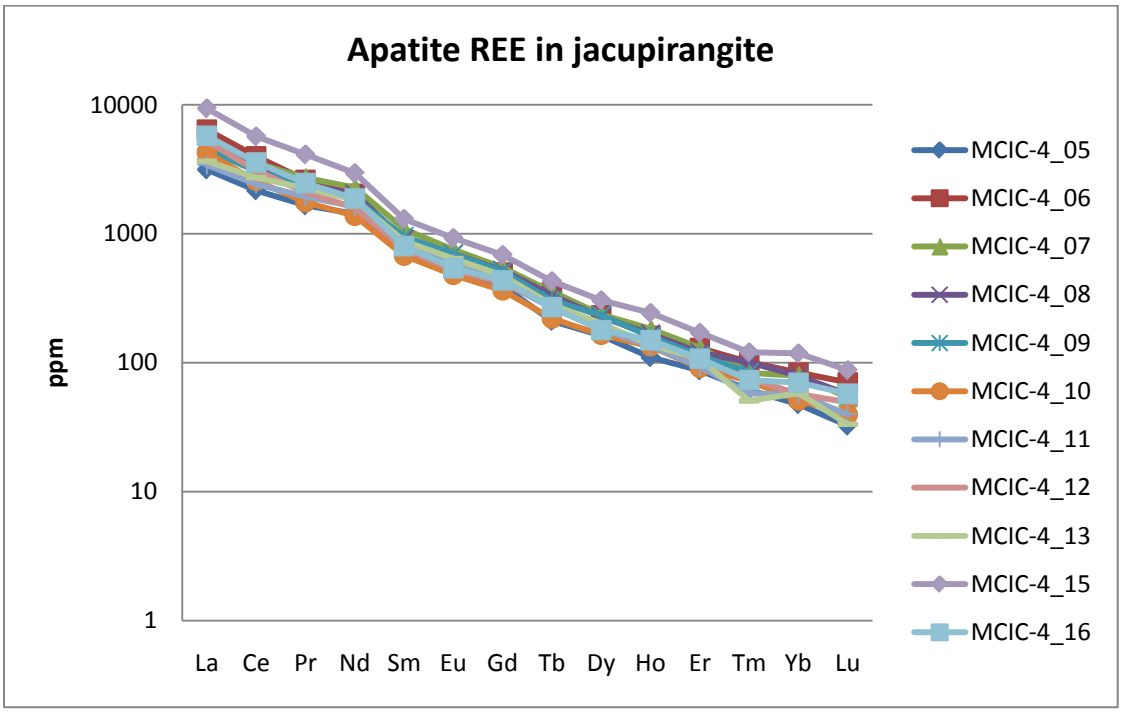
Apatite REE in jacupirangite
10000
1000
100
10
1
ppm
La Ce Pr Nd Sm Eu Gd Tb Dy Ho Er Tm Yb Lu
MCIC-4_05
MCIC-4_06
MCIC-4_07
MCIC-4_08
MCIC-4_09
MCIC-4_10
MCIC-4_11
MCIC-4_12
MCIC-4_13
MCIC-4_15
MCIC-4_16

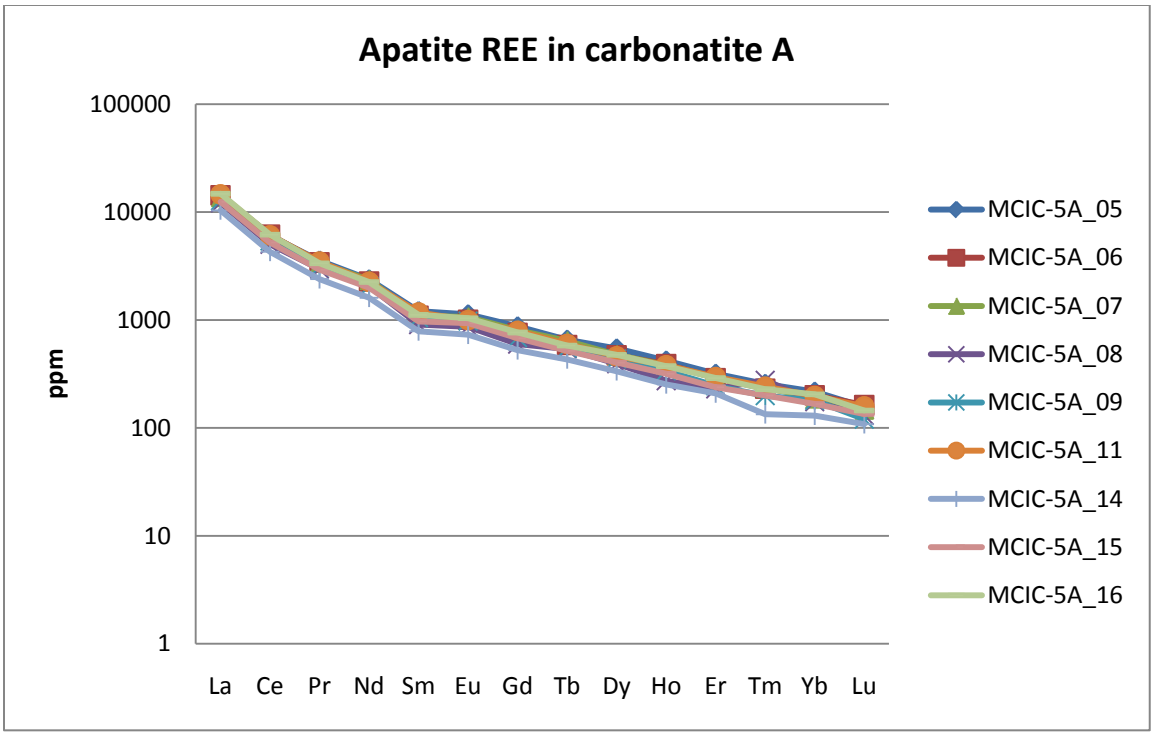
Apatite REE in carbonatite A
100000
10000
1000
100
10
1
ppm
La Ce Pr Nd Sm Eu Gd Tb Dy Ho Er Tm Yb Lu
MCIC-5A_05
MCIC-5A_06
MCIC-5A_07
MCIC-5A_08
MCIC-5A_09
MCIC-5A_11
MCIC-5A_14
MCIC-5A_15
MCIC-5A_16

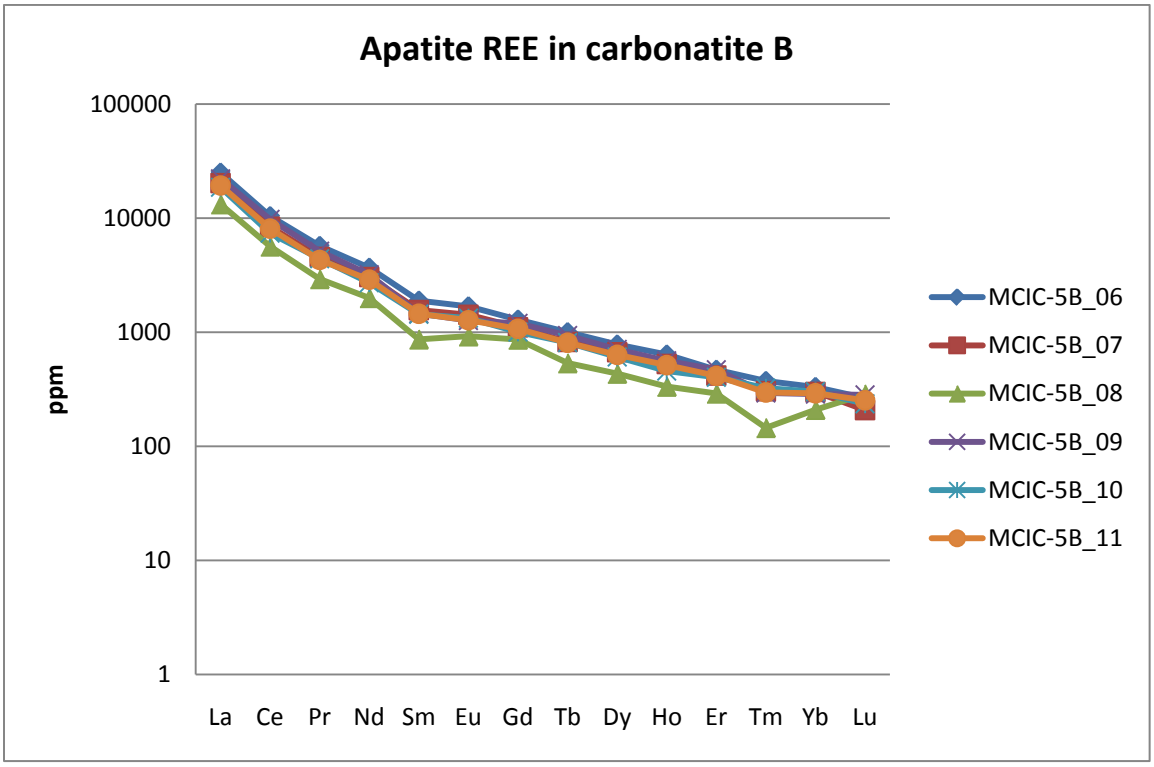
Apatite REE in carbonatite B
100000
10000
1000
100
10
1
ppm
La Ce Pr Nd Sm Eu Gd Tb Dy Ho Er Tm Yb Lu
MCIC-5B_06
MCIC-5B_07
MCIC-5B_08
MCIC-5B_09
MCIC-5B_10
MCIC-5B_11

Appendix 10

MCIC apatite volatile composition, AST, and fugacity ratios

MCIC-1 (Trachyte-phonolite)

X(FAp)	X(CAp)	X(HAp)	X(CAp/HAp)	X(FAp/HAp)	AST(Cel.)	f(HCl/H2O)	f(HF/H2O)	AST(Kelvin)	f(HCl/H2O)	f(HF/H2O)
0.8934	0.0016	0.1050	0.0155	8.5125	700	5.56E-05	4.92E-05	1048	2.34E-06	5.12E-08
0.8894	0.0015	0.1091	0.0137	8.1527	700	4.92E-05	4.71E-05	1048	2.07E-06	4.90E-08
0.8714	0.0003	0.1283	0.0022	6.7930	700	7.79E-06	3.93E-05	1048	3.28E-07	4.09E-08
0.9196	0.0011	0.0793	0.0145	11.6017	700	5.17E-05	6.71E-05	1048	2.18E-06	6.98E-08
0.8664	0.0019	0.1318	0.0140	6.5741	700	5.03E-05	3.80E-05	1048	2.12E-06	3.95E-08
0.7960	0.0022	0.2018	0.0107	3.9435	700	3.83E-05	2.28E-05	1048	1.61E-06	2.37E-08
0.9041	0.0030	0.0929	0.0324	9.7348	700	1.16E-04	5.63E-05	1048	4.89E-06	5.85E-08
0.9045	0.0018	0.0937	0.0193	9.6492	700	6.90E-05	5.58E-05	1048	2.91E-06	5.80E-08
0.8474	0	0.1526	0	5.5536	700	0	3.21E-05	1048	0	3.34E-08
0.8678	0.0020	0.1302	0.0152	6.6658	700	5.45E-05	3.85E-05	1048	2.30E-06	4.01E-08
0.8367	0.0019	0.1615	0.0116	5.1814	700	4.14E-05	2.99E-05	1048	1.74E-06	3.12E-08
0.8036	0.0027	0.1938	0.0138	4.1470	700	4.94E-05	2.40E-05	1048	2.08E-06	2.49E-08
0.8475	0.0026	0.1500	0.0172	5.6516	700	6.17E-05	3.27E-05	1048	2.60E-06	3.40E-08
0.8479	0.0020	0.1501	0.0136	5.6488	700	4.87E-05	3.26E-05	1048	2.05E-06	3.40E-08
0.7654	0.0014	0.2332	0.0060	3.2813	700	2.14E-05	1.90E-05	1048	9.02E-07	1.97E-08
0.7720	0.0015	0.2265	0.0064	3.4081	700	2.30E-05	1.97E-05	1048	9.68E-07	2.05E-08
0.7730	0.0015	0.2255	0.0068	3.4279	700	2.43E-05	1.98E-05	1048	1.02E-06	2.06E-08
0.8124	0.0023	0.1853	0.0126	4.3842	700	4.51E-05	2.53E-05	1048	1.90E-06	2.64E-08
0.7921	0.0023	0.2056	0.0111	3.8522	700	3.99E-05	2.23E-05	1048	1.68E-06	2.32E-08
0.8003	0.0016	0.1981	0.0080	4.0394	700	2.87E-05	2.33E-05	1048	1.21E-06	2.43E-08
0.7964	0.0001	0.2035	0.0006	3.9139	700	2.33E-06	2.26E-05	1048	9.79E-08	2.35E-08
0.8112	0.0008	0.1880	0.0043	4.3159	700	1.54E-05	2.49E-05	1048	6.48E-07	2.60E-08
0.8449	0.0018	0.1533	0.0118	5.5112	700	4.22E-05	3.19E-05	1048	1.78E-06	3.31E-08
0.9205	0.0014	0.0781	0.0173	11.782	700	6.19E-05	6.81E-05	1048	2.61E-06	7.09E-08
0.7854	0.0007	0.2139	0.0032	3.6711	700	1.16E-05	2.12E-05	1048	4.86E-07	2.21E-08
0.9937	0.0011	0.0052	0.2101	189.52	700	7.52E-04	1.10E-03	1048	3.17E-05	1.14E-06

MCIC-2 (Garnet pseudoleucite nepheline syenite)

X(FAp)	X(CAp)	X(HAp)	X(CAp/HAp)	X(FAp/HAp)	AST(Cel.)	f(HCl/H2O)	f(HF/H2O)	AST(Kelvin)	f(HCl/H2O)	f(HF/H2O)
0.8354	0.0001	0.1646	0.0005	5.0766	700	1.07E-06	8.59E-06	948	3.80E-08	6.24E-09
0.9086	0.0005	0.0909	0.0057	9.9973	700	1.13E-05	1.69E-05	948	4.01E-07	1.23E-08
0.8818	0.0005	0.1176	0.0046	7.4958	700	9.23E-06	1.27E-05	948	3.28E-07	9.21E-09
0.8779	0.0021	0.1200	0.0171	7.3159	700	3.43E-05	1.24E-05	948	1.22E-06	8.99E-09
0.7861	0.0003	0.2135	0.0016	3.6818	700	3.16E-06	6.23E-06	948	1.12E-07	4.53E-09
0.8612	0.0007	0.1381	0.0050	6.2337	700	9.99E-06	1.06E-05	948	3.55E-07	7.66E-09
0.8783	0.0007	0.1210	0.0059	7.2570	700	1.19E-05	1.23E-05	948	4.22E-07	8.92E-09
0.9826	0.0013	0.0161	0.0803	61.0491	700	1.61E-04	1.03E-04	948	5.70E-06	7.50E-08
1.0942	0.0006	-0.0948	-0.0060	-11.5411	700	-1.21E-05	-1.95E-05	948	-4.29E-07	-1.42E-08
1.0303	0.0006	-0.0309	-0.0190	-33.3677	700	-3.80E-05	-5.65E-05	948	-1.35E-06	-4.10E-08

MCIC-3 (Biotite ijolite, part 1)

X(FAp)	X(CAp)	X(HAp)	X(CAp/HAp)	X(FAp/HAp)	AST(Cel.)	f(HCl/H2O)	f(HF/H2O)	AST(Kelvin)	f(HCl/H2O)	f(HF/H2O)
0.3964	0.0020	0.6017	0.0033	0.6588	700	5.51E-06	7.65E-07	921	1.86E-07	5.00E-10
0.3864	0.0021	0.6115	0.0034	0.6318	700	5.66E-06	7.33E-07	921	1.91E-07	4.80E-10
0.3663	0.0010	0.6327	0.0016	0.5789	700	2.60E-06	6.72E-07	921	8.78E-08	4.40E-10
0.4207	0.0018	0.5775	0.0031	0.7286	700	5.14E-06	8.46E-07	921	1.74E-07	5.53E-10
0.4413	0.0019	0.5568	0.0035	0.7926	700	5.78E-06	9.20E-07	921	1.95E-07	6.02E-10
0.4169	0.0022	0.5809	0.0037	0.7177	700	6.21E-06	8.33E-07	921	2.10E-07	5.45E-10
0.4067	0.0023	0.5910	0.0038	0.6882	700	6.40E-06	7.99E-07	921	2.16E-07	5.23E-10
0.4046	0.0019	0.5934	0.0032	0.6819	700	5.42E-06	7.91E-07	921	1.83E-07	5.18E-10
0.4104	0.0023	0.5873	0.0039	0.6988	700	6.52E-06	8.11E-07	921	2.20E-07	5.31E-10
0.3949	0.0025	0.6026	0.0042	0.6553	700	6.97E-06	7.61E-07	921	2.35E-07	4.98E-10
0.4373	0.0016	0.5610	0.0029	0.7795	700	4.86E-06	9.05E-07	921	1.64E-07	5.92E-10
0.4283	0.0016	0.5701	0.0029	0.7512	700	4.78E-06	8.72E-07	921	1.61E-07	5.71E-10
0.4160	0.0019	0.5821	0.0032	0.7147	700	5.31E-06	8.30E-07	921	1.79E-07	5.43E-10
0.4004	0.0027	0.5968	0.0046	0.6709	700	7.65E-06	7.79E-07	921	2.58E-07	5.10E-10
0.4277	0.0023	0.5700	0.0041	0.7503	700	6.89E-06	8.71E-07	921	2.33E-07	5.70E-10
0.4261	0.0015	0.5725	0.0025	0.7443	700	4.25E-06	8.64E-07	921	1.43E-07	5.65E-10
0.4583	0.0020	0.5397	0.0036	0.8492	700	6.05E-06	9.86E-07	921	2.04E-07	6.45E-10
0.4351	0.0013	0.5636	0.0022	0.7719	700	3.75E-06	8.96E-07	921	1.27E-07	5.86E-10
0.4332	0.0021	0.5647	0.0037	0.7670	700	6.26E-06	8.90E-07	921	2.11E-07	5.83E-10
0.4221	0.0024	0.5756	0.0041	0.7333	700	6.87E-06	8.51E-07	921	2.32E-07	5.57E-10
0.4784	0.0001	0.5215	0.0001	0.9174	700	2.35E-07	1.06E-06	921	7.95E-09	6.97E-10
0.4335	0.0021	0.5644	0.0038	0.7680	700	6.31E-06	8.91E-07	921	2.13E-07	5.83E-10
0.4241	0.0034	0.5726	0.0059	0.7406	700	9.90E-06	8.60E-07	921	3.35E-07	5.62E-10
0.4318	0.0018	0.5663	0.0032	0.7625	700	5.37E-06	8.85E-07	921	1.82E-07	5.79E-10
0.4126	0.0025	0.5849	0.0043	0.7055	700	7.13E-06	8.19E-07	921	2.41E-07	5.36E-10
0.4116	0.0025	0.5859	0.0043	0.7026	700	7.16E-06	8.16E-07	921	2.42E-07	5.34E-10
0.4501	0.0026	0.5474	0.0047	0.8222	700	7.80E-06	9.54E-07	921	2.64E-07	6.24E-10
0.4351	0.0021	0.5628	0.0037	0.7731	700	6.19E-06	8.97E-07	921	2.09E-07	5.87E-10
0.3604	0.0045	0.6351	0.0071	0.5675	700	1.18E-05	6.59E-07	921	3.98E-07	4.31E-10
0.3964	0.0017	0.6019	0.0029	0.6586	700	4.85E-06	7.64E-07	921	1.64E-07	5.00E-10
0.3994	0.0013	0.5993	0.0022	0.6666	700	3.65E-06	7.74E-07	921	1.23E-07	5.06E-10
0.3771	0.0031	0.6199	0.0050	0.6083	700	8.28E-06	7.06E-07	921	2.80E-07	4.62E-10
0.4417	0.0009	0.5574	0.0017	0.7923	700	2.82E-06	9.20E-07	921	9.52E-08	6.02E-10
0.4315	0.0011	0.5674	0.0019	0.7606	700	3.16E-06	8.83E-07	921	1.07E-07	5.78E-10
0.4132	0.0008	0.5860	0.0013	0.7052	700	2.22E-06	8.19E-07	921	7.50E-08	5.36E-10
0.3739	0.0018	0.6244	0.0028	0.5988	700	4.72E-06	6.95E-07	921	1.59E-07	4.55E-10
0.3988	0.0024	0.5988	0.0040	0.6660	700	6.68E-06	7.73E-07	921	2.26E-07	5.06E-10

MCIC-3 (Biotite ijolite, part 2)

X(FAp)	X(CAp)	X(HAp)	X(CAp/HAp)	X(FAp/HAp)	AST(Cel.)	f(HCl/H2O)	f(HF/H2O)	AST(Kelvin)	f(HCl/H2O)	f(HF/H2O)
0.3615	0.0020	0.6365	0.0032	0.5679	700	5.36E-06	6.59E-07	921	1.81E-07	4.31E-10
0.3670	0.0015	0.6315	0.0023	0.5811	700	3.89E-06	6.75E-07	921	1.31E-07	4.41E-10
0.3760	0.0014	0.6226	0.0022	0.6040	700	3.71E-06	7.01E-07	921	1.25E-07	4.59E-10
0.3445	0.0013	0.6542	0.0020	0.5265	700	3.41E-06	6.11E-07	921	1.15E-07	4.00E-10
0.3392	0.0011	0.6597	0.0017	0.5141	700	2.83E-06	5.97E-07	921	9.55E-08	3.90E-10
0.3496	0.0023	0.6480	0.0036	0.5395	700	6.02E-06	6.26E-07	921	2.03E-07	4.10E-10
0.3520	0.0022	0.6457	0.0035	0.5451	700	5.82E-06	6.33E-07	921	1.96E-07	4.14E-10
0.3855	0.0015	0.6131	0.0024	0.6287	700	3.96E-06	7.30E-07	921	1.34E-07	4.77E-10
0.3705	0.0028	0.6266	0.0045	0.5913	700	7.60E-06	6.86E-07	921	2.57E-07	4.49E-10
0.3717	0.0026	0.6257	0.0042	0.5941	700	6.94E-06	6.90E-07	921	2.35E-07	4.51E-10
0.3864	0.0014	0.6123	0.0022	0.6311	700	3.69E-06	7.33E-07	921	1.25E-07	4.79E-10
0.3670	0.0018	0.6312	0.0028	0.5814	700	4.71E-06	6.75E-07	921	1.59E-07	4.42E-10
0.3595	0.0016	0.6389	0.0025	0.5628	700	4.19E-06	6.53E-07	921	1.41E-07	4.27E-10
0.3611	0.0015	0.6375	0.0023	0.5664	700	3.81E-06	6.57E-07	921	1.29E-07	4.30E-10
0.3690	0.0028	0.6282	0.0045	0.5874	700	7.58E-06	6.82E-07	921	2.56E-07	4.46E-10
0.3734	0.0030	0.6237	0.0047	0.5987	700	7.91E-06	6.95E-07	921	2.67E-07	4.55E-10
0.3709	0.0027	0.6264	0.0043	0.5922	700	7.13E-06	6.87E-07	921	2.41E-07	4.50E-10
0.4060	0.0024	0.5916	0.0041	0.6862	700	6.89E-06	7.97E-07	921	2.33E-07	5.21E-10
0.4182	0.0021	0.5797	0.0036	0.7214	700	6.06E-06	8.37E-07	921	2.05E-07	5.48E-10
0.4107	0.0023	0.5870	0.0040	0.6998	700	6.61E-06	8.12E-07	921	2.23E-07	5.31E-10
0.4173	0.0032	0.5795	0.0056	0.7200	700	9.32E-06	8.36E-07	921	3.15E-07	5.47E-10
0.3529	0.0028	0.6443	0.0044	0.5478	700	7.32E-06	6.36E-07	921	2.47E-07	4.16E-10
0.3574	0.0016	0.6410	0.0025	0.5575	700	4.10E-06	6.47E-07	921	1.38E-07	4.23E-10
0.3636	0.0035	0.6329	0.0055	0.5746	700	9.19E-06	6.67E-07	921	3.11E-07	4.36E-10
0.3787	0.0026	0.6187	0.0042	0.6122	700	6.94E-06	7.11E-07	921	2.35E-07	4.65E-10
0.4095	0.0010	0.5895	0.0017	0.6946	700	2.91E-06	8.06E-07	921	9.85E-08	5.28E-10
0.4294	0.0015	0.5691	0.0026	0.7545	700	4.31E-06	8.76E-07	921	1.46E-07	5.73E-10
0.3945	0.0020	0.6035	0.0034	0.6536	700	5.61E-06	7.59E-07	921	1.90E-07	4.96E-10
0.3949	0.0011	0.6040	0.0019	0.6537	700	3.13E-06	7.59E-07	921	1.06E-07	4.96E-10
0.4072	0.0022	0.5906	0.0038	0.6895	700	6.32E-06	8.00E-07	921	2.13E-07	5.24E-10
0.4057	0.0017	0.5926	0.0028	0.6845	700	4.72E-06	7.95E-07	921	1.60E-07	5.20E-10
0.4108	0.0022	0.5871	0.0037	0.6997	700	6.19E-06	8.12E-07	921	2.09E-07	5.31E-10
0.4076	0.0026	0.5898	0.0044	0.6912	700	7.41E-06	8.02E-07	921	2.50E-07	5.25E-10
0.3960	0.0023	0.6017	0.0039	0.6581	700	6.49E-06	7.64E-07	921	2.19E-07	5.00E-10
0.4127	0.0027	0.5846	0.0046	0.7061	700	7.68E-06	8.20E-07	921	2.60E-07	5.36E-10
0.4675	0.0008	0.5318	0.0015	0.8791	700	2.45E-06	1.02E-06	921	8.26E-08	6.68E-10
0.3972	0.0015	0.6012	0.0026	0.6606	700	4.29E-06	7.67E-07	921	1.45E-07	5.02E-10

MCIC-4 (Jacupirangite, part 1)

X(FAp)	X(CAp)	X(HAp)	X(CAp/HAp)	X(FAp/HAp)	AST(Cel.)	f(HCl/H2O)	f(HF/H2O)	AST(Kelvin)	f(HCl/H2O)	f(HF/H2O)
0.5463	0.0025	0.4512	0.0055	1.2110	700	2.29E-05	9.58E-06	1077	1.01E-06	1.10E-08
0.5457	0.0021	0.4522	0.0046	1.2067	700	1.92E-05	9.54E-06	1077	8.45E-07	1.09E-08
0.5364	0.0023	0.4613	0.0050	1.1627	700	2.09E-05	9.19E-06	1077	9.22E-07	1.05E-08
0.5380	0.0026	0.4594	0.0057	1.1711	700	2.36E-05	9.26E-06	1077	1.04E-06	1.06E-08
0.5441	0.0036	0.4522	0.0081	1.2033	700	3.35E-05	9.52E-06	1077	1.48E-06	1.09E-08
0.5491	0.0020	0.4488	0.0045	1.2234	700	1.89E-05	9.67E-06	1077	8.33E-07	1.11E-08
0.5436	0.0060	0.4504	0.0134	1.2068	700	5.55E-05	9.54E-06	1077	2.45E-06	1.09E-08
0.5449	0.0031	0.4520	0.0068	1.2057	700	2.82E-05	9.53E-06	1077	1.24E-06	1.09E-08
0.6302	0.0019	0.3679	0.0052	1.7130	700	2.17E-05	1.35E-05	1077	9.58E-07	1.55E-08
0.6028	0.0011	0.3960	0.0029	1.5222	700	1.19E-05	1.20E-05	1077	5.23E-07	1.38E-08
0.5487	0.0019	0.4494	0.0042	1.2211	700	1.75E-05	9.66E-06	1077	7.72E-07	1.11E-08
0.6078	0.0031	0.3891	0.0079	1.5622	700	3.29E-05	1.24E-05	1077	1.45E-06	1.42E-08
0.6086	0.0040	0.3874	0.0103	1.5708	700	4.28E-05	1.24E-05	1077	1.89E-06	1.42E-08
0.5802	0.0021	0.4176	0.0051	1.3893	700	2.13E-05	1.10E-05	1077	9.41E-07	1.26E-08
0.5998	0.0020	0.3982	0.0051	1.5063	700	2.11E-05	1.19E-05	1077	9.32E-07	1.37E-08
0.7317	0.0027	0.2656	0.0102	2.7554	700	4.25E-05	2.18E-05	1077	1.87E-06	2.50E-08
0.6874	0.0030	0.3096	0.0097	2.2202	700	4.02E-05	1.76E-05	1077	1.77E-06	2.01E-08
0.5797	0.0034	0.4169	0.0081	1.3904	700	3.38E-05	1.10E-05	1077	1.49E-06	1.26E-08
0.6652	0.0031	0.3317	0.0092	2.0054	700	3.83E-05	1.59E-05	1077	1.69E-06	1.82E-08
0.4869	0.0074	0.5057	0.0146	0.9627	700	6.08E-05	7.61E-06	1077	2.68E-06	8.73E-09
0.5711	0.0053	0.4236	0.0126	1.3483	700	5.24E-05	1.07E-05	1077	2.31E-06	1.22E-08
0.5567	0.0044	0.4389	0.0100	1.2683	700	4.17E-05	1.00E-05	1077	1.84E-06	1.15E-08
0.5751	0.0032	0.4217	0.0077	1.3639	700	3.20E-05	1.08E-05	1077	1.41E-06	1.24E-08
0.5912	0.0034	0.4054	0.0085	1.4584	700	3.52E-05	1.15E-05	1077	1.55E-06	1.32E-08
0.5478	0.0018	0.4505	0.0040	1.2160	700	1.65E-05	9.62E-06	1077	7.29E-07	1.10E-08
0.6023	0.0023	0.3955	0.0058	1.5229	700	2.39E-05	1.20E-05	1077	1.05E-06	1.38E-08
0.5581	0.0022	0.4398	0.0049	1.2690	700	2.05E-05	1.00E-05	1077	9.05E-07	1.15E-08
0.4795	0.0041	0.5164	0.0080	0.9286	700	3.32E-05	7.34E-06	1077	1.46E-06	8.42E-09
0.5518	0.0037	0.4445	0.0083	1.2416	700	3.46E-05	9.82E-06	1077	1.53E-06	1.13E-08
0.5304	0.0054	0.4642	0.0116	1.1426	700	4.82E-05	9.04E-06	1077	2.13E-06	1.04E-08
0.5466	0.0031	0.4502	0.0070	1.2140	700	2.90E-05	9.60E-06	1077	1.28E-06	1.10E-08
0.5604	0.0032	0.4363	0.0074	1.2845	700	3.09E-05	1.02E-05	1077	1.36E-06	1.17E-08
0.5725	0.0026	0.4249	0.0062	1.3474	700	2.59E-05	1.07E-05	1077	1.14E-06	1.22E-08
0.6044	0.0028	0.3927	0.0072	1.5390	700	2.98E-05	1.22E-05	1077	1.32E-06	1.40E-08
0.5884	0.0027	0.4089	0.0066	1.4389	700	2.76E-05	1.14E-05	1077	1.22E-06	1.31E-08
0.6760	0.0034	0.3206	0.0105	2.1087	700	4.38E-05	1.67E-05	1077	1.93E-06	1.91E-08
0.6386	0.0062	0.3552	0.0174	1.7978	700	7.23E-05	1.42E-05	1077	3.19E-06	1.63E-08

MCIC-4 (Jacupirangite, part 2)

X(FAp)	X(CAp)	X(HAp)	X(CAp/HAp)	X(FAp/HAp)	AST(Cel.)	f(HCl/H2O)	f(HF/H2O)	AST(Kelvin)	f(HCl/H2O)	f(HF/H2O)
0.6351	0.0017	0.3632	0.0048	1.7485	700	1.98E-05	1.38E-05	1077	8.74E-07	1.59E-08
0.6495	0.0015	0.3490	0.0043	1.8613	700	1.78E-05	1.47E-05	1077	7.86E-07	1.69E-08
0.5469	0.0029	0.4502	0.0065	1.2149	700	2.71E-05	9.61E-06	1077	1.20E-06	1.10E-08
0.5355	0.0022	0.4623	0.0048	1.1583	700	1.99E-05	9.16E-06	1077	8.79E-07	1.05E-08
0.5408	0.0029	0.4563	0.0063	1.1850	700	2.62E-05	9.37E-06	1077	1.16E-06	1.07E-08
0.5516	0.0037	0.4447	0.0083	1.2402	700	3.43E-05	9.81E-06	1077	1.51E-06	1.12E-08
0.5692	0.0037	0.4271	0.0086	1.3328	700	3.59E-05	1.05E-05	1077	1.58E-06	1.21E-08
0.5725	0.0033	0.4242	0.0077	1.3497	700	3.21E-05	1.07E-05	1077	1.41E-06	1.22E-08
0.5818	0.0039	0.4143	0.0094	1.4043	700	3.92E-05	1.11E-05	1077	1.73E-06	1.27E-08
0.5663	0.0034	0.4303	0.0079	1.3161	700	3.28E-05	1.04E-05	1077	1.44E-06	1.19E-08
0.5932	0.0038	0.4030	0.0094	1.4719	700	3.91E-05	1.16E-05	1077	1.72E-06	1.34E-08
0.5971	0.0057	0.3972	0.0143	1.5031	700	5.94E-05	1.19E-05	1077	2.62E-06	1.36E-08
0.5775	0.0026	0.4199	0.0061	1.3753	700	2.53E-05	1.09E-05	1077	1.11E-06	1.25E-08
0.5588	0.0022	0.4390	0.0051	1.2729	700	2.13E-05	1.01E-05	1077	9.38E-07	1.15E-08
0.5813	0.0015	0.4171	0.0037	1.3935	700	1.54E-05	1.10E-05	1077	6.77E-07	1.26E-08

MCIC-5A (Carbonatite)

X(FAp)	X(CAp)	X(HAp)	X(CAp/HAp)	X(FAp/HAp)	AST(Cel.)	f(HCl/H2O)	f(HF/H2O)	AST(Kelvin)	f(HCl/H2O)	f(HF/H2O)
0.2770	0.0013	0.7217	0.0018	0.3838	700	7.36E-06	3.04E-06	472	3.24E-07	3.48E-09
0.2724	0.0015	0.7261	0.0021	0.3751	700	8.80E-09	1.47E-12	472	3.07E-11	8.01E-18
0.2924	0.0010	0.7066	0.0014	0.4138	700	5.80E-09	1.62E-12	472	2.02E-11	8.84E-18
0.3121	0.0019	0.6860	0.0028	0.4550	700	1.17E-08	1.78E-12	472	4.07E-11	9.72E-18
0.3023	0.0003	0.6974	0.0004	0.4335	700	1.87E-09	1.69E-12	472	6.52E-12	9.26E-18
0.3250	0.0012	0.6738	0.0018	0.4823	700	7.74E-09	1.89E-12	472	2.70E-11	1.03E-17
0.3146	0.0014	0.6840	0.0020	0.4599	700	8.53E-09	1.80E-12	472	2.97E-11	9.82E-18
0.3221	0.0007	0.6771	0.0011	0.4758	700	4.67E-09	1.86E-12	472	1.63E-11	1.02E-17
0.3008	0.0012	0.6980	0.0017	0.4309	700	7.38E-09	1.68E-12	472	2.57E-11	9.21E-18
0.3164	0.0022	0.6814	0.0032	0.4643	700	1.37E-08	1.81E-12	472	4.76E-11	9.92E-18
0.3168	0.0020	0.6813	0.0029	0.4649	700	1.23E-08	1.82E-12	472	4.29E-11	9.93E-18
0.3272	0.0009	0.6719	0.0014	0.4869	700	5.91E-09	1.90E-12	472	2.06E-11	1.04E-17
0.2897	0.0021	0.7082	0.0030	0.4090	700	1.25E-08	1.60E-12	472	4.37E-11	8.74E-18
0.3061	0.0003	0.6936	0.0005	0.4413	700	1.97E-09	1.72E-12	472	6.86E-12	9.43E-18
0.2863	0.0009	0.7128	0.0013	0.4016	700	5.31E-09	1.57E-12	472	1.85E-11	8.58E-18
0.2997	0.0014	0.6989	0.0020	0.4288	700	8.52E-09	1.68E-12	472	2.97E-11	9.16E-18
0.3131	0.0008	0.6861	0.0011	0.4564	700	4.79E-09	1.78E-12	472	1.67E-11	9.75E-18
0.3079	0.0020	0.6901	0.0028	0.4462	700	1.20E-08	1.74E-12	472	4.17E-11	9.53E-18
0.2908	0.0020	0.7072	0.0028	0.4112	700	1.18E-08	1.61E-12	472	4.13E-11	8.78E-18
0.3110	0.0018	0.6871	0.0027	0.4526	700	1.13E-08	1.77E-12	472	3.94E-11	9.67E-18
0.2661	0.0005	0.7334	0.0007	0.3629	700	2.96E-09	1.42E-12	472	1.03E-11	7.75E-18
0.2561	0.0005	0.7434	0.0006	0.3446	700	2.67E-09	1.35E-12	472	9.31E-12	7.36E-18
0.2385	0.0003	0.7612	0.0004	0.3133	700	1.87E-09	1.22E-12	472	6.54E-12	6.69E-18
0.2327	0.0012	0.7661	0.0016	0.3037	700	6.80E-09	1.19E-12	472	2.37E-11	6.49E-18
0.3114	0.0013	0.6874	0.0018	0.4530	700	7.76E-09	1.77E-12	472	2.71E-11	9.68E-18
0.3291	0.0007	0.6702	0.0010	0.4911	700	4.17E-09	1.92E-12	472	1.45E-11	1.05E-17
0.3240	0.0017	0.6743	0.0026	0.4805	700	1.10E-08	1.88E-12	472	3.82E-11	1.03E-17
0.3375	0.0014	0.6611	0.0021	0.5105	700	8.82E-09	2.00E-12	472	3.08E-11	1.09E-17
0.2556	0.0012	0.7432	0.0016	0.3439	700	6.68E-09	1.34E-12	472	2.33E-11	7.35E-18
0.2533	0.0008	0.7459	0.0011	0.3396	700	4.49E-09	1.33E-12	472	1.57E-11	7.26E-18
0.2413	0.0014	0.7574	0.0018	0.3186	700	7.54E-09	1.25E-12	472	2.63E-11	6.81E-18
0.2485	0.0020	0.7494	0.0027	0.3316	700	1.15E-08	1.30E-12	472	4.01E-11	7.08E-18
0.2961	0.0006	0.7033	0.0009	0.4210	700	3.88E-09	1.65E-12	472	1.35E-11	8.99E-18
0.3242	0.0011	0.6746	0.0017	0.4806	700	7.08E-09	1.88E-12	472	2.47E-11	1.03E-17
0.2893	0.0008	0.7099	0.0011	0.4076	700	4.81E-09	1.59E-12	472	1.68E-11	8.71E-18

MCIC-5B (Carbonatite)

X(FAp)	X(CAp)	X(HAp)	X(CAp/HAp)	X(FAp/HAp)	AST(Cel.)	f(HCl/H2O)	f(HF/H2O)	AST(Kelvin)	f(HCl/H2O)	f(HF/H2O)
0.2240	0.0019	0.7741	0.0025	0.2894	700	1.04E-08	1.13E-12	472	3.63E-11	6.18E-18
0.2344	0.0010	0.7646	0.0014	0.3065	700	5.76E-09	1.20E-12	472	2.01E-11	6.55E-18
0.2421	0.0011	0.7567	0.0015	0.3200	700	6.40E-09	1.25E-12	472	2.23E-11	6.84E-18
0.2383	0.0013	0.7605	0.0017	0.3133	700	7.10E-09	1.22E-12	472	2.48E-11	6.69E-18
0.2456	0.0019	0.7524	0.0026	0.3265	700	1.09E-08	1.28E-12	472	3.80E-11	6.97E-18
0.2490	0.0017	0.7493	0.0023	0.3323	700	9.52E-09	1.30E-12	472	3.32E-11	7.10E-18
0.2758	0.0003	0.7239	0.0004	0.3810	700	1.63E-09	1.49E-12	472	5.68E-12	8.14E-18
0.2744	0.0014	0.7243	0.0019	0.3788	700	7.88E-09	1.48E-12	472	2.75E-11	8.09E-18
0.2414	0.0014	0.7572	0.0018	0.3188	700	7.62E-09	1.25E-12	472	2.66E-11	6.81E-18
0.2464	0.0014	0.7522	0.0018	0.3276	700	7.59E-09	1.28E-12	472	2.65E-11	7.00E-18
0.2274	0.0019	0.7707	0.0025	0.2950	700	1.06E-08	1.15E-12	472	3.71E-11	6.30E-18
0.2408	0.0004	0.7588	0.0005	0.3174	700	2.04E-09	1.24E-12	472	7.13E-12	6.78E-18
0.3116	0.0014	0.6870	0.0020	0.4535	700	8.31E-09	1.77E-12	472	2.90E-11	9.69E-18
0.3122	0.0013	0.6865	0.0019	0.4548	700	7.95E-09	1.78E-12	472	2.77E-11	9.72E-18
0.3110	0.0014	0.6876	0.0020	0.4523	700	8.57E-09	1.77E-12	472	2.99E-11	9.66E-18
0.3037	0.0018	0.6946	0.0025	0.4372	700	1.07E-08	1.71E-12	472	3.74E-11	9.34E-18
0.2634	0.0017	0.7349	0.0023	0.3585	700	9.88E-09	1.40E-12	472	3.44E-11	7.66E-18
0.3012	0.0006	0.6981	0.0009	0.4315	700	3.82E-09	1.69E-12	472	1.33E-11	9.22E-18
0.3081	0.0018	0.6901	0.0026	0.4464	700	1.10E-08	1.74E-12	472	3.82E-11	9.54E-18
0.2886	0.0018	0.7095	0.0026	0.4068	700	1.08E-08	1.59E-12	472	3.78E-11	8.69E-18
0.2943	0.0009	0.7047	0.0013	0.4177	700	5.63E-09	1.63E-12	472	1.96E-11	8.92E-18
0.2868	0.0020	0.7111	0.0028	0.4033	700	1.20E-08	1.58E-12	472	4.20E-11	8.62E-18
0.2975	0.0011	0.7014	0.0016	0.4241	700	6.90E-09	1.66E-12	472	2.41E-11	9.06E-18
0.2864	0.0019	0.7117	0.0027	0.4024	700	1.14E-08	1.57E-12	472	3.98E-11	8.60E-18
0.2919	0.0006	0.7075	0.0008	0.4126	700	3.51E-09	1.61E-12	472	1.22E-11	8.81E-18

Appendix 11

Standards Used

EPMA Standards/Elements

Fluorine: Synthetic apatite-(CaF)

Chlorine and sulfur: Scapolite

Calcium and phosphorus: Natural apatite

Strontium: Strontianite or Durango apatite

Manganese: Rhodonite

Silicon, sodium, iron: Hornblende

REE: Synthetic single REE phosphates

LA-ICP-MS Standards/Elements

REE: NIST-610

All other elements: BHVO

Appendix 12

Backscattered electron images of minerals analyzed using LA-ICP-MS

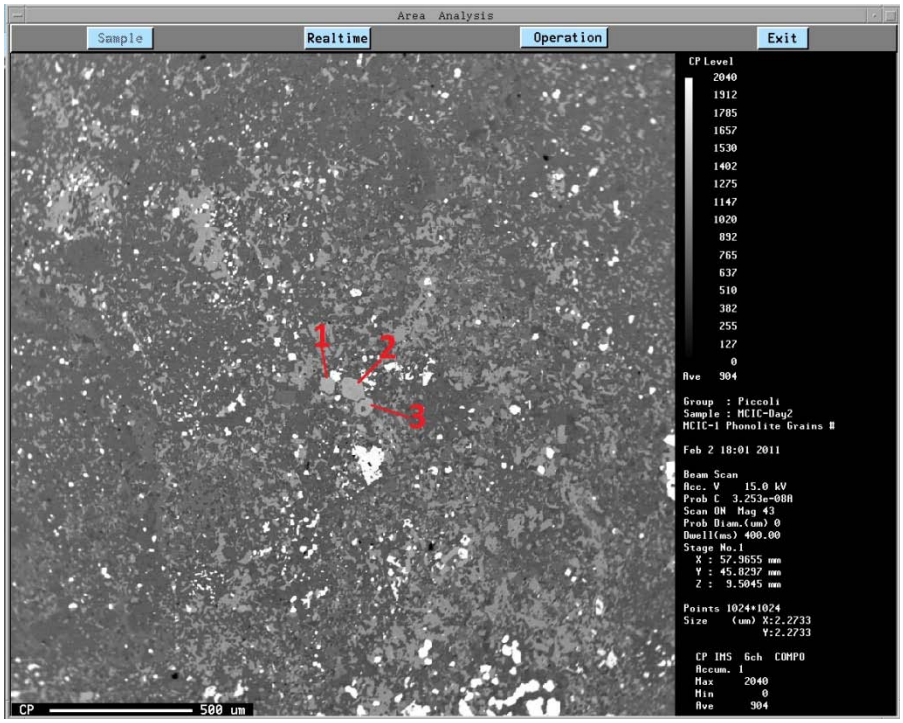

MCIC-1 Apatite 1-3

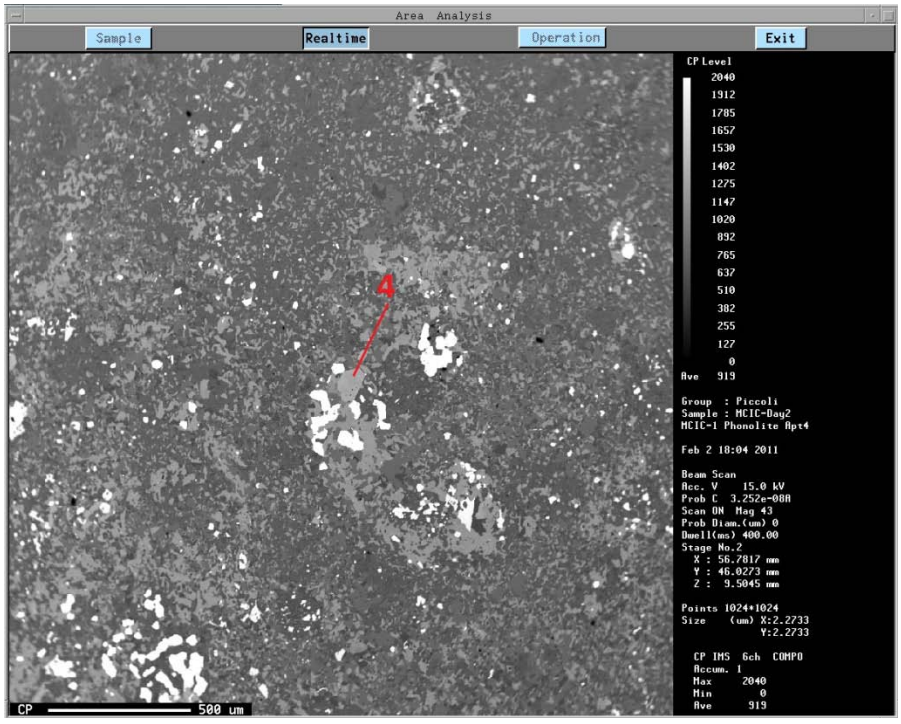

MCIC-1 Apatite 4

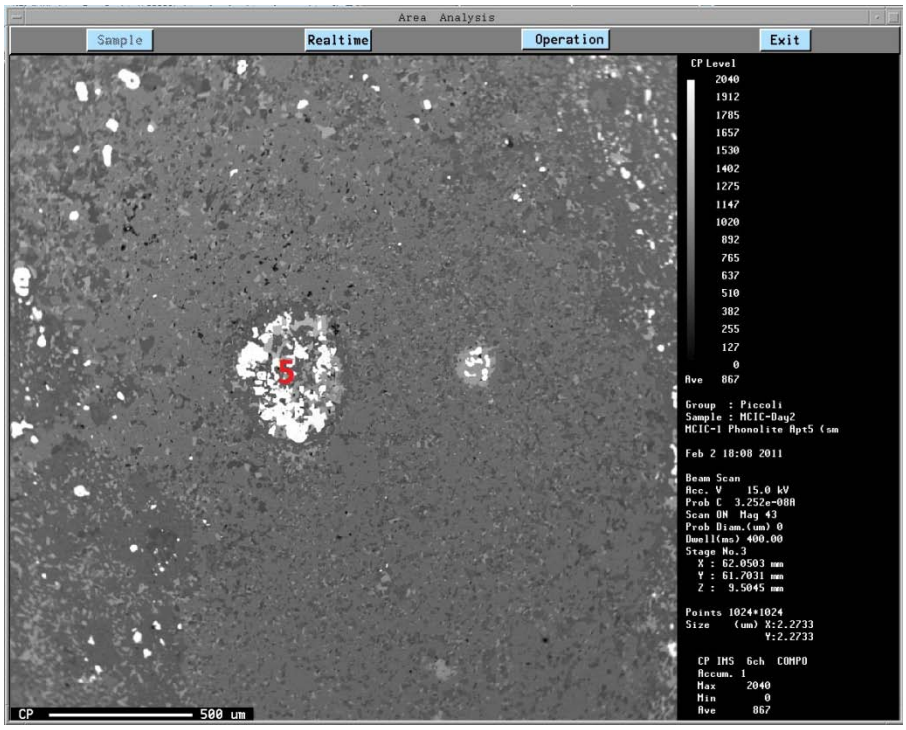

MCIC-1 Apatite 5

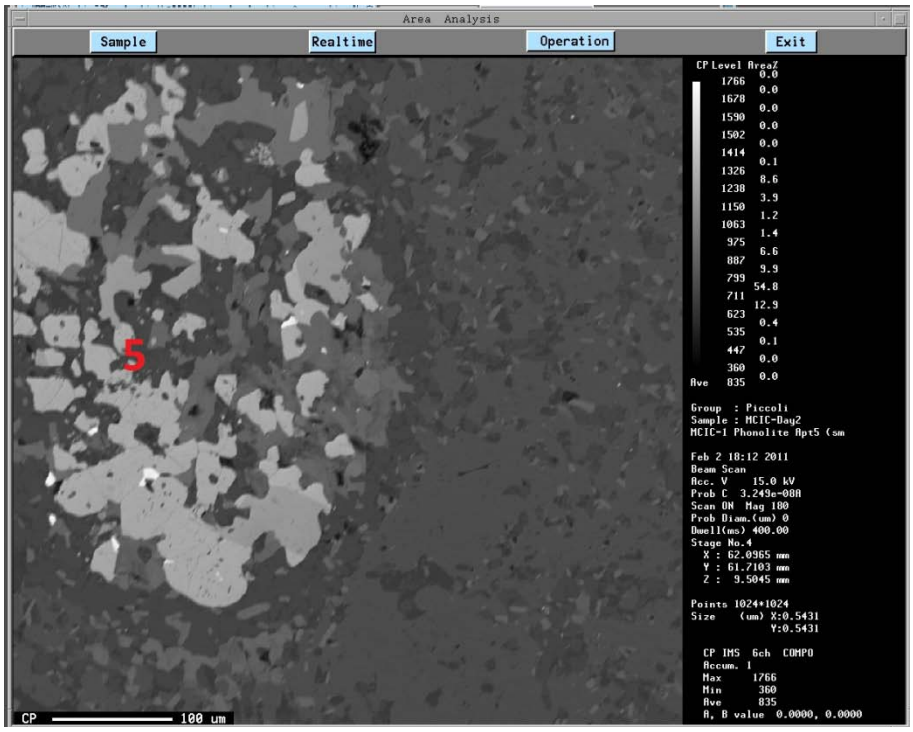

MCIC-1 Apatite 5 close-up

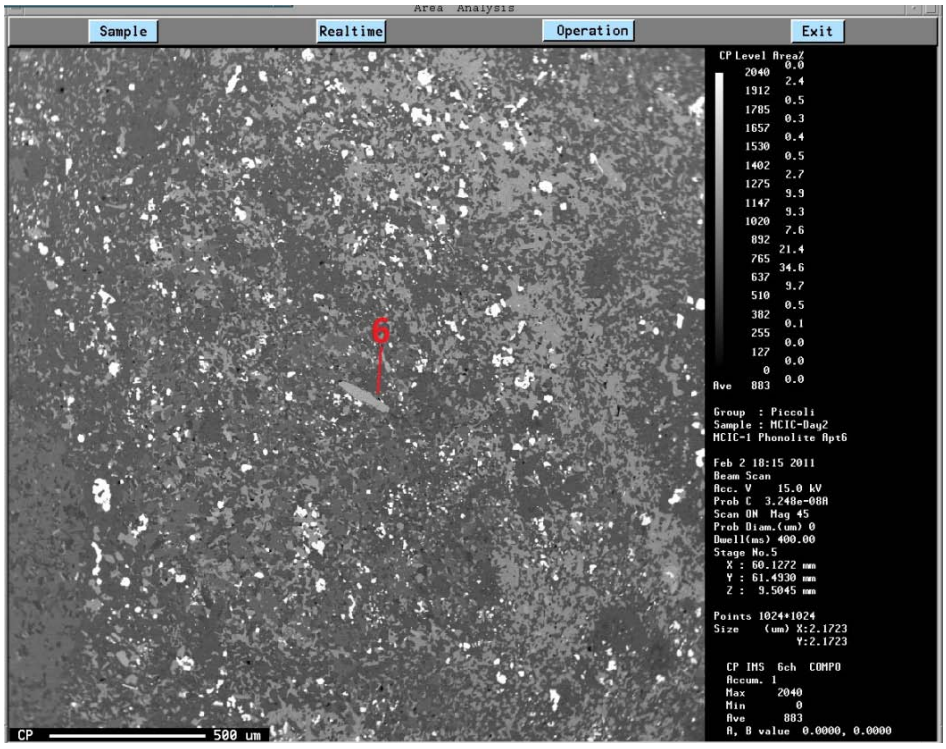

MCIC-1 Apatite 6

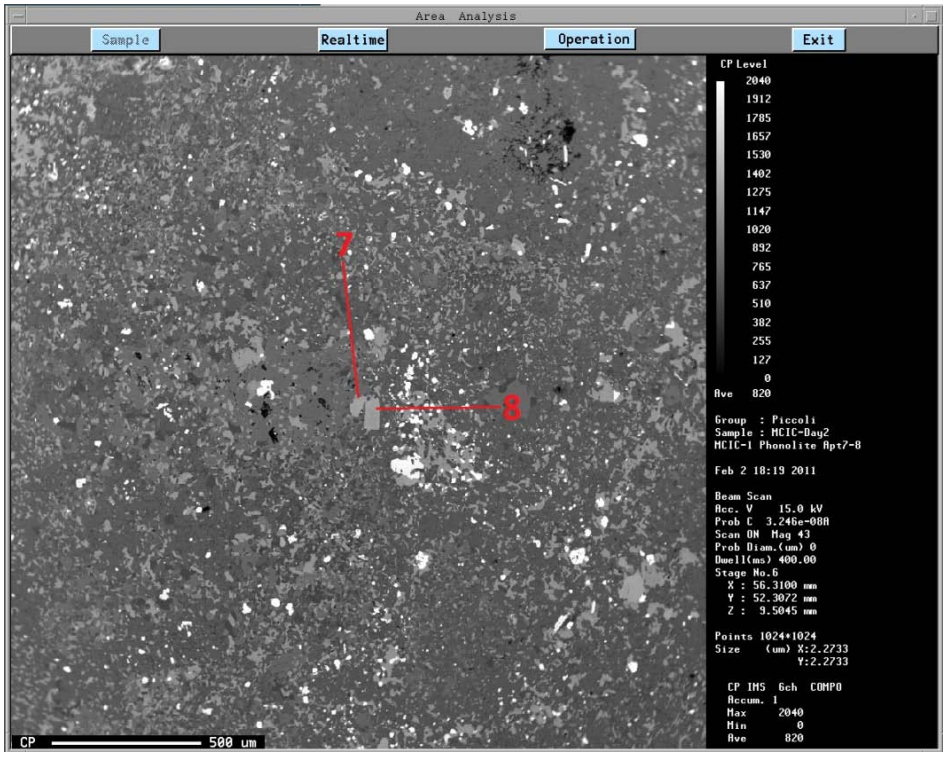

MCIC-1 Apatite 7 and 8

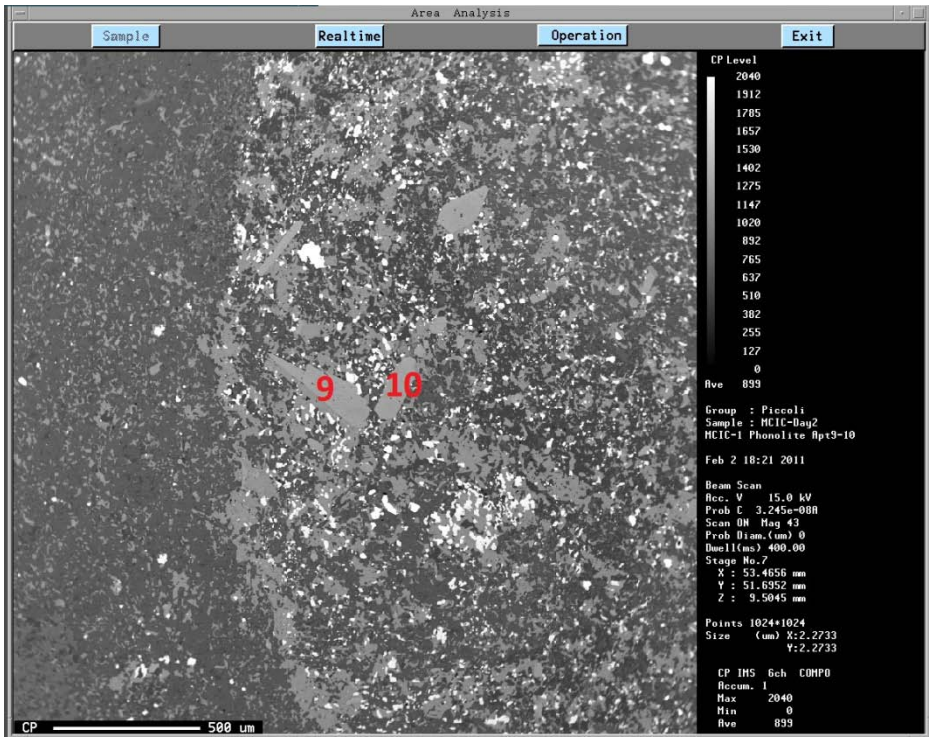

MCIC-1 Apatite 9 and 10

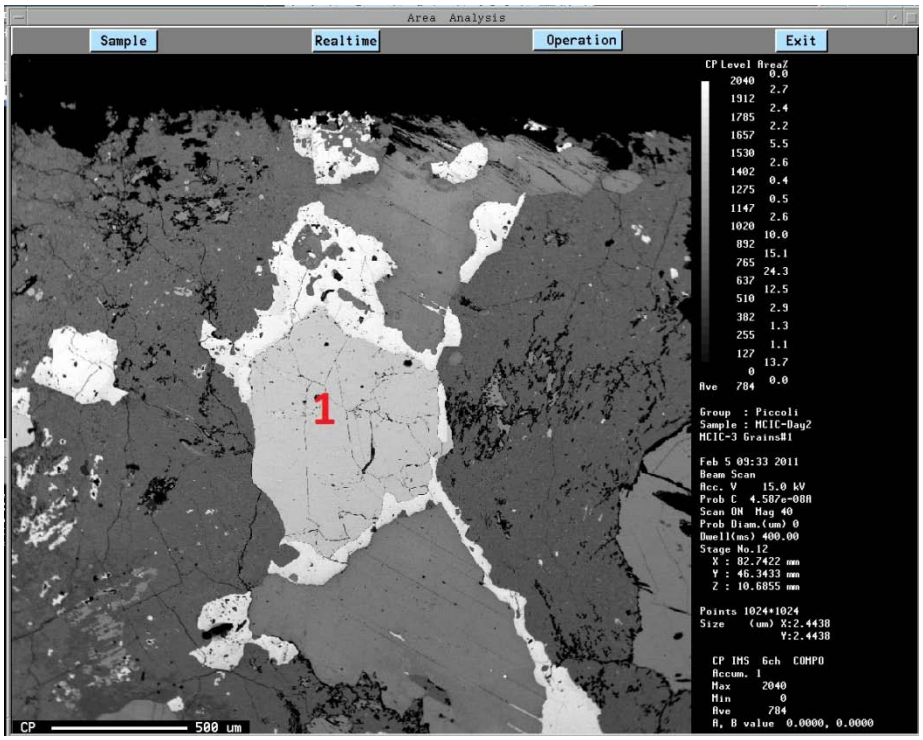

MCIC-3 Apatite 1

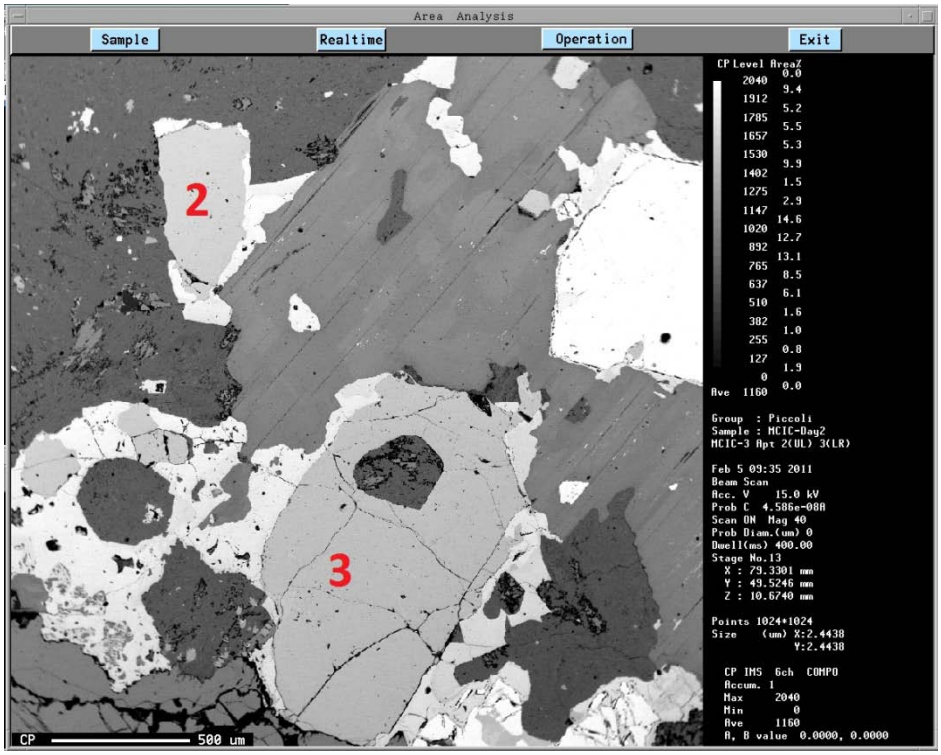

MCIC-3 Apatite 2 and 3

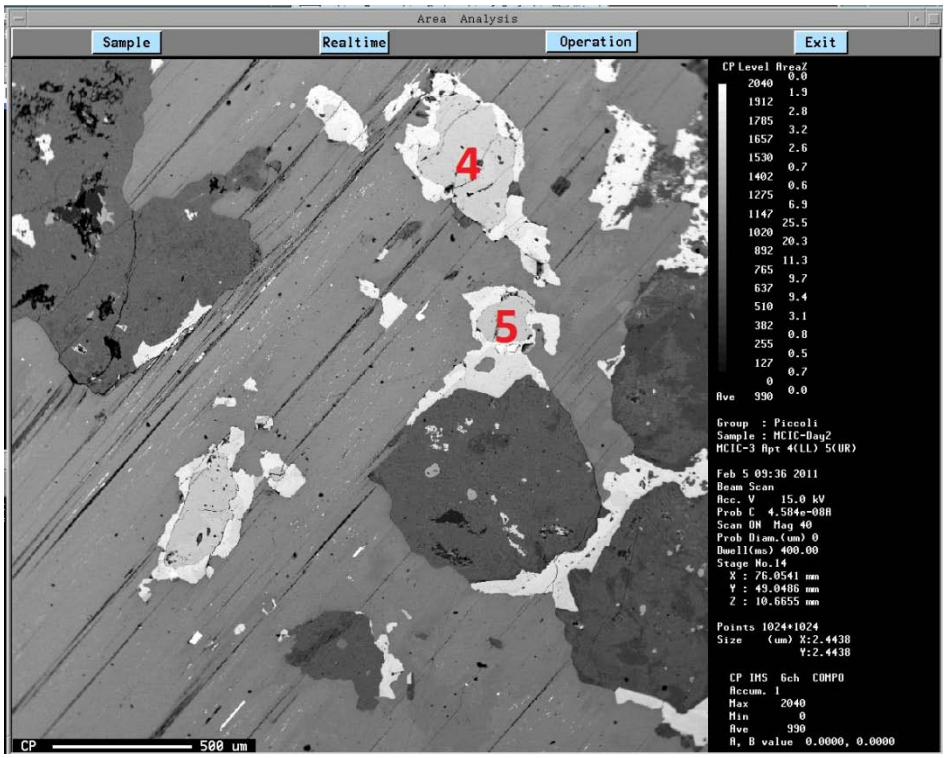

MCIC-3 Apatite 4 and 5

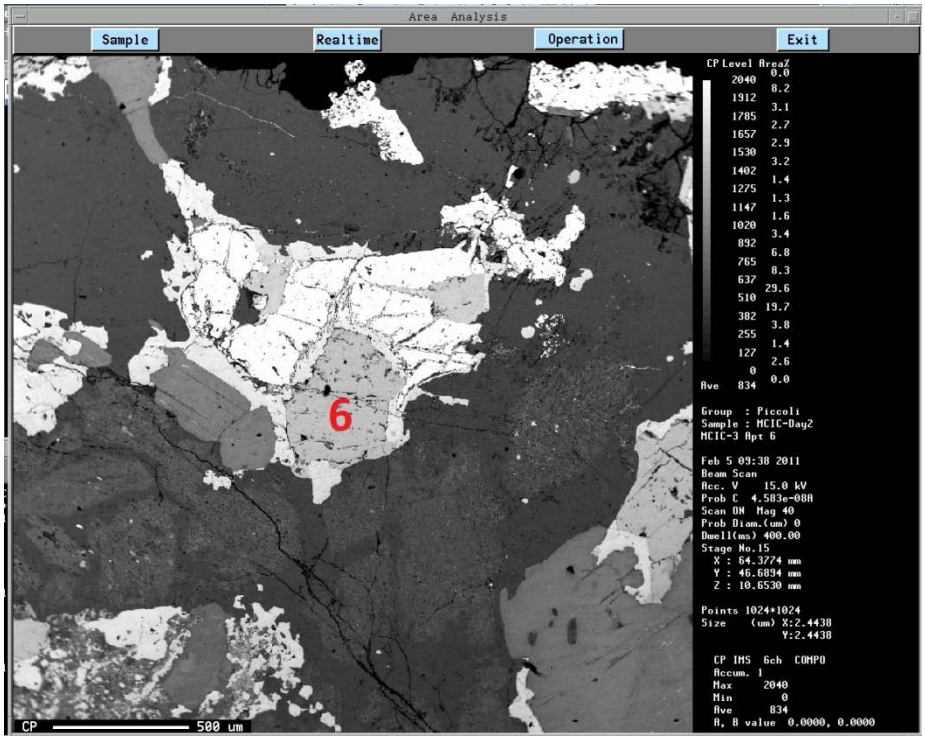

MCIC-3 Apatite 6

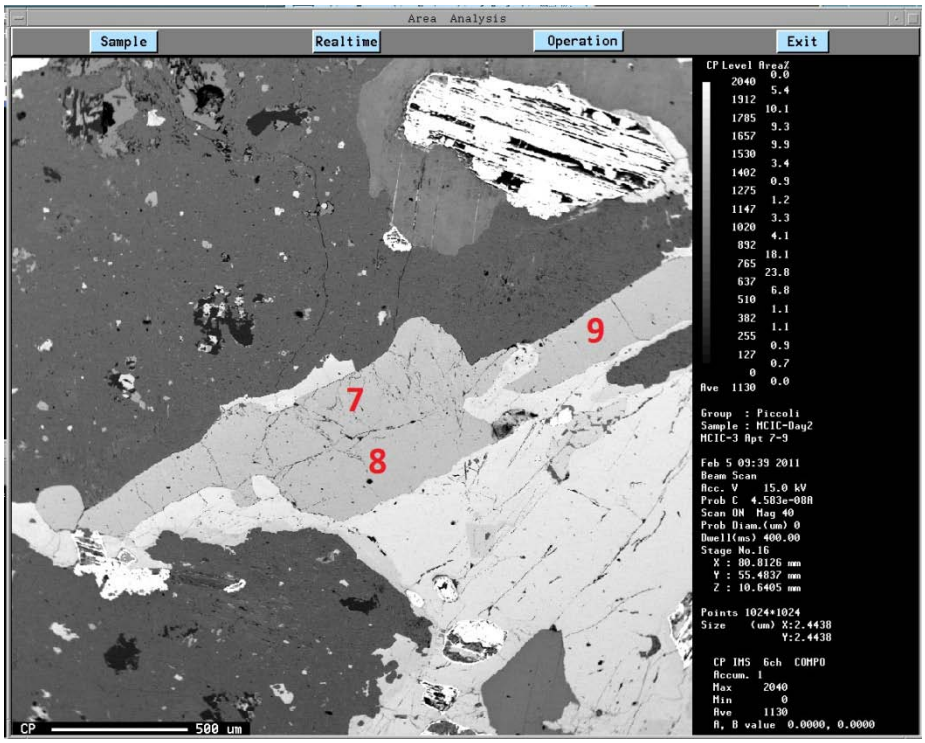

MCIC-3 Apatite 7-9

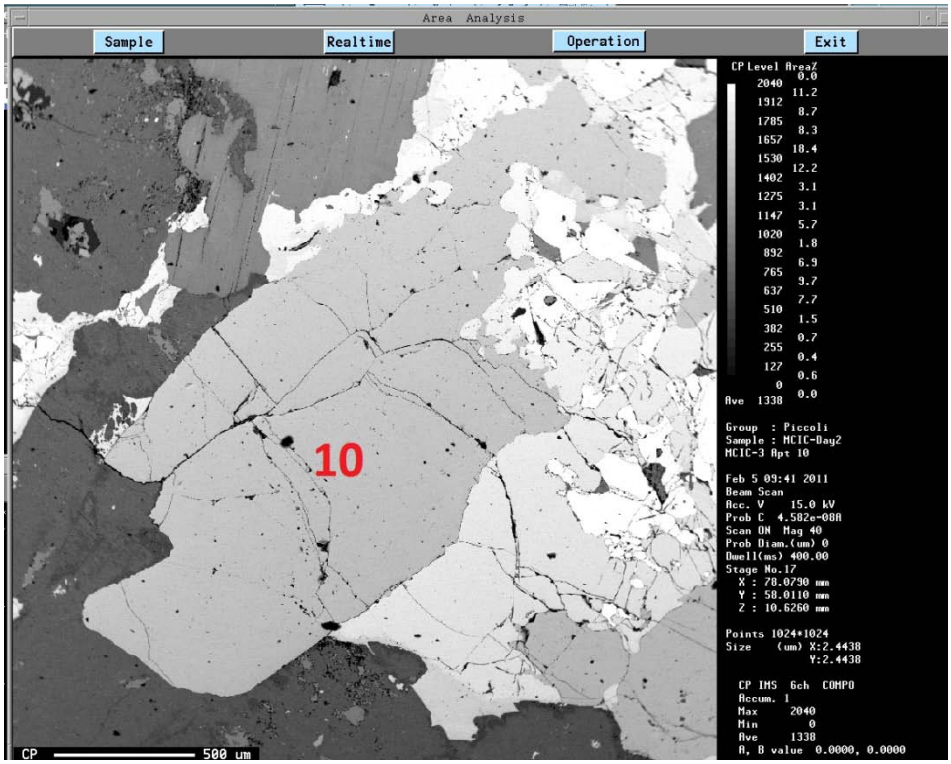

MCIC-3 Apatite 10

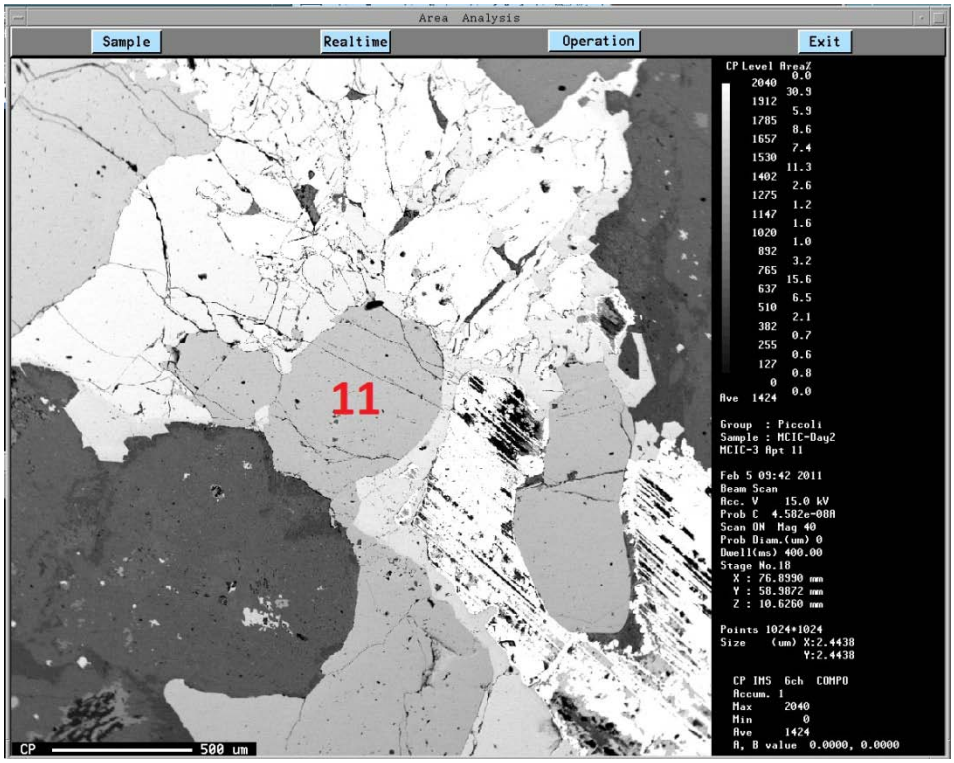

MCIC-3 Apatite 11

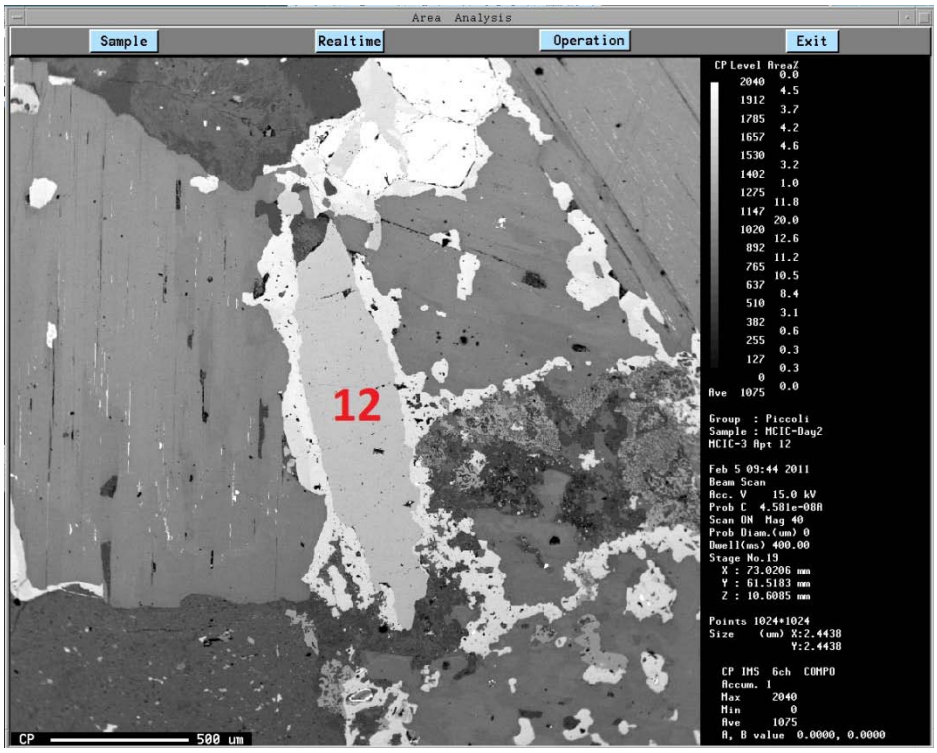

MCIC-3 Apatite 12

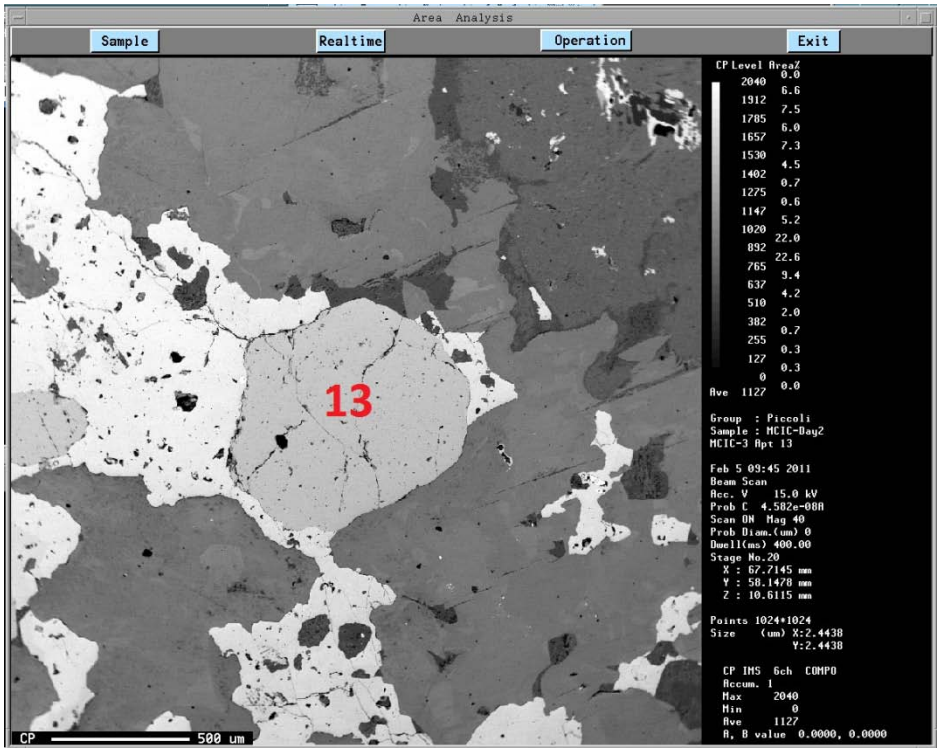

MCIC-3 Apatite 13

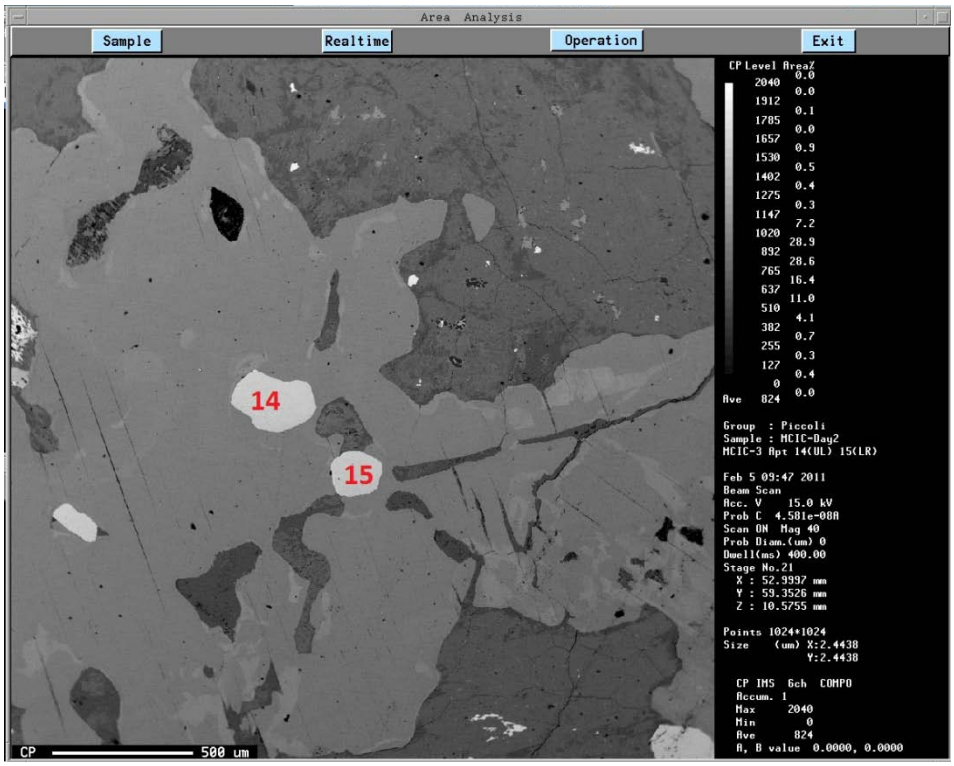

MCIC-3 Apatite 14 and 15

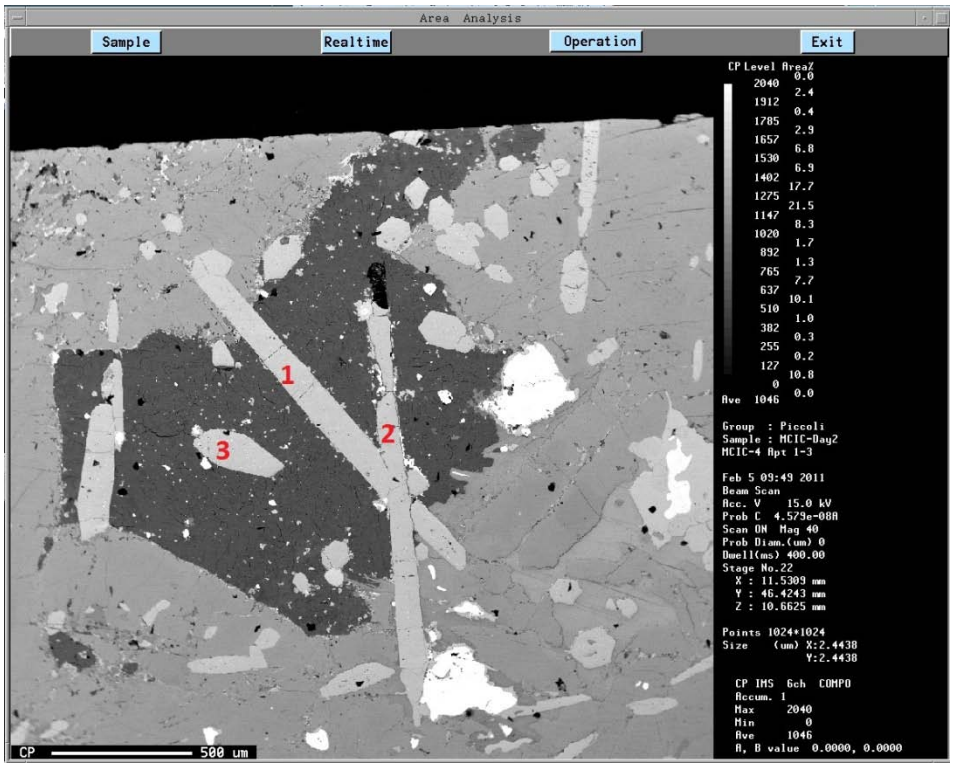

MCIC-4 Apatite 1-3

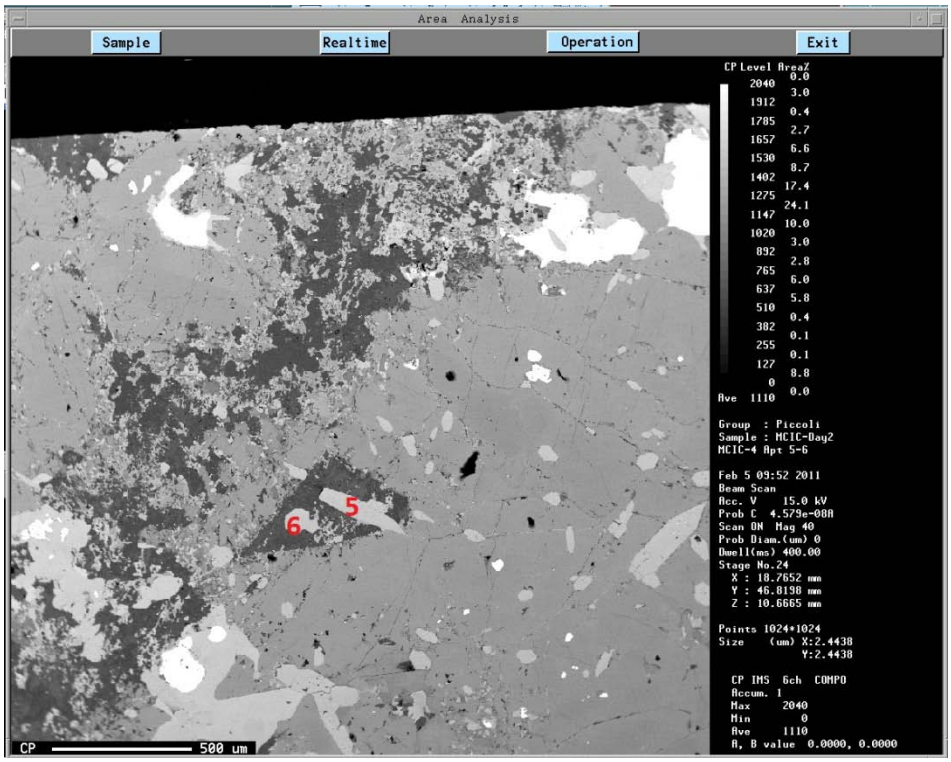

MCIC-4 Apatite 5 and 6

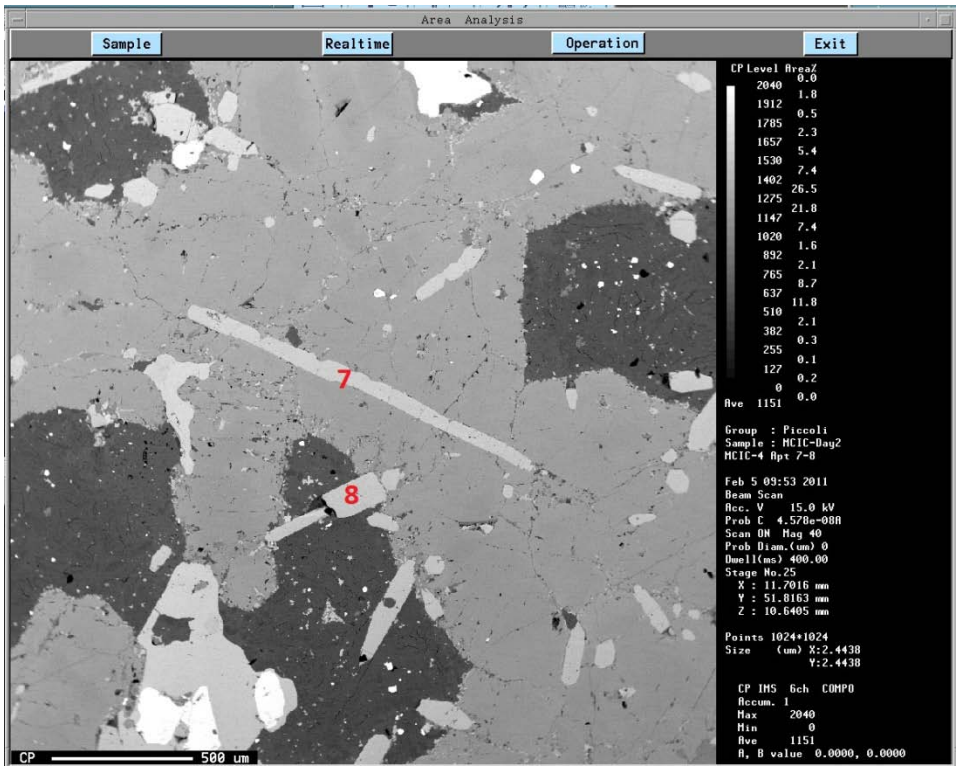

MCIC-4 Apatite 7 and 8

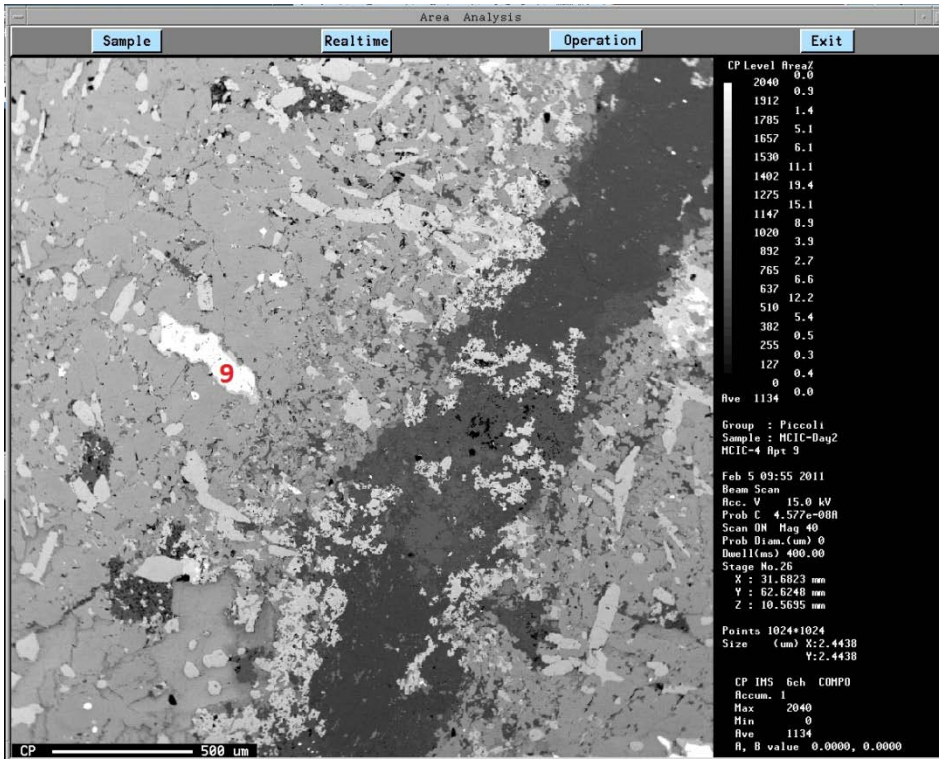

MCIC-4 Apatite 9

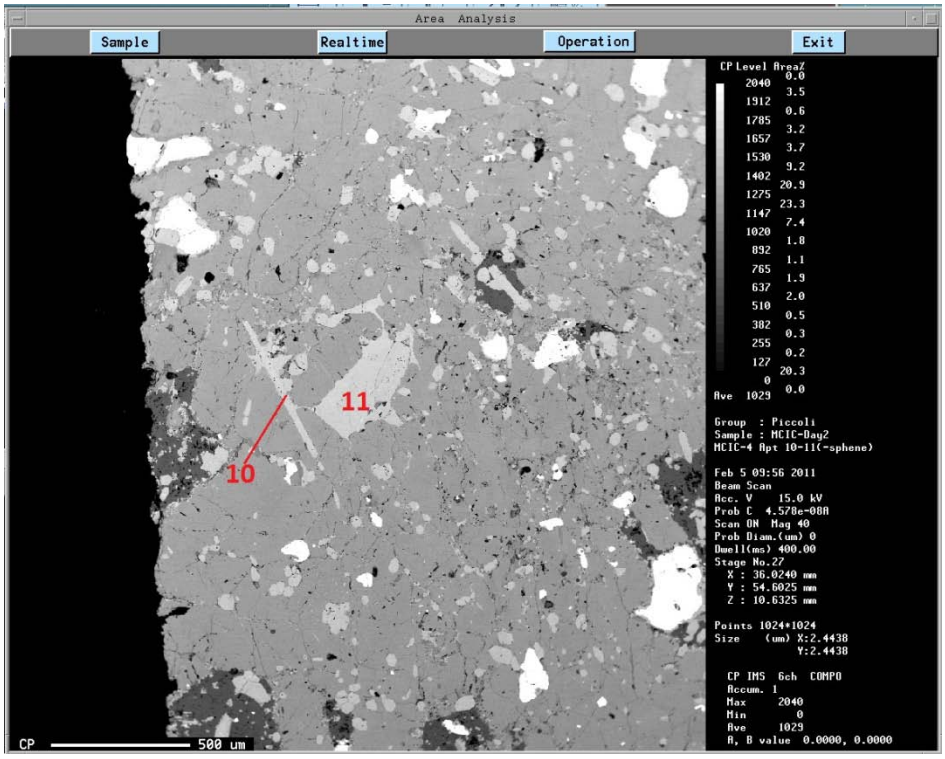

MCIC-4 Apatite 10 and 11

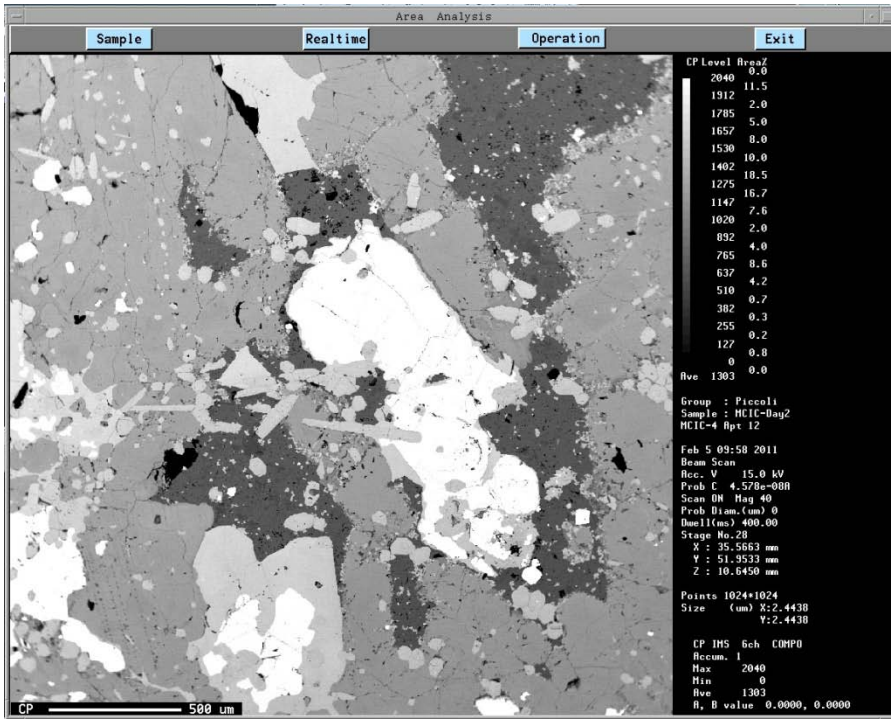

MCIC-4 Apatite group 12

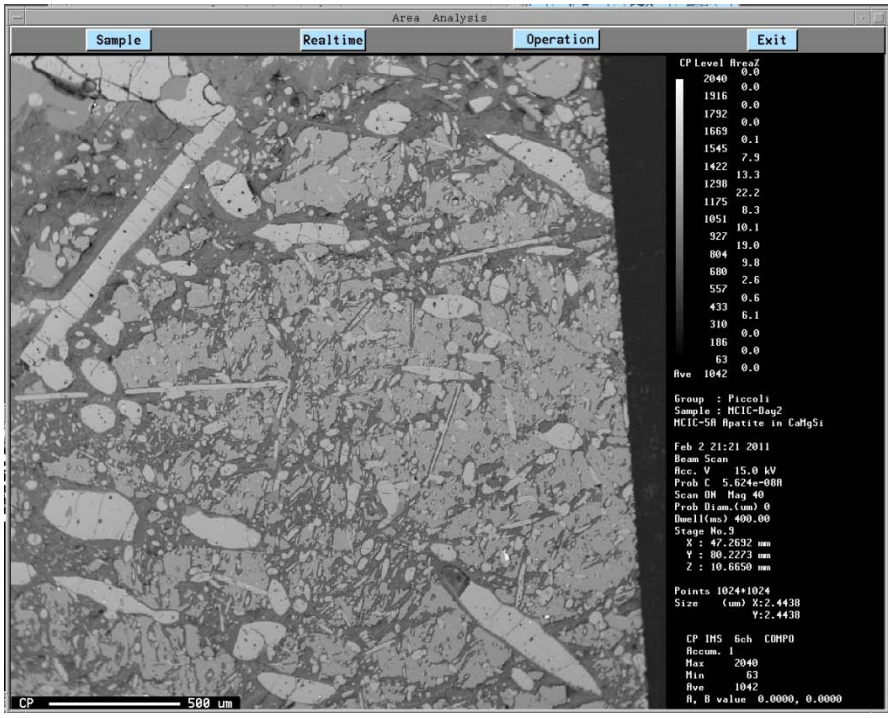

MCIC-5A Apatite in pyroxene cluster

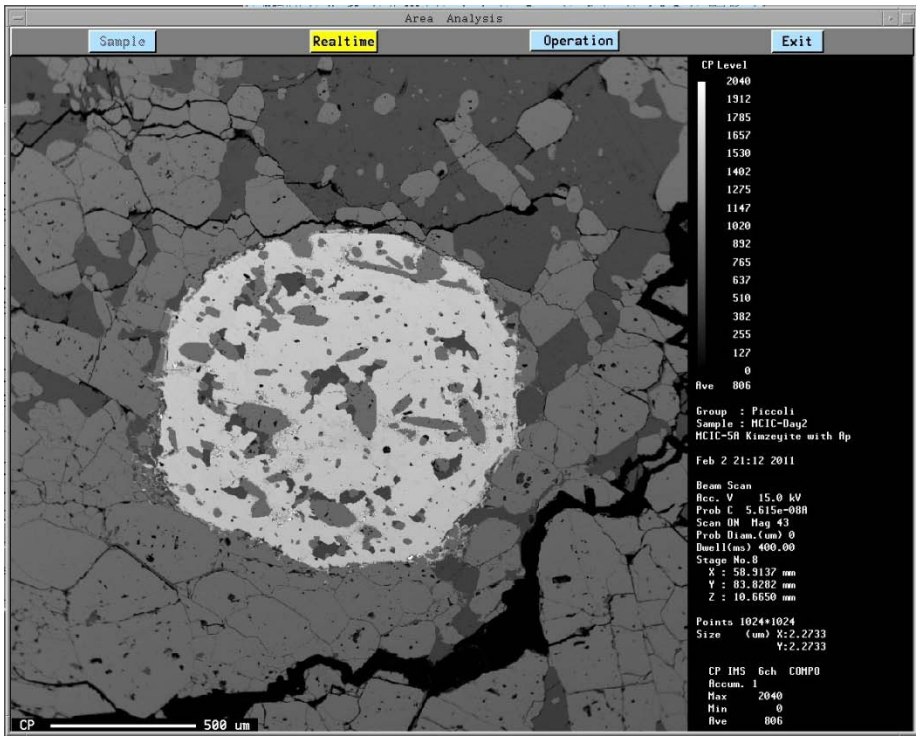

MCIC-5A Kimzeyite

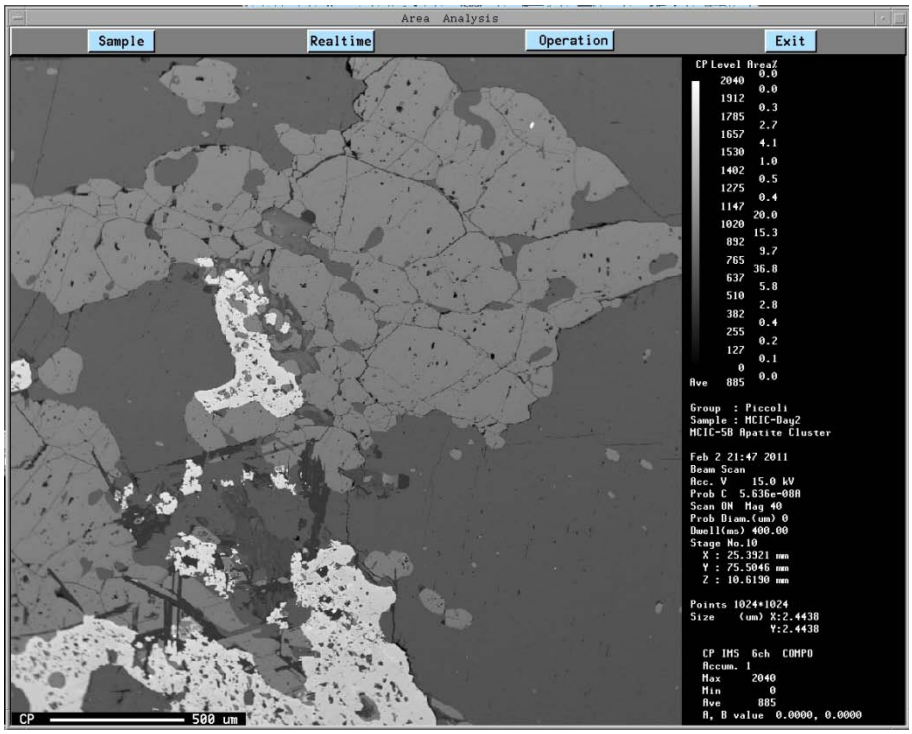

MCIC-5B Apatite cluster

Appendix 13

Thin section scans

MCIC-1 (Trachyte-phonolite)

MCIC-2 (Garnet pseudoleucite nepheline syenite)

MCIC-3 (Biotite ijolite)

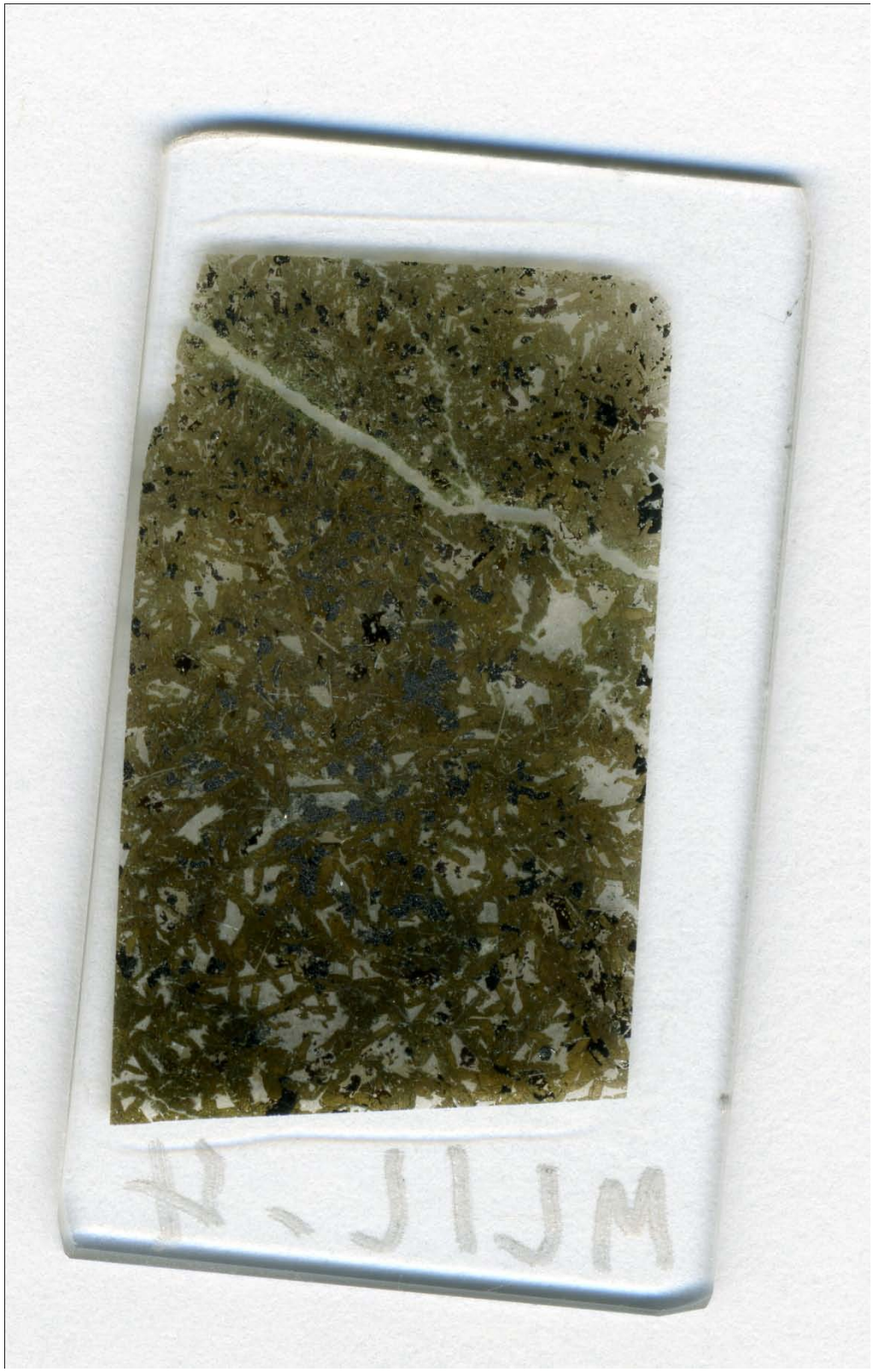

MCIC-4 (Jacupirangite)

MCIC-5A (Carbonatite)

MCIC-5B (Carbonatite)

Appendix 14

Sample thin section photos

PPL= plane polarized light

XPL= cross polarized light

FOV= field of view

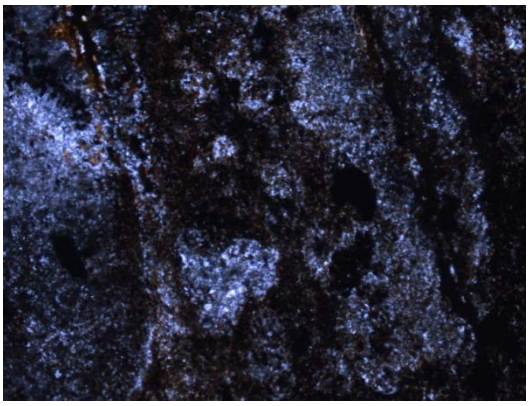

MCIC-1 PPL, 5x, FOV=2.7 mm

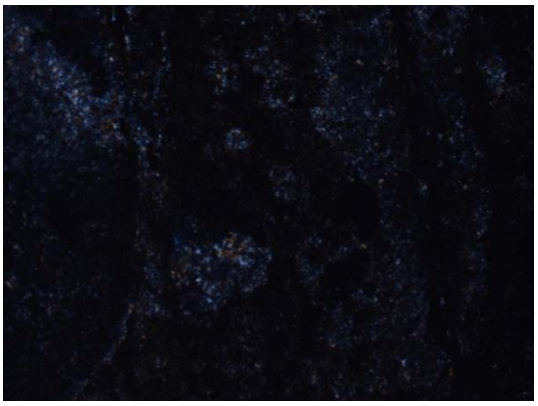

MCIC-1 XPL, 5x, FOV=2.7 mm

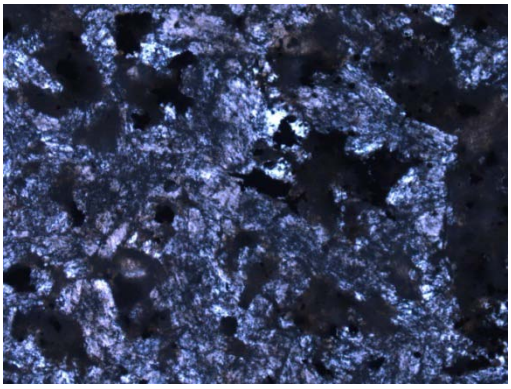

MCIC-2 PPL, 5x, FOV=2.7 mm

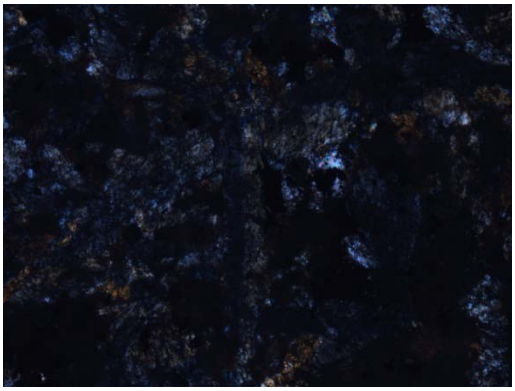

MCIC-2 XPL, 5x, FOV=2.7 mm

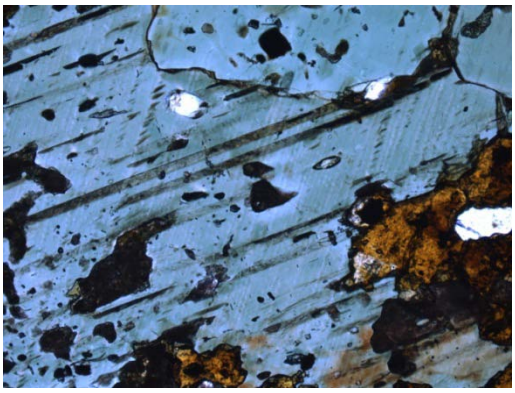

MCIC-3 PPL, 5x, FOV=2.7 mm

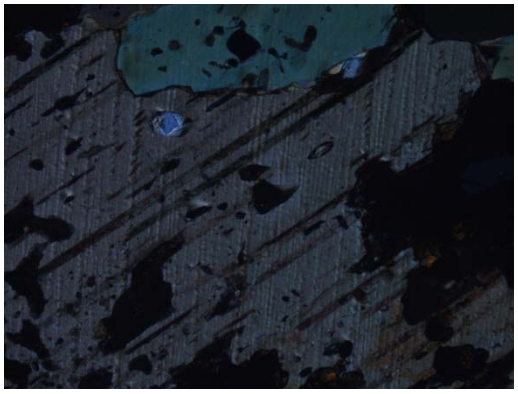

MCIC-3 XPL, 5x, FOV=2.7 mm

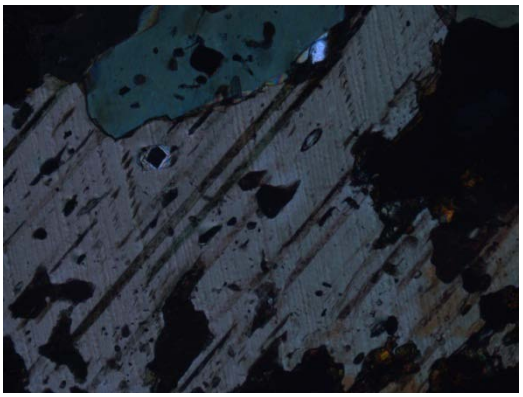

MCIC-3 XPL, 5x, FOV=2.7 mm

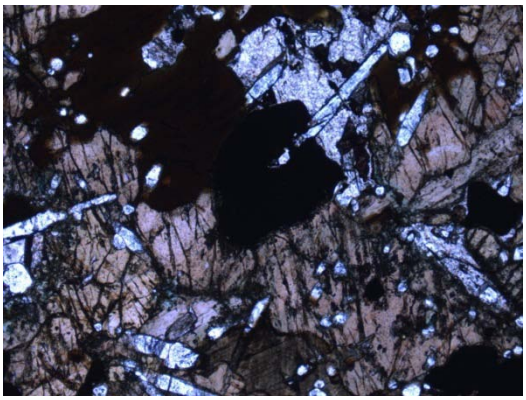

MCIC-4 PPL, 5x, FOV=2.7 mm

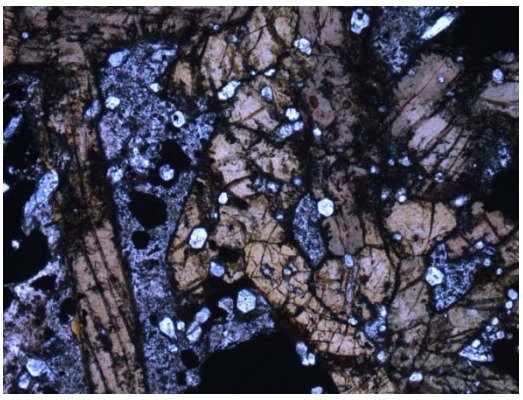

MCIC-4 PPL, 5x, FOV=2.7 mm

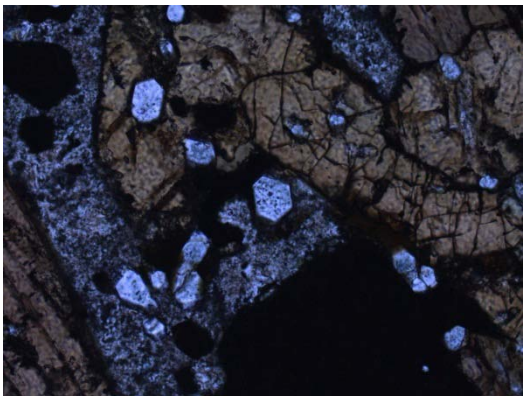

MCIC-4 PPL, 10x, FOV=1.4 mm

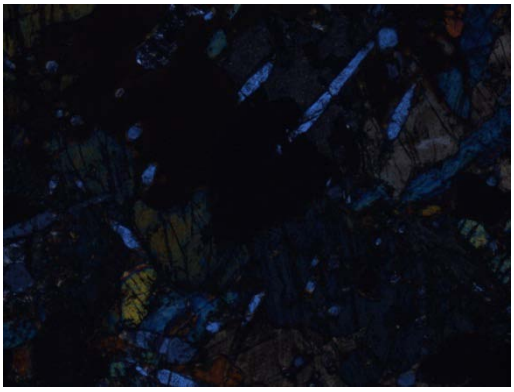

MCIC-4 XPL, 5x, FOV=2.7 mm

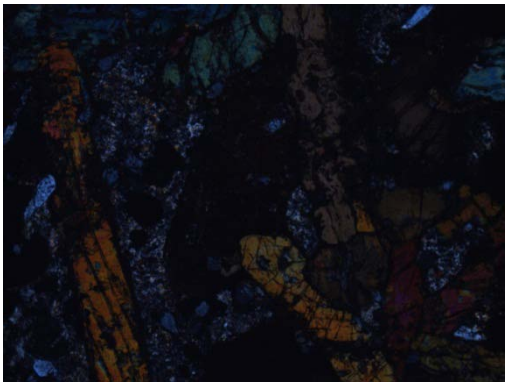

MCIC-4 XPL, 5x, FOV=2.7 mm

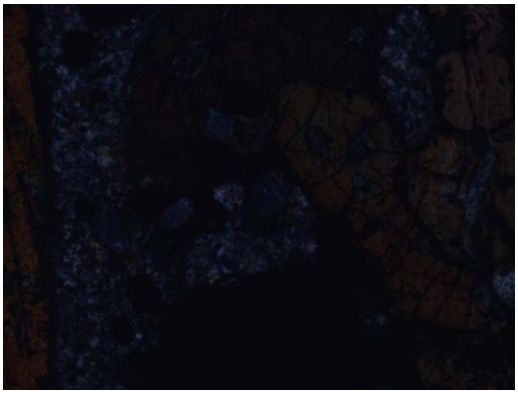

MCIC-4 XPL, 10x, FOV=1.4 mm

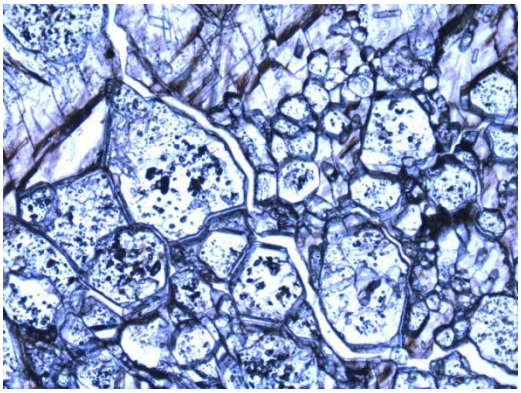

MCIC-5A PPL, 5x, FOV=2.7 mm

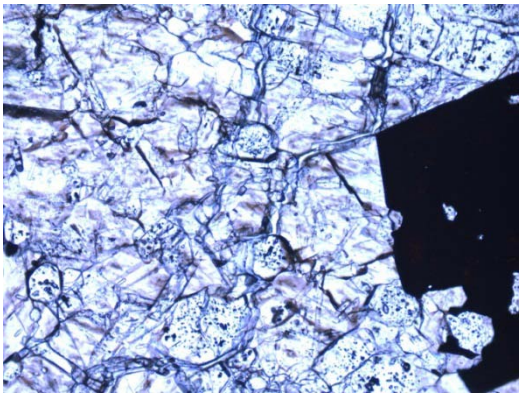

MCIC-5A PPL, 5x, FOV=2.7 mm

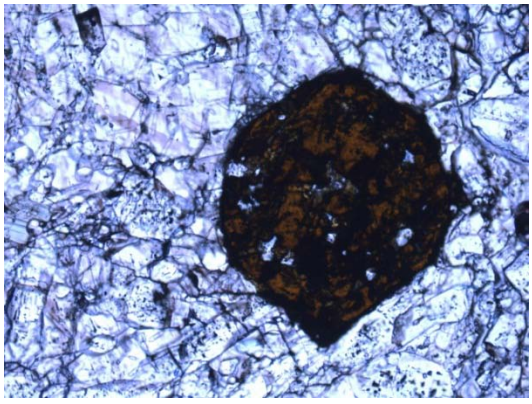

MCIC-5A PPL, 5x, FOV=2.7 mm

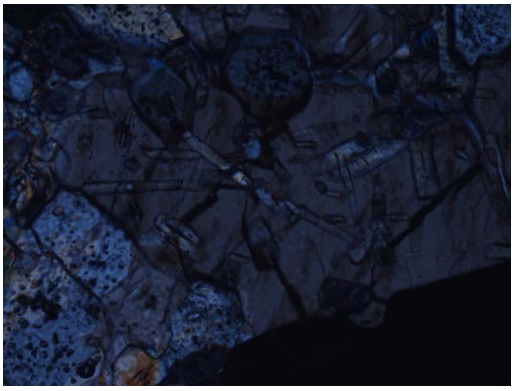

MCIC-5A PPL, 10x, FOV=1.4 mm

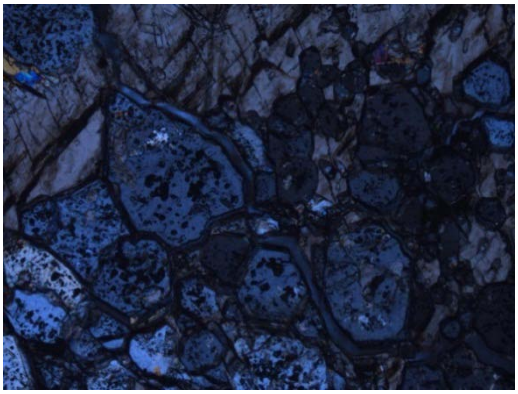

MCIC-5A XPL, 5x, FOV=2.7 mm

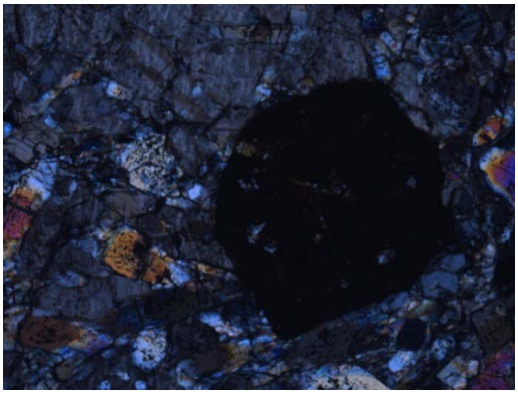

MCIC-5A XPL, 5x, FOV=2.7 mm

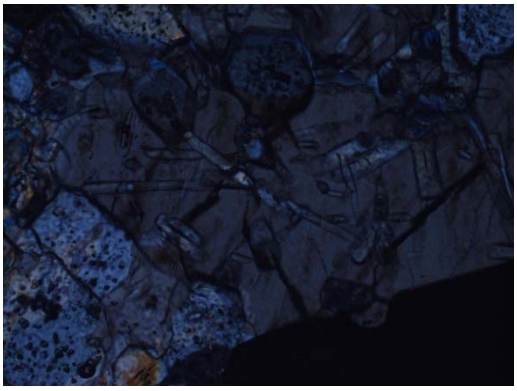

MCIC-5A XPL, 10x, FOV=1.4 mm

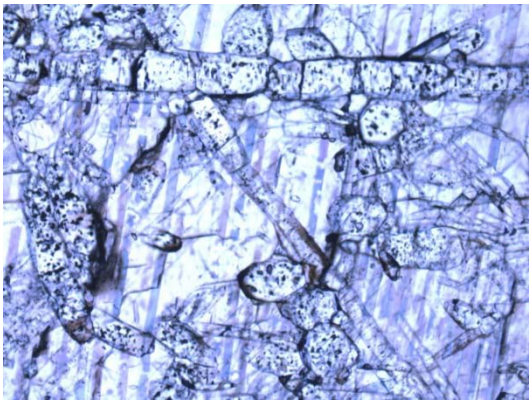

MCIC-5B PPL, 5x, FOV=2.7 mm

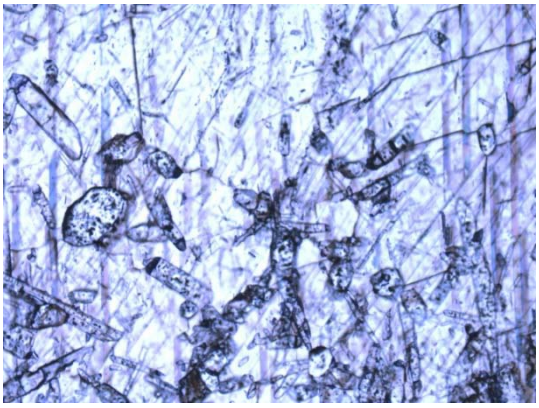

MCIC-5B PPL, 5x, FOV=2.7 mm

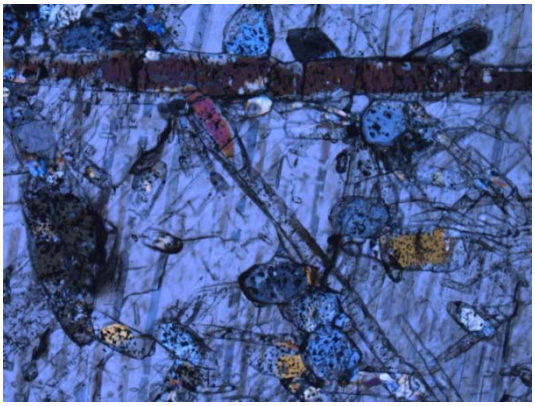

MCIC-5B XPL, 5x, FOV=2.7 mm

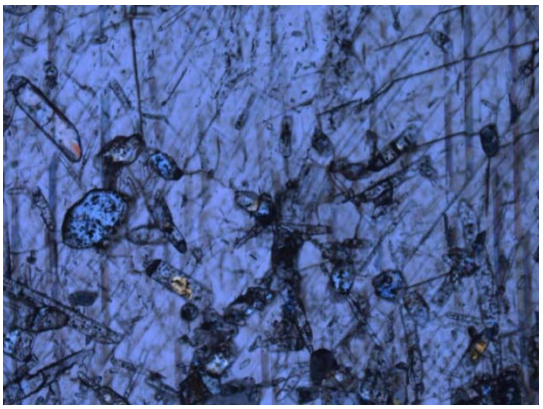

MCIC-5B XPL, 5x, FOV=2.7 mm